Musculoskeletal Modelling of Three Sit-to-Stand Strategies in Elderly People

Maud Hendriksen (4905113)
Supervisors: Dr. ir. E. van der Kruk and Prof. dr. F.C.T. van der Helm

April 2021

Abstract

Introduction: A thigh push-off is often used as a compensation strategy for standing up by elderly people. However, the biomechanics of this movement are not known. In this thesis the standing-up movement with the use of the thigh push-off strategy (TP), the armrest push-off strategy (AR) and the no arm aid strategy (NA) was analysed. The aim was to find out why TP for standing up is being used as a compensation strategy by elderly people.
Method: We examined upper and lower limb joint moments and lower limb muscle forces in three different sit-to-stand strategies in nine healthy elderly men. Inverse dynamics and static optimisation were done in OpenSim using a 3D musculoskeletal model.
Results: The lumbar extension moment in TP was significantly lower compared to NA ($p=0.04$). Rectus femoris force is lower in phase 2 in TP compared to AR. AR upper limb joint moments were significantly larger in dominant and non-dominant shoulder external rotation ($p=0.02$, $p<0.01$), elbow extension ($p<0.001$, $p<0.001$), and wrist flexion ($p=0.04$, $p=0.02$) compared to TP. Also, dominant shoulder abduction ($p=0.04$) moment was higher in AR compared to TP.
Conclusion: Elderly people probably use a thigh push-off to unload the lower back, but this could also be accomplished with AR. However, AR upper limb loading is higher compared to TP. TP is used to unload the lower back and upper limb joints.

Keywords: Ageing, Musculoskeletal modeling, OpenSim, Compensation, Movement objectives, Capacity, Sit-to-stand, Thigh push-off, Armrest push-off

Abbreviations

Abbreviation	Full term
Abd	abduction
ADL	activities of daily living
AP	anterior-posterior
AR	the armrest push-off strategy
BicFem (lh)	biceps femoris long head
BW	body weight
CoP	center of pressure
D	dominant
DoF	degrees of freedom
EMG	electromyography
Exrot	external rotation
Ext	extension
Flex	flexion
GasMed	medial gastrocnemius
GlMax	gluteus maximus
GlMed	gluteus medius
GRF	ground reaction force
Ham	hamstring muscle group
ID	inverse dynamics
IK	inverse kinematics
Inr	internal rotation
ML	medial-lateral
MR	magnetic resonance
n	number of participants
NA	the no arm aid strategy
ND	non-dominant
Quad	quadriceps femoris muscle group
RecFem	rectus femoris
Semimem	semimembranosus
SO	static optimisation
STS	sit-to-stand
STW	sit-to-walk
TibAnt	tibialisanterior
TibPost	tibialis posterior
TP	the thigh/knee push-off strategy
TTS	time to stand
TUG	timed-up-and-go
VasInt	vastus intermedius
VasLat	vastus lateralis
Vasmed	vastus medialis

1 Introduction

The population of people over 65-year has increased tenfold in the past century in The Netherlands and will increase over the next years [1]. The population of 80 years and over will even be tripled by 2050 [2], which has serious implications for health and social services [3]. Ageing may lead to mobility issues, which can hinder one's ability to manage activities of daily living and may lead to the need of help and decrease in social well-being [4].

To be able to prevent elderly from getting impaired, the concept of functional redundancy should be better understood. Functional redundancy is the redundancy in the muscle architecture of the human body [5]. Due to this redundancy age-related mobility impairments do not immediately arise at the onset of physical decline. Therefore redundancy is a key element in understanding how much age-related decline can be tolerated by elderly before actual movement impairments occur. A result of functional redundancy has been defined as neuromusculoskeletal (NMSK) compensation, further referred to as compensation [5]. Compensation is defined as an adjustment in movement strategy in relation to a baseline (e.g., previous state or a control group) [5]. Compensation strategies can be an early indicator of age-related decline and therefore important clinically [5].

Two types of compensation are proposed by Van der Kruk et al. [5]: compensation by changes in kinematics or compensation by changes in muscle recruitment. The form of compensation by changes in kinematics is a change in people's movement trajectory. Examples of changing the movement trajectory are using a handrail when climbing the stairs or using the armrests to stand up from a chair. An example of compensation based on altering muscle recruitment is using more co-contraction to increase stability. The reasons for compensation can be categorised into two forms: compensation for capacity and compensation for movement objectives. Compensation for capacity is defined as a change in recruitment of NMSK resources due to a low reserve in any part of the NMSK capacity at any moment during the task [5]. The NMSK capacity is defined as the physiological abilities of the NMSK system [5]. Reserve is the difference between capacity and task demand and varies throughout the task. The part with the highest task demand may result in failure when there is no reserve, unless compensation can occur. Compensation for movement objectives is explained as changes in kinematics as a result of different weighting of movement objectives (e.g., energy, stability, pain avoidance, safety and/or velocity). To maintain mobility in elderly in the long term, knowledge about reserve and compensation are important. Compensation strategies may benefit mobility in the short-term but may lead to injuries in the long term due to over- or underuse of physiological abilities [6].

The sit-to-stand (STS) movement is a widely studied activity of a daily living task in elderly people. This movement is performed when getting out of bed, standing up from a chair, or leaving the toilet. Standing up is a requirement of independent living and an important activity of daily living (ADL). If the STS movement is impaired, in-home care or moving to an elderly home is required [5]. Due to the importance of the STS movement, this movement has been reviewed by Van der Kruk et al. [6] with the concept of compensation. An overview of the current compensation strategies in standing up was created. Compensation strategies for movement objectives and/or for capacity of the STS movement that have been found in literature include: arm and/or trunk movements, pacing, and asymmetry of foot placement [6]. Van der Kruk et al. [7] imply that future research should consider upper extremity loading values and strategies, asymmetries, and sit-to-walk (STW). In literature the STS movement has generally been studied with the arms crossed in front of the body. Only a few studies allowed arm swing, the use of armrests, and/or a thigh push-off. However, 52% of the healthy elderly population was unable

to stand up without the use of their arms and only 40% of the elderly preferred to stand up without the use of their arms [7]. Asymmetric foot positioning was also present in standing up, but is poorly reflected in existing literature [7].

Pushing-off on the thighs/knees to stand up from a chair is prevalent in over 50% of the observed STW trials performed by elderly people [8]. Besides investigating the prevalence, the thigh push-off strategy (TP) has not been studied so far. Although the high prevalence of using TP, the biomechanical advantage is not known. In clinic this strategy is not used for the reason that clinicians suspect this might overload the lower back and shoulders. Nonetheless, data from an instrumented hip implant and vertebral body replacement showed a reduction in peak force in the hip for 7 out of 10 patients and a reduction in the peak force load in the L3 vertebral body [7; 9]. The hip peak force was measured in ten patients and peak force load in the L3 vertebral body was measured in three patients [9]. No data of TP is yet available for healthy individuals.

In this thesis the standing-up movement with the use of TP, the armrest push-off strategy (AR) and the no arm aid strategy (NA) will be analysed. The aim is to find out why TP for standing up is being used by elderly people. This will be done by quantifying the full-body joint moments and lower limb muscle forces in standing up for the three different strategies. We hypothesize that TP reduces lower back loading compared to standing up without arm aid and reduces shoulder loading compared to standing up with an armrest push-off. Also, we expect lower hip extension muscle forces due to a smaller hip joint moment [9].

2 Method

2.1 Participants

Twenty-seven healthy young men and females (YM, YF) (20-35years, 13 men) and 23 relatively healthy older females and men (EF, EM) (65-92 years, 11 men) participated in the study. Participants were recruited between July and November 2019 in London, United Kingdom. Participants took part in a 3-4 hours experiment at the Charing Cross Hospital. Exclusion from participation included being assessed as 'moderately' or 'severely' frail by the Edmonton Frail Scale [10], any history of severe mobility-limiting pathologies, any known allergy to adhesives, unable to speak or read English at a sufficient level to give informed consent, suffering from a psychiatric illness or mental state that limits informed consent, any systemic inflammatory, connective tissue disorders or medical disorders limiting exercise, pregnancy or having a pacemaker. Ethical approval was granted by the institutional ethics committee. All participants gave written informed consent. Due to time limitations only EM were studied within this thesis (Table 1). Two elderly men were excluded after the measurements had taken place due to missing marker and force data.

Table 1: Participant information. The mean and standard deviations are given for each variable.

Age group	n	Age (years)	Weight (kg)	Height (m)
Older men (EM)	9	78±7.73	77.27±14.78	1.74±0.08

Abbreviations: n=number of participants.

2.2 Participant characteristics

A questionnaire was conducted to assess levels of activity, diet, general health, (former) profession, any joint related pain or surgery, level of frailty, fear of falling (FES-I short) [11], level of dizziness and hand dominance [12]. Participants were also asked on a visual analogue scale (VAS) from 0-10 if they were experiencing any pain at the start and end of the experiment. The FES-I score is a measure of fear of falling, where 7 is no concern about falling at all and 28 is a severe concern about falling.

2.3 Experiments

The experiments that have been conducted include sit-to-stand (STS) movements, sit-to-walk (STW) movements, a timed-up-and-go (TUG) test, and capacity measures. Capacity measures include measurements on isokinetic strength, balance, proprioception, hand grip strength, joint range of motion, and a nerve conduction study. The capacity measures, STW, and TUG are explained in detail in Appendix B, but results were not used for this thesis.

2.3.1 Task measures

Participants were instrumented with markers (Figure 2) and Appendix A:Table 9) and 16 electromyography (EMG) sensors, to be able to track the full body motion and activity of the lower limb muscles. The EMG sensors were placed on muscle groups (Appendix A:Table 10) according to European guidelines to be able to track the activity of these muscles. The seat height was adjusted to knee height approximately. Before the different strategies were measured a static

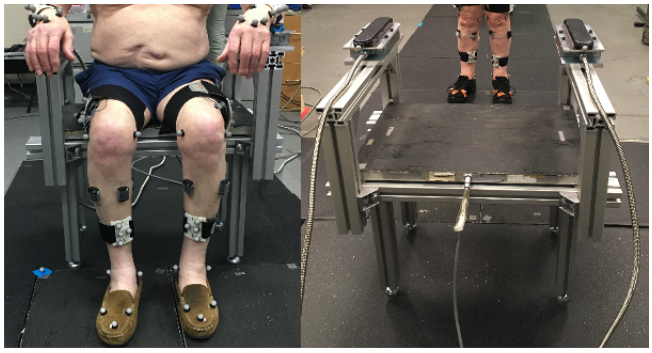

Figure 1: The back and front of the instrumented chair. At the back the cables are visible where the force plates are connected with. Two force plates were placed on the ground and one was placed on the seat. On both sides a force plate was attached to the armrest and wheelchair armrest pads were connected on top of the armrest force plates.

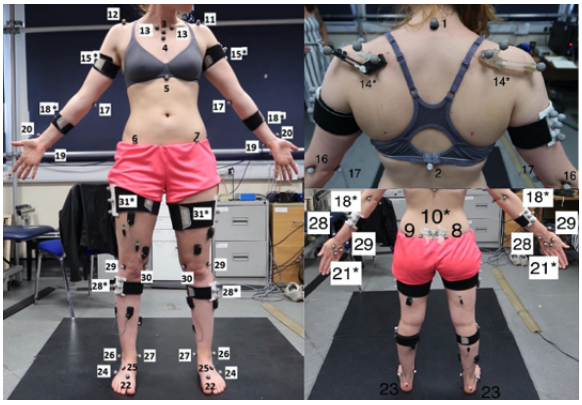

Figure 2: Marker and EMG sensors placed on a participant. Definitions of marker positions can be found in Appendix A.

and dynamic trial was recorded. The three different arm strategies were tested in STS: standing up with the use of the armrests push-off strategy (AR), with the use of the thigh/knee push-off strategy (TP) and the no arm aid strategy (NA). Participants were seated on the instrumented chair and asked to stand up in one of the three strategies. All three strategies were performed three times and standing up with the use of TP was followed by twice performing STW with TP. Besides the arm strategy no other instructions were given. All participants were able to execute all the tasks. Participants were equipped with self-made force gloves in TP trials to be able to measure the reaction force of the thigh.

The STS transfer of each strategy was divided into three phases. Phase 1 started when the participant started to move their CoM forward. This was notified by a posterior acceleration of the torso ($>2m/s^2$). Phase 1 ended before seat off, just before the force plate on the seat reported no forces. Phase 2 started when there was no contact with the seat anymore and ended when the ankle was in maximal dorsiflexion. Phase 3 started just after maximal dorsiflexion and lasted until maximum hip extension ($<3°/s$).

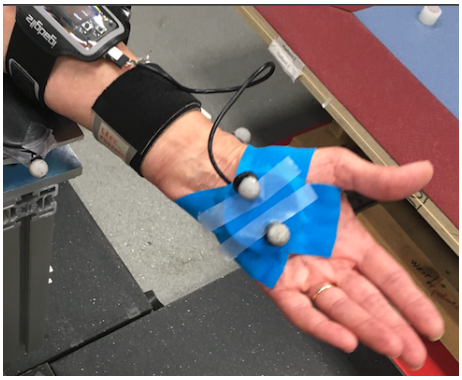

Figure 3: The self-made force glove. On the hand the attached single disc load cell and on the forearm in the top left corner the Raspberry Pi is connected. Markers on the force glove are removed before the trials started.

2.3.2 Motion Capture

The markers were placed on the thorax, pelvis, arms, legs, scapula and feet, either as a cluster of four or as separate markers (Appendix A: Table 9). Except for the scapulae, which was measured using a locator cluster and a separate tracker during the dynamic trial. Kinematics were captured using a 10-camera motion capture system (Vicon Motion Systems, Oxford, UK), sampled at 100Hz. Ground reaction forces (GRFs) were measured using two Kistler force plates on the floor under each foot, one on the seat of the instrumented chair and two force plates on the armrests of the instrumented chair, with a sampling frequency of 1000Hz (Kistler Holding AG, Winterthur, Switzerland). The armrest force plates were covered by wheelchair armrest pads to be able to grasp the armrest (Figure 1). To measure the reaction force of the thighs on the hands in TP, force gloves were made, which were placed on the palm of both hands (Figure 3). The force gloves consisted of a single disc load cell, which translated the load applied to the surface into an electrical signal, working on Raspberry Pi [13]. The force gloves had a sampling frequency of 100Hz. The force measured by the load cell was calibrated with the armrest force plate by pressing three times on the armrest with the force glove every trial.

To capture muscle activity a wireless Delsys EMG system was used. The muscle activity was sampled with a frequency of 2000Hz. EMG signals were rectified and 2^{nd} order Butterworth low pass filtered with a cutoff frequency of 20Hz [14]. EMG signals were also adjusted to determine the times at which muscles turn on and off. The Hilbert transform was used to take the linear envelope with a cutoff frequency of 50Hz and smoothed the signal with a 50-milisecond window. An adaptive threshold detected the activity of the signal [15].

2.4 Data analysis

All force plate and kinematic data was input into a 3D muskuloskeletal (MSK) model in OpenSim [16; 17]. C3d motion files from Vicon were converted to .trc files in Matlab to use in OpenSim for scaling and inverse kinematics (IK). The data was rotated accordingly. Forces were converted with Matlab to motion files to use in OpenSim. The reaction force of the seat was splitted into two forces that are applied to the center of pressure (CoP) of the thigh on the longitudinal axis. Axis were also converted in Matlab to match the OpenSim axis. All data were input into a MSK model. Kinematic data and force plate data were filtered with a low-pass cut-off frequency of 4.7Hz and 10Hz respectively.

2.4.1 Model

All data were input into a MSK model developed by Lai et al. [18]. This model is an updated version of an earlier developed MSK model [19]. It is a full-body model with twenty-two segments. The MSK model has muscle-actuated lower extremities and a torque-actuated torso and upper extremities. The model consists of rigid body representations of an averaged-sized adult male (mass=75kg, height=1.70m) [19]. Bones are connected with joints and the full body model consists of 37 degrees of freedom (DoF): 7 in each leg, 6 at the pelvis, and 17 in the torso and upper extremities. The model is driven by 80 Hill-type muscle-tendon units to generate moment around the lower limb joints and 17 torque generators that move the upper extremities and torso. The model was suitable for analysing movements with up to 140° of knee flexion and 120° of hip flexion. The muscle parameters in this model were based on cadaver-based estimates [20] and on magnetic resonance (MR) imaging results of young adults [21]. The optimal muscle fiber lengths, tendon slack length, and pennation angles were derived from a study on 21 elderly cadavers [20] and the maximum isometric force was based on an estimate of the muscle's physiological cross-sectional area (PCSA) and assumed specific tension of $60 N/cm^2$ from the MR image results of young adults [19; 21]. In this thesis elderly men were studied, therefore the maximum isometric forces were adjusted to the values obtained from the cadaver-based study [20; 22].

The pronation and supination range of the forearm were extended. In previous literature search a mean range from 77.7° of pronation and 82.4° of supination was found in elderly people [23], while the existing model was only able to perform 90° between maximal pronation and maximal supination. Pronation is a crucial movement in TP and AR. The model's range between maximal pronation and maximal supination was adjusted to 150°. With the generic MSK model the following simulations were executed: scaling, IK, inverse dynamics (ID) and static optimisation (SO) (Figure 4).

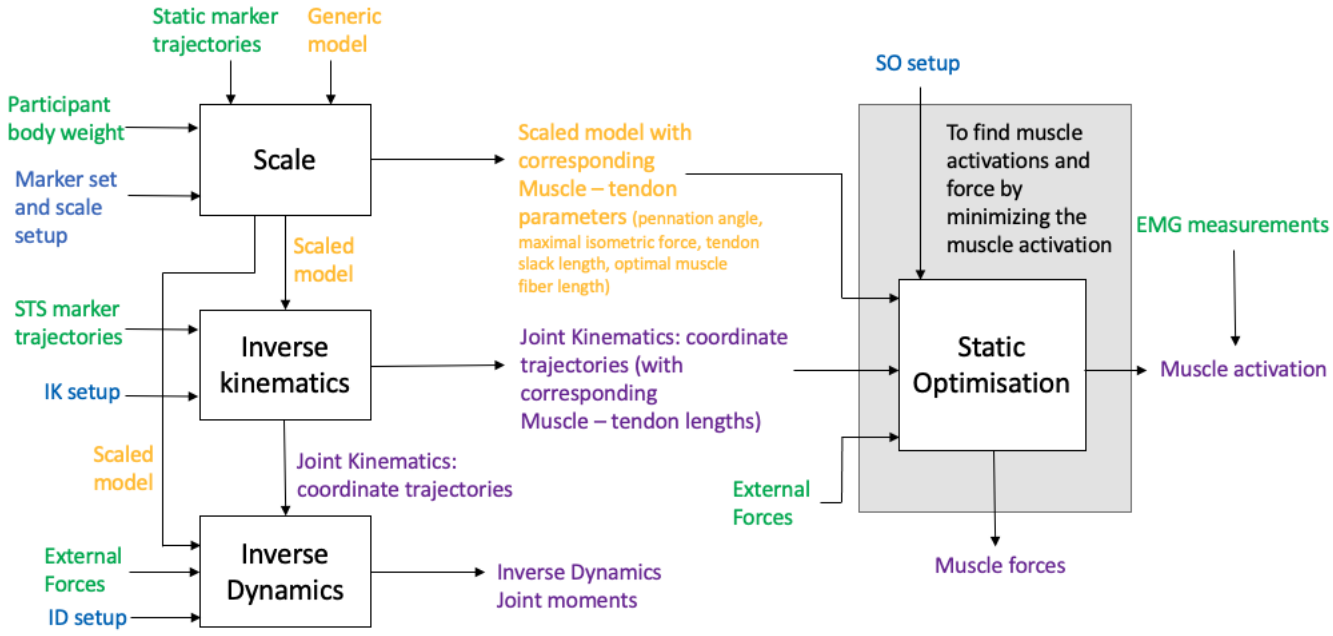

Figure 4: Process diagram for simulations used in this thesis. The OpenSim simulation tool boxes are shown in black. Experimental data are shown in green, setup files are shown in blue, the OpenSim files are shown in yellow, and the simulation files generated by the toolbox are shown in purple.

2.4.2 Scaling

Scale setups were made for every individual and was done using OpenSim. Inputs into the generic model were the static trial marker trajectories, marker set, scale setup, and participant body weight (BW). Segments were scaled with scale factors from measurements in the scale tool with the use of markers either automatically or manually. Every participant had their own adjusted generic model with markers adjusted where necessary when compared to photos taken in static position. This was done to correct for inaccurate marker placement on bony landmarks. The scale setup consisted of marker weightings and scale factors. Cluster markers were weighted zero, since these are not positioned on bony landmarks hence their position is less reliable.

2.4.3 Inverse Kinematics

IK was performed with all joints unlocked except for the metatarsophalangeal and subtalar joints. Inputs for IK were the scaled model, marker trajectories of each trial and the IK setup which consisted of the weights of the markers. Motion segment markers are weighted more heavily compared to the markers attached to the anatomical landmark. The outputs of IK from OpenSim are position, velocity and acceleration of the joints and of the center of mass (CoM) of the segments.

2.4.4 Inverse Dynamics

Armrest and seat forces were put to zero when it was certain that there was no relevant force applied to the force plates. Force plates were corrected where necessary. Force glove data was only collected in the vertical direction in the local frame of the hand. A matrix was made with zeros in the x and z direction and the synchronised sampled data in the y direction. The force vectors were implemented into the .mot force file for use in OpenSim. All forces were expressed in the ground frame, except for the force on the hand in TP trials, these were expressed in the local frame of the corresponding hand. In NA the .mot file consisted of the force and CoP of the ground force plates, and the seat force plate (splitted into two forces acting on the thigh), in TP the force of the force gloves (CoP was the CoM of the hand) were included and in AR the force and CoP of the armrests were included. The force measured by the force glove is the force exerted on the hand by the thigh. All inputs into OpenSim were in meters. The inputs for ID in OpenSim were the scaled model, the moment arms, the segment mass, segment acceleration, inertia, segment angular velocity, and the external load data (Figures in Appendix H). Outputs were the ID joint moments.

The body forces at joints analysis from the ID simulation in OpenSim give a zero force vector output. This is a common problem known by other OpenSim users. A work around is to take a static optimisation force file output that matches the model and give an input of zero to all muscle forces. Run the joint reaction tool in the analyse toolbox of OpenSim with all muscles put to zero, which should give decent body force estimates. Eventhough, this is not the best way to solve for joint reaction forces, the relative joint reactions in the different strategies can be compared. Also, a joint reaction analysis is performed with the muscle force outputs for the lower limb joints, which calculates the joint forces and moments transferred between two connected bodies as a result of all forces acting on the model [24].

2.4.5 Static optimisation

Static optimisation (SO) is used to estimate muscle forces from experimental data. It is a widely used tool in OpenSim due to its speed and usability. The input for SO were external load data, motion files containing time histories of the generalized coordinates that describe the movement of the model, the scaled model, and the SO setup. The setup consisted of the exponent for the activation-based cost function to be minimised, and a file containing the residual and reserve actuators [24]. The residual and reserve actuators are necessary to correct for the dynamic inconsistency between the estimated model accelerations and the external forces in the first free joint in the model. In this study the first free joint in the model is the ground-pelvis joint. Every DoF should be corrected with one actuator.

The outputs are muscle forces and their activation. The EMG data was compared with the simulated activation after normalising the EMG by the peak value of that muscle's simulated activation. The final SO results were verified to make sure the results were solely from muscle-tendon actuators and not from reserve or residual actuators, which would mean extra joint torques to increase muscle forces [24]. The hip, knee, and ankle normalised ID joint torques (Nm/kg) were compared with the joint torques calculated from SO, which is the sum of the product of muscle moment arms and muscle forces (Appendix C: Eq.11,12,13) [25].

The gluteus maximus and adductor magnus muscles were modeled as multiple actuators. Therefore their forces were calculated by summing the values reported for every single actuator [26]. The activation was multiplied by a weighing factor and these were summed up. This weighing factor was based on the maximum isometric force a single actuator could produce with respect to the sum of all actuators making up the muscle. Also, the muscles belonging to the hamstring and quadriceps femoris muscle groups were added up to form the muscle groups and to be able to compare our results to literature.

EMG signals are normalised to the maximum activation of the SO results. Also, the on-off EMG signal is normalised to the maximum activation of the SO results.

2.5 Statistics

Repeated measures ANOVA was done to compare the three strategies on values of time to stand (TTS), peak ground reaction force (GRF), joint moments, and muscle force for the complete STS transfer and for the individual phases. Also, repeated measures ANOVA was performed to compare the phases within the strategies for muscle force and joint moment. Peak armrest force components, peak armrest resultant force with and without the medio-lateral component, and peak and sum of the force measured by the force glove were also determined using repeated measures ANOVA. Differences between dominant and non-dominant leg were compared using the paired-sample t-test. We defined the dominant leg according to the largest vertical GRF during STS transfer for the majority of the trials. Also, the relation between the hand placement on the thighs and the muscle force, peak hand force, and joint moments were determined. The relation between the FES-I score and the sum and peak force on the hand in TP and AR were analysed as well.

Normality was checked using the Shapiro-Wilk's test ($p>0.05$). Most variables were normally distributed according to Shapiro-Wilk's test. Partial omega squared were calculated for effect sizes, where $\omega^2=0.01$ is considered a small effect, $\omega^2=0.06$ is considered a medium effect and $\omega^2=0.14$ is considered a large effect [27]. A p-value of less than 0.05 was assumed to be significant. Statistical tests were performed in Matlab.

3 Results

Due to measurement issues with the motion capture system (1 trial), force plate data (1 participant) and force glove data (4 participants), we have performed IK for 9 participants and 80 trials, ID for 68 trials, and SO also for 68 trials (Table 2). TP was analysed for 6 participants due to missing force glove data. The results included in the tables and figures represent the results of six participants unless stated otherwise. In Appendix G tables and figures were included which show the results of 9 participants in AR and NA.

Table 2: The number of trials and number of participants per technique for which IK, ID, and SO are performed in this study

	IK		ID		SO	
	participants	trials	participants	trials	participants	trials
TP	9	27	6	15	6	15
AR	9	26	9	26	9	26
NA	9	27	9	27	9	27

3.1 Time to Stand

In phase 1 participants were faster in NA compared to TP (Table 3). Phase 3 was performed significantly faster in AR compared to TP. The standard deviation of the duration of a full STS of both TP and NA are higher compared to AR. This is due to the fact that the oldest participant (93y) had more difficulty standing up without the use of armrests. The TTS without including this participant (P2237) are: NA 1.45±0.13s, AR 1.53±0.17s, TP 1.76±0.34s.

Table 3: The mean and standard deviation of the duration of the phases and full time to stand in seconds.

Elderly people	TP (s)	AR (s)	NA (s)
Phase 1	0.54 ± 0.09^{c}	0.55±0.15	0.44 ± 0.03^{c}
Phase 2	0.18±0.16	0.12±0.08	0.22±0.15
Phase 3	1.23 ± 0.47^{a}	0.91 ± 0.27^{a}	1.0 ±0.59
Full STS	1.96±0.66	1.59±0.24	1.67±0.67

[a]: Significant difference between TP and AR.
[c]: Significant difference between TP and NA.

3.2 Joint Moments and Joint Reaction Forces

Dominant and non-dominant hip, non-dominant knee and lumbar peak joint moments in AR were significantly lower compared to TP ($p<0.05$) (Table 4 and Figure 5). Non-dominant hip, dominant knee and lumbar peak joint moments in AR were significantly lower compared to NA. Including all participants tested with AR and NA (9 participants) the hip and knee peak joint moments on both sides were significantly lower in AR compared to NA as expected. The lumbar peak joint moment was 0.75 Nm/kg and 0.49 Nm/kg lower compared to NA and TP respectively, which is significant ($p<0.001$, $p=0.003$). In all phases the lumber extension moment is lower in AR compared to NA and TP. Also, the lumbar extension moment in TP is significantly lower compared to NA (0.26 Nm/kg, $p=0.04$).

Knee peak joint moments were reached in phase 2 and ankle peak joint moments were reached in phase 3 in all three strategies. Lumbar and hip peak joint moments were reached in phase 2 in AR and NA and in phase 3 in TP, which would imply that in TP lumbar and hip peak joint moments were reached after maximum dorsiflexion.

In phase 1 the non-dominant hip joint moment was significantly lower in AR compared to both TP and NA. In phase 2 the non-dominant ankle and hip joint moments were significantly lower in AR compared to NA and the knee and hip joint moments were lower in AR compared to TP. In phase 3 the hip joint moment was significantly lower in AR compared to TP. Significant differences in lower limb joint moments between phases within strategies can be found in Appendix D.

The overall CoM and the CoM of the torso, and pelvis do not differ substantially in TP compared to NA.

As expected, all NA upper limb joint moments in 9 participants were significantly smaller compared to AR joint moments, except for the joint moments in dominant shoulder flexion, dominant wrist extension, and non-dominant and dominant elbow flexion. Significant differences between TP and NA were found in dominant shoulder flexion ($p=0.04$), dominant and non-dominant shoulder internal rotation ($p=0.02$, $p=0.05$), dominant shoulder adduction ($p=0.03$), and dominant elbow extension ($p=0.03$), where all joint moments were higher in TP compared to NA (Table 5).

Table 4: Lower limb peak joint moments in three different techniques in elderly men. Peak joint moments are shown in Nm/kg.

	TP		AR		NA	
	(D)	(ND)	(D)	(ND)	(D)	(ND)
Hip	-1.03 ± 0.17[a]	-0.90 ± 0.09[a]	-0.58 ± 0.12[a]	-0.50± 0.19[a,b]	-0.92 ± 0.34	-0.92 ± 0.15[b]
Knee	-0.78 ± 0.22	-0.69 ± 0.09[a]	-0.63 ± 0.23[b]	-0.59±0.08[a]	-0.82 ± 0.2[b]	-0.72 ± 0.15
Ankle	-0.64 ± 0.15	-0.56 ± 0.09	-0.49 ± 0.22	-0.46 ± 0.19	-0.51 ± 0.18	-0.55 ± 0.11
Lumbar	1.74 ± 0.25[a,c]		1.25 ± 0.32[a,b]		2.0 ± 0.31[b,c]	

[a]: Significant difference between TP and AR.
[b]: Significant difference between AR and NA.
[c]: Significant difference between TP and NA.
Abbreviations: D=dominant, ND=non-dominant.

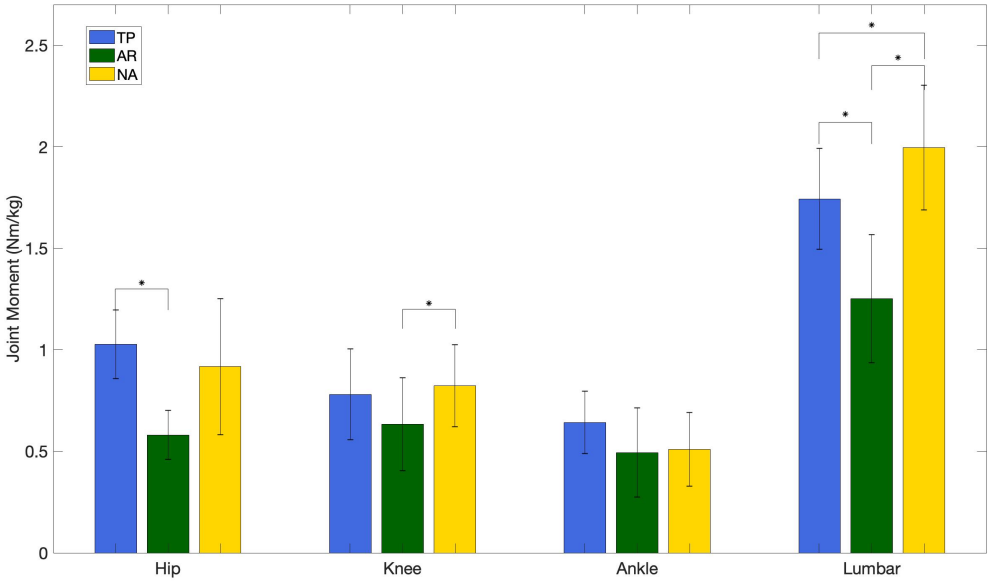

Figure 5: Peak lower limb joint moments of the dominant leg for the hip, knee and ankle in TP (blue), AR (green), and NA (yellow) with error bars representing one standard deviation.

AR upper limb joint moments were significantly larger in dominant and non-dominant shoulder external rotation ($p=0.02$, $p<0.01$), elbow extension ($p<0.001$, $p<0.001$), and wrist flexion ($p=0.04$, $p=0.02$) compared to TP. Also, dominant shoulder abduction ($p=0.04$) moment was higher in AR compared to TP.

There are no significant differences between the dominant and non-dominant lower and upper limb joint moments.

The joint reaction forces obtained without muscle force interaction did not give reasonable results with respect to magnitudes. It did show significant lower shoulder and elbow loading in TP compared to AR (shoulder: $p<0.01$, elbow: $p=0.01$). Also in the joint reaction force analysis including muscle forces, the non-dominant shoulder ($p<0.01$) and dominant and non-dominant elbow ($p=0.04$, $p<0.01$) loading were lower in TP compared to AR. The lower back loading was significantly lower in both AR and TP compared to NA ($p=0.001$, $p<0.01$).

All significant differences had large effect sizes ($\omega^2>0.14$) except for the dominant knee joint moment ($\omega^2=0.07$), non-dominant knee joint moment ($\omega^2=0.04$), dominant elbow joint moment ($\omega^2=0.07$) and the dominant shoulder flexion joint moment ($\omega^2=0.09$).

Table 5: Upper limb peak joint torques in three different STS techniques. Peak joint moments are shown in Nm/kg.

	TP		AR		NA	
	(D)	(ND)	(D)	(ND)	(D)	(ND)
Shoulder Flex	0.29 ± 0.16^{c}	0.31 ± 0.2	0.17 ± 0.08	0.22 ± 0.11	0.09 ± 0.06^{c}	0.09 ± 0.05
Shoulder Ext	-0.04 ± 0.02	-0.04 ± 0.02	-0.19 ± 0.14	-0.14 ± 0.08^{b}	-0.03 ± 0.03	-0.02 ± 0.03^{b}
Shoulder Exr	0.01 ± 0.01^{a}	0.01 ± 0.01^{a}	$0.1 \pm 0.05^{a,b}$	$0.10 \pm 0.04^{a,b}$	0.0 ± 0.01^{b}	0.0 ± 0.01^{b}
Shoulder Inr	-0.13 ± 0.07^{c}	-0.21 ± 0.13^{c}	-0.05 ± 0.02	-0.03 ± 0.01	-0.02 ± 0.01^{c}	-0.02 ± 0.01^{c}
Shoulder Abd	-0.04 ± 0.02^{a}	-0.07 ± 0.03	$-0.11 \pm 0.05^{a,b}$	-0.09 ± 0.02^{b}	-0.04 ± 0.03^{b}	-0.04 ± 0.03^{b}
Elbow Ext	$-0.01 \pm 0.02^{a,c}$	-0.03 ± 0.03^{a}	$-0.26 \pm 0.06^{a,b}$	$-0.26 \pm 0.04^{a,b}$	$0.01 \pm 0.01^{b,c}$	0.01 ± 0.01^{b}
Wrist Flex	0 ± 0^{a}	0 ± 0^{a}	$0.05 \pm 0.03^{a,b}$	$0.03 \pm 0.02^{a,b}$	0 ± 0^{b}	0 ± 0^{b}

[a]: Significant difference between TP and AR.
[b]: Significant difference between AR and NA.
[c]: Significant difference between TP and NA.
Abbreviations: Ext=extension, Flex=flexion, Exr=external rotation, Inr=internal rotation, Abd=abduction.

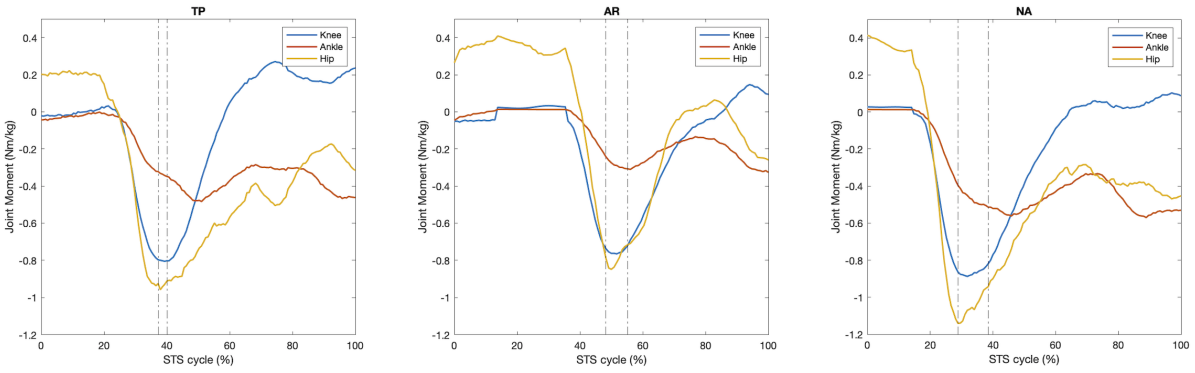

Figure 6: The hip, knee and ankle joint moments are plotted for every condition for one participant in one trial of each STS strategy. The dashed lines indicate the phases: the first dashed line indicated the seat-off (start phase 2) and the second dashed-line indicates the maximum dorsiflexion angle (start phase 3).

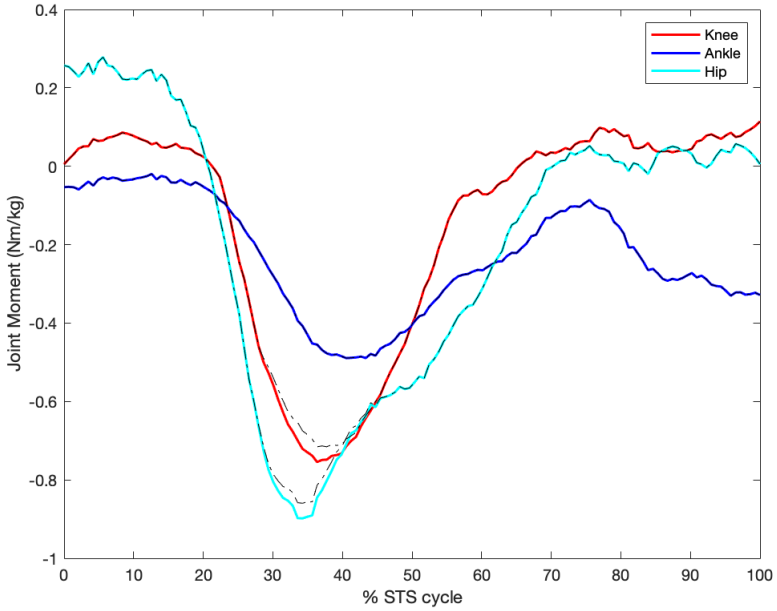

Figure 7: Comparison of the joint moments obtained from inverse dynamics to those obtained using static optimisation (dashed lines). The values derived from static optimisation match the inverse dynamic values across the entire STS cycle for the three joints examined.

3.3 Static Optimisation

In Figure 7 one trial is shown for the comparison between SO and ID results. The SO result of the hip and knee joint moments are lower, but this deviation is negligible. In the majority of the trials the SO result favorably matched the ID values across the entire STS cycle for the ankle, knee and hip joint.

In Table 6 the peak muscle forces per strategy are presented for the muscles with a considerable contribution (>0.1N/BW). Most significant differences in muscle forces were found between AR and NA (Figure 8). Muscles that exerted significantly lower forces in AR compared to NA are non-dominant soleus, vasti muscles, gluteus maximus, hamstring muscle group, and the quadriceps muscles. Also, the dominant gluteus maximus exerts lower force in AR compared to NA.

Significant lower muscle forces in AR compared to TP were found in non-dominant vasti muscles, non-dominant adductor magnus, non-dominant quadriceps muscle group and both semimembranosus, and gluteus maximus. The muscle force exerted by the dominant medial gastrocnemius is higher in TP compared to NA. No other significant differences were found between TP and NA.

Within phases the muscles that exert more force in TP compared to NA is the dominant medial gastrocnemius in phase 3 ($p<0.01$). Moreover, within phase 2 the dominant rectus femoris muscle force exerts significantly less force in TP compared to AR ($p<0.01$). Statistical differences between phases within the STS strategies can be found in Appendix E.

Interlimb muscle force difference was only significant for the medial gastrocnemius in AR ($p=0.04$).

The significant differences in muscle forces between strategies had large effect sizes (ω^2>0.14) except for the dominant gluteus maximus (ω^2=0.08), non-dominant soleus(ω^2=0.06), vastus intermedius(ω^2=0.02,) vastus lateralis (ω^2=0.12), vastus medialis (ω^2=0.06), and quadriceps femoris (ω^2=0.04).

Including all participants analysed in AR and NA, more muscle forces were significantly different between AR and NA (Appendix G).

SO results were compared to the EMG activation (Figure 9). The EMG signals do not favorably match the SO results. The SO gluteus maximus activation does not match the EMG activation in any of the trials. The SO vastus lateralis activation does match the on-off EMG activation. The SO activation of the soleus, medial gastrocnemius, tibialis anterior, biceps femoris long head and the gluteus medialis do partially match the EMG activation. Also, large differences between dominant and non-dominant leg are found in the EMG muscle activation patterns and not in the SO muscle activation patterns.

Table 6: Muscle forces with most contribution to the standing up movements in N/BW.

Muscle	TP		AR		NA	
	(D)	(ND)	(D)	(ND)	(D)	(ND)
BicFem (lh)	0.96 ± 0.51	0.89 ± 0.49	0.93 ± 0.48	0.65 ± 0.46	1.03 ± 0.49	0.86 ± 0.56
GasMed	0.3 ± 0.07[c]	0.3 ± 0.1	0.2 ± 0.09	0.23 ± 0.07	0.17 ± 0.05[c]	0.2 ± 0.05
RecFem	1.08 ± 0.72	0.9 ± 0.42	1.26 ± 0.69	0.89 ± 0.35	1.29 ± 0.7	0.92 ± 0.43
Semimem	0.4 ± 0.12[a]	0.34 ± 0.08[a]	0.18 ± 0.08[a]	0.17 ± 0.11[a]	0.25 ± 0.13	0.28 ± 0.11
Soleus	1.83 ± 0.74	1.51 ± 0.38	1.36 ± 0.67	1.21 ± 0.46[b]	1.71 ± 0.83	1.59 ± 0.34[b]
TibAnt	0.46 ± 0.28	0.3 ± 0.14	0.4 ± 0.21	0.33 ± 0.13	0.51 ± 0.23	0.36 ± 0.16
TibPost	0.56 ± 0.38	0.42 ± 0.18	0.56 ± 0.23	0.51 ± 0.22	0.68 ± 0.24	0.56 ± 0.22
VasInt	0.69 ± 0.35	0.62 ± 0.26[a]	0.53 ± 0.34	0.43 ± 0.25[a,b]	0.73 ± 0.32	0.63 ± 0.28[b]
VasLat	1.95 ± 0.45	2.06 ± 0.38[a]	1.67 ± 0.61	1.6 ± 0.53[a,b]	2.07 ± 0.43	2.03 ± 0.31[b]
VasMed	1.08 ± 0.43	1.06 ± 0.34[a]	0.88 ± 0.45	0.75 ± 0.36[a,b]	1.16 ± 0.37	1.07 ± 0.35[b]
Glmax	1.71 ± 0.46[a]	1.57 ± 0.4[a]	1.31 ± 0.45[a,b]	1.01 ± 0.37[a,b]	1.89 ± 0.7[b]	1.63 ± 0.35[b]
Glmed	0.49 ± 0.25	0.53 ± 0.25	0.36 ± 0.22	0.34 ± 0.18	0.38 ± 0.19	0.46 ± 0.21
AddMag	0.93 ± 0.71	0.72 ± 0.37[a]	0.68 ± 0.52	0.42 ± 0.24[a,b]	1.08 ± 0.77	0.79 ± 0.35[b]
Ham	1.09 ± 0.47	1.06 ± 0.44	0.99 ± 0.45	0.75 ± 0.39	1.18 ± 0.47	1.01 ± 0.51
Quad	4.59 ± 1.87	4.5 ± 1.32[a]	4.17 ± 1.94	3.54 ± 1.3 [a,b]	5.11 ± 1.42	4.63 ± 1.17[b]

[a]: Significant difference between TP and AR.
[b]: Significant difference between AR and NA.
[c]: Significant difference between TP and NA.
Abbreviations: BicFem (lh)=biceps femoris long head, GasMed=medial gastrocnemius, Semimem=semimembranosus, TibAnt=tibialisanterior, TibPost=tibialis posterior, VasInt=vastus intermedius, VasLat=vastus lateralis, VasMed=vastus medialis,Glmax=gluteus maximalis, Glmed=gluteus medialis, Ham=hamstring muscle group, Quad=quadriceps femoris muscle group.

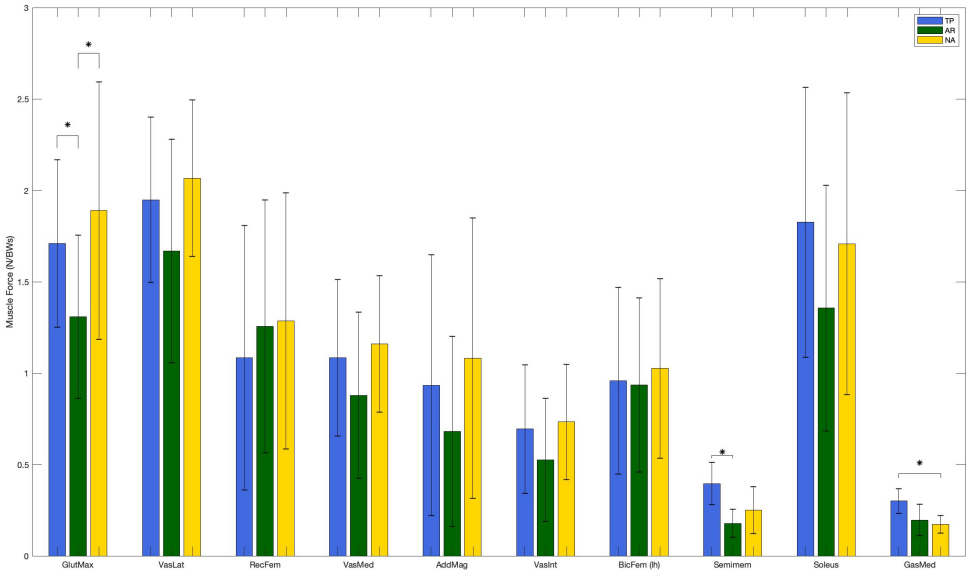

Figure 8: Peak lower limb muscle forces in N/BW of the dominant leg. The asterisk displays a significant difference between muscle force in TP (blue), AR (green), and NA (yellow).

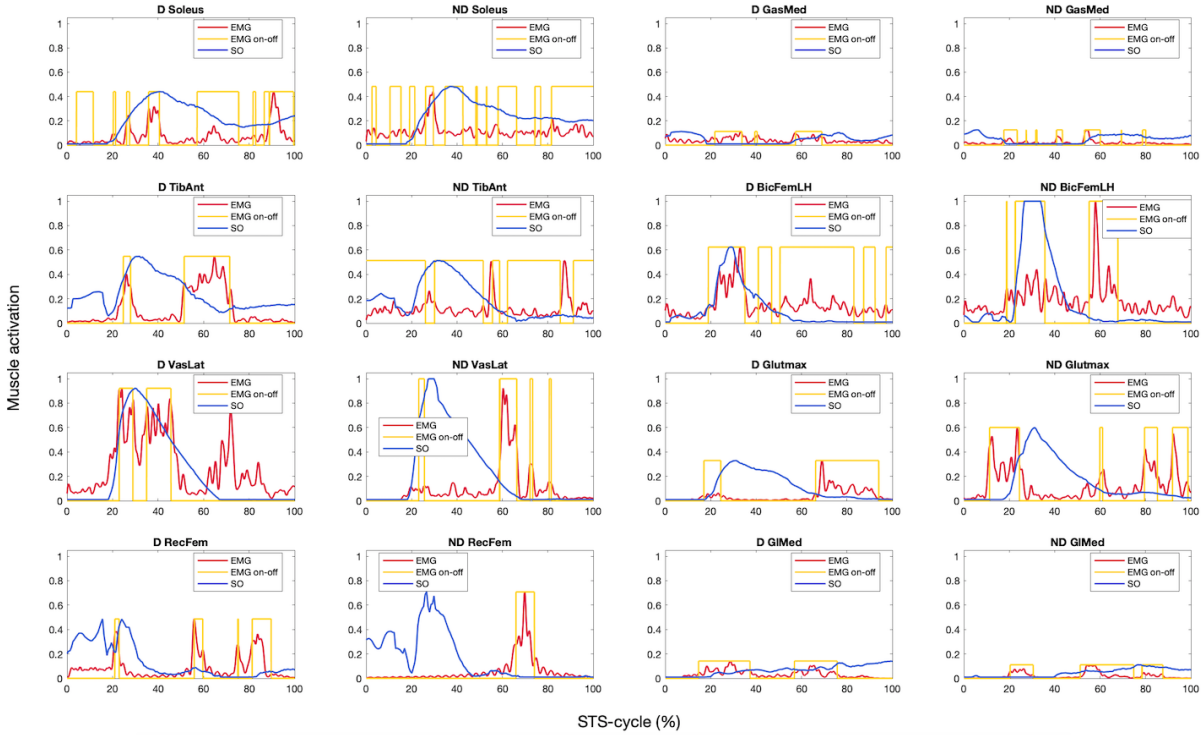

Figure 9: EMG activation patterns and SO muscle activation patterns (blue line) of one trial in NA. The EMG activation patterns are shown as the on-off signal derived with the Hilbert transform (yellow line), and as the linearly enveloped EMG signal (red line).

3.4 Force plates and force gloves

Peak GRFs of the non-dominant leg in AR are significantly lower compared to NA (p=0.02). No significant differences were found between dominant and non-dominant peak GRFs.

Table 7: The peak ground reaction force of each STS technique in N/BW for both the dominant and non-dominant leg.

	TP		AR		NA	
	D	ND	D	ND	D	ND
GRF (N/BW)	0.71±0.09	0.64±0.08	0.61±0.04	0.55±0.07[b]	0.64±0.09	0.62±0.07[b]

[b]: Significant difference between AR and NA.

The hand placement on the thighs in TP with respect to the hip and knee joint center has been determined on a scale from 0 to 100 percent, where 0 percent is at the hip joint center and 100 percent is at the knee joint center (Figure 10). The lowest peak force exerted on the hands is a participant who had placed their hands closest to the hip and the highest exerted peak force is exerted by a participant having the hands closest to the knee. However, the other participants do not show a relation between the position of the hand on the thigh and the amount of force exerted on the thighs. Moreover, there is no relation between the position of the hand and the rectus femoris muscle force or the lumbar extension moment. Rectus femoris is shown due to its significantly lower muscle force in TP compared to AR in phase 2. The other muscles are not shown, but there is no relation in the other lower limb muscles.

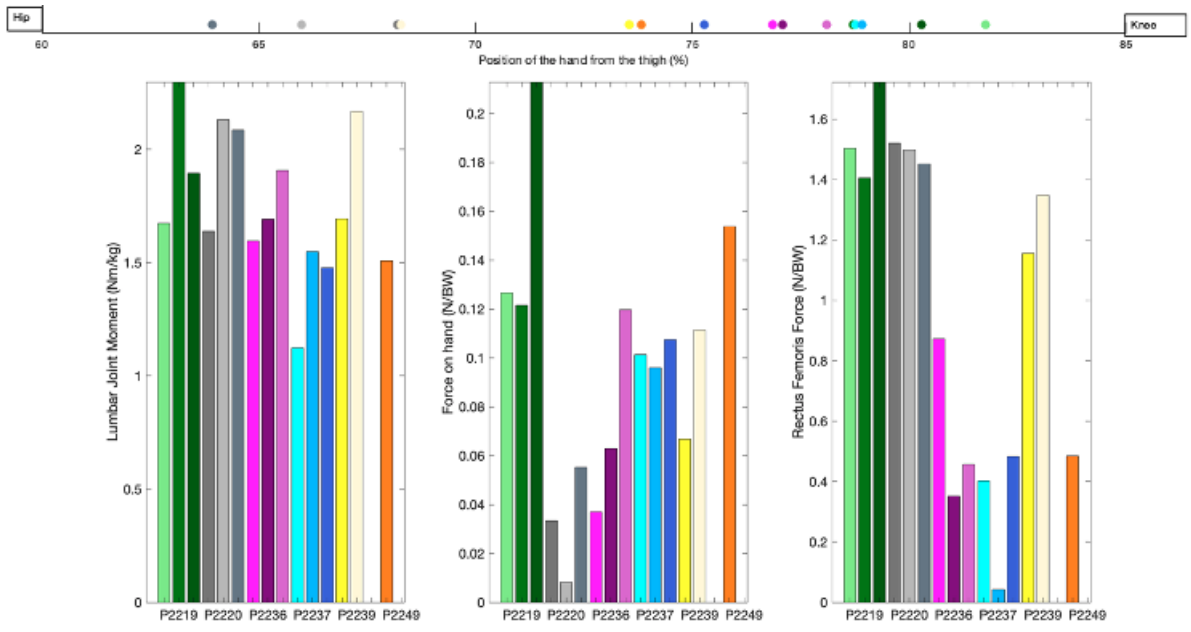

Figure 10: The lumbar joint moment, peak force measured by the force gloves and the rectus femoris muscle force for all TP trials. The forces and moments are shown in the bars and the position of the hand with respect to the thigh is shown on top. Zero percent is the hand placement at the hip joint center and 100 percent is at the knee joint center.

A relation exist between the sum of the force on the hands and the FES-I score (Figure 11). Participant P2237 has the highest FES-I score of 21 and also the highest sum of force on the hand. Participant P2249 has a score of 12 and has second largest sum on the hand. P2219 has a score of 8, which has slightly higher sum of force on the hands compared to the others with a FES-I score of 7. No relation between the peak force exerted on the armrests and the FES-I score was visible.

The armrest forces were measured for 9 participants, but for two participants the ML and AP component were lacking in one of the armrests, thus the results are calculated for 7 participants. The resultant force measured at the armrest in AR was calculated with and without the mediolateral (ML) component. The difference between the resultant force with and without ML component is very small (7.9e-04 N/BW). The vertical force is significantly different compared to the resultant force with ($p=0.048$, $\omega^2=0.07$). The peak ML component force is 11% of the peak resultant force, the peak AP component force is 32% of the peak resultant force, and the peak vertical component force is 97% of the peak resultant force. Onset of peak component forces showed no significant differences between components. The timing of the peak component forces and resultant force were in the same range as the peak upper limb joint moments.

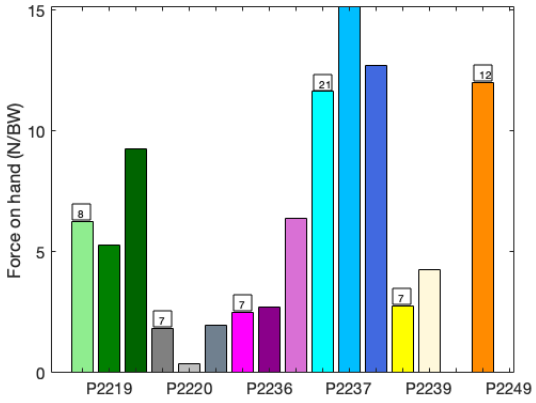

Figure 11: The sum of the force measured by the force gloves (N/BW). This is the force exerted on the hands by the thigh. FES-I scores are shown on top of the bars. The FES-I score is a score from 7-28, where 7 is no concern about falling at all and 28 is a severe concern about falling.

Table 8: Peak forces and the timing of peak forces (N/BW) of all components on the armrest in AR of the dominant side of 7 participants. Two participants were excluded from this analysis due to missing ML component.

	Resultant Force	Resultant Force no ML component	Vertical component	AP component	ML component
Peak Force (N/BW)	0.20±0.06[a]	0.20±0.05	0.20±0.06[a]	0.07±0.02	0.02±0.01
Timing (s)	0.61±0.14	0.62±0.16	0.61±0.14	0.76±0.14	0.54±0.1
Timing (%)	40.3±9.4	40.5±10.3	40.0±9.5	49.4±5.8	36.3±10.8

[a]: Significant difference between resultant force and vertical component.

4 Discussion

The purpose of this study was to find out why elderly people use a thigh push-off to stand up from a seated position. The prevalence of this strategy is high and to our knowledge the biomechanics were not known before this study had taken place. To be able to find out why elderly use this compensation strategy, the upper and lower limb joint moments and the lower limb muscle forces were determined for three different STS strategies. Clinicians suspect that TP might overload the lower back. However, we hypothesised a decreased joint moment in the lumbar joint, and hip joint moment compared to NA and a lower shoulder loading compared to AR. The results partially confirm our hypothesis; the lumbar extension joint moment is lower in TP compared to NA and the shoulder loading is lower in TP compared to AR.

To our knowledge this is the first study measuring the force on the hands, quantifying muscle forces and joint moments in TP. Also, we have included a force plate on the seat of the chair, which incorporates the interaction between the thigh and the seat. These aspects all together make the study unique.

4.1 Time to Stand

The TTS of NA are comparable to literature. TTS reported in literature measured in NA in an elderly cohort were 1.5s and 1.4s, where our TTS is 1.67s and without the oldest participant 1.46s [28; 29]. In the study of Smith et al. [30] the TTS was longer in NA compared to AR, but the difference was not significant. In our study TTS in NA was also longer compared to AR and no significance was found. To our knowledge TP had never been timed before, hence not comparable to literature.

4.2 Joint Moments in the Upper and Lower Limb

The lumbar joint moment is lower in TP compared to NA, which is in accordance with instrumented implant results. Orthoload [9] reported a decrease of the peak force load of 33% and in our study the lumbar extension moment is 13% lower. Instrumented implant data also showed a lower peak force in the hip in seven out of ten patients. This is not the case in the current participant group. In one out of six participants the dominant peak hip joint moment is lower and in four out of six the non-dominant peak hip joint moment is lower in TP compared to NA. Also, the shoulder and elbow loading was significantly lower in TP compared to AR. Shoulder external rotation, shoulder abduction, elbow extension, and wrist flexion showed significant lower joint moments in TP compared to AR.

Kinematic and dynamic results were comparable to literature. The STS movement has a lot of determinants that influence the dynamics, which makes it a complex and dynamic movement. Therefore in literature there are many different results. Yoshioka et al. [31] measured peak hip, knee, and ankle joint moments in a 2D model in a young cohort in NA (hip: 1 Nm/kg, knee: 0.9 Nm/kg and ankle: 0.5 Nm/kg). The joint moments are comparable to our results (hip:0.92 Nm/kg, knee:0.82 Nm/kg and ankle:0.51 Nm/kg). Mak et al. [28] measured hip joint moments around 0.91 Nm/kg, knee joint moments of 1.17 Nm/kg and ankle joint moments of 0.64 Nm/kg in a 2D model in NA for elderly people, which are higher in the knee and ankle joints compared to our results. The elderly participants included by Mak et al. [28] are younger compared to our participants and this might explain the higher knee and ankle joint moments.

Van der Kruk et al. estimated the joint moments in STW without instructions for the same

subjects measured in this thesis. Measured values of hip joint moment in the stance leg were between 0.6 and 1.4 Nm/kg, knee joint moment between 0.5 and 1 Nm/kg, and ankle joint moment between 0.4 and 0.8 Nm/kg in the phase from sit to swing. These values are in the same magnitude as the current study. Also, the hip joint moments were higher compared to the knee joint moments in the STW which is comparable to our results. These results are not determined using OpenSim hence independent from our results.

Scientific literature shows that the use of armrests resulted in lower joint moments in the hip and knee, and an increase in stability compared to no arm aid [32; 33; 34]. A lower hip and knee joint moment in AR in our study is in accordance with scientific literature. However, the increase in upper limb strain was not investigated in these studies. We have investigated the upper limb loading and difference between TP and AR are evident. Smith et al. [30] did analyse the joint reaction forces of the shoulder in AR, which was 2.06 times BW, where Anglin et al. [35] reported 1.8 times BW for elderly people. In this thesis the shoulder loading in AR was significantly higher compared to TP, but the joint reaction loads are not in the same magnitudes compared to literature.

The upper limb loading in TP had never been studied before, but our findings show higher shoulder internal rotation, and shoulder flexion joint moments compared to NA. Studying the kinematics of this strategy these are logical findings. Upperlimb kinematics can explain the dynamics in TP; due to a forward movement of the arms the shoulder flexion moment increases and the shoulder internal rotation moment is also caused by the forward motion of the arms.

The lumbar extension joint moment in TP is lower compared to NA, this could be a result of different muscle recruitment or a change in CoM. The overall CoM and the CoM of the torso, and pelvis do not differ substantially in TP compared to NA. The lower limb muscle recruitment was determined in this study and discussed below.

4.3 Muscle Forces and Activation

The muscle forces in TP have never been studied before and are therefore not comparable to literature. Hip extensor and flexor muscle forces were expected to be lower in TP compared to NA due to the hypothesis of lower hip joint moment. However, the hip joint moment was not lower and the muscle forces were not lower. The muscle recruitment in the lower limb did not differ significantly in TP compared to NA. In phase 2 the rectus femoris muscle force was lower in TP compared to AR, but this is also due to the fact that the hip joint moment was highest in phase 3 in TP and in phase 2 in AR.

As expected, the muscles in the lower limb exert less muscle force in AR compared to NA, but not significant for all muscles. In STS rectus femoris, gluteus maximus, soleus and vasti muscles have the highest contribution, which is comparable to literature [26; 30]. Gluteus maximus activation is smaller compared to vastus lateralis activation, which is the opposite in Caruthers et al. [26]. However, Yoskioka et al. [31] and Ellis et al. [36] estimated the gluteus maximus to be smaller compared to the quadriceps muscles, like our result. Maximal muscle forces in NA for quadriceps femoris, hamstrings and gastrocnemius found in literature were 5.29, 0.69 and 0.71 (times BW) compared to 5.11, 1.18 and 0.17 (times BW) in our study [26]. In AR muscle forces found in literature were 3.94, 1.59 and 0.58 (times BW) [36], while ours were 4.17, 0.99 and 0.20 (times BW). In literature gluteal muscles were greater contributors to hip extension than the hamstrings. However, in our study the hamstrings contributed more to the hip extension compared to the gluteal muscles. Our gastrocnemius muscle forces are lower compared to the

aforementioned studies, but the soleus in our study exerts more muscle force and this even leads to higher calf muscle forces. The reason for the higher soleus activity could be due to a higher ankle joint moment in our study and the unrestricted foot positioning. Soleus muscle force in literature is higher in elderly people in NA and AR compared to young adults [30]. Elderly people have lower quadriceps forces and higher activity in the hamstring and calf muscles compared to young adults in STS [30]. Caruthers et al. [26] and Ellis et al. [36] have measured healthy young individuals. Even though the quadriceps muscle forces are lower in NA in our results, we would have expected even lower muscle forces in the quadriceps in our study compared to the healthy young. This could be due to relatively strong elderly subjects. The hamstring and calf muscle forces are higher in the elderly men in our study compared to young cohort in literature in NA.

SO results do not completely match the EMG activation patterns. This could be due to badly placed EMG sensors, sitting on top of the EMG sensors leading to interaction with the chair, and/or not shaven the legs. The SO activation patterns do match the muscle activation patterns reported in STS movement in literature [26]. Thus the SO results are more reliable compared to the EMG activation, mainly due to large dominant and non-dominant leg differences in the EMG activation which would not be expected in these large quantities in the STS task.

4.4 Compensation for Movement Objectives

TP as a compensation strategy could be explained by two types of compensation: compensation for movement objectives (energy, stability, pain avoidance, and velocity) and compensation for capacity [5]. Based on the TTS of TP we can conclude velocity is not a movement objective TP is compensated for. Higher energy efficiency is not achieved by only a lower lumbar extension joint moment compared to NA. The longer TTS, equal lower limb joint moments, and higher upper limb joint moments compared to NA are in contrast with higher energy efficiency. The knee, hip and ankle joints are not significantly unloaded with respect to NA or AR, thus pain avoidance as an objective in these joints can be rejected. However, the lumbar extension moment is lower with respect to NA and lower back loading as a result of all loads acting on the model is also significantly lower. Therefore the possibility of using TP as a consequence of lower back pain is a reasonable explanation.

Another objective to compensate for is stability. Studying stability was beyond the scope of this thesis. Nevertheless, preliminary results of an ongoing research with a new method studying stability show an increase in stability in TP compared to NA. This method is based on the stability basin, which differentiates between less and more stable STS strategies for an individual [37]. Furthermore, a decrease in skeletal capacity results in an increase in fear of falling. An increase in fear of falling puts more emphasis on stability as a movement objective [6]. Elderly people and young adults that consistently choose TP to stand up in all trials have a significant higher FES-I score compared to the group standing up without arm aid [38]. This would imply that people use TP to be more stable. Also, in this thesis participants with a higher FES-I score exerted more force on the hands in TP.

Pain avoidance of the lower back could not be the only objective to stand up with TP, since the back loading in AR is even lower compared to TP. Upper limb loading should be taken into account as well. From literature it is known that AR is being used for more stability [33], but it is expected that TP also serves for more stability and for lower loading of the upper limb. The loading in the upper limb is lower in TP compared to AR and thus pain avoidance in the shoulder could explain TP.

4.5 Compensation for Capacity

A lack of muscular capacity can result in compensation strategies which we identify as compensation for capacity [5]. Besides the rectus femoris muscle force in phase 2, there was no significant lower muscle force calculated in TP compared to NA or AR. Therefore, TP as a compensation strategy could not be explained by compensation for capacity in the lower limb muscles. TP as a compensation strategy of NA could be explained as a consequence of compensation for capacity in the torso. The abdomen muscles are significantly reduced due to ageing [39]. Therefore SO should be performed with a model including the abdomen muscle activation to check for the abdomen muscle forces in TP, NA, and AR.

Capacity in the upper limb has been studied before. Although the capacity measures are hugely varying among studies due to differences in measurement setups and participant groups, the trend of a lower upper limb joint capacity in elderly is evident [40; 41; 42]. Decline in maximal joint moment in the shoulder is greater compared to the reduction in the elbow and wrist maximal joint moment [41]. The reason for this could be the more frequent use of elbow and wrist during activities of daily living. In healthy older individuals the decline in shoulder abduction and adduction are almost equal in literature [42]. Murgia et al. [42] measured an age related decline of 57% and 48% in elderly men in shoulder abduction and flexion respectively. External and internal rotation declined in elderly people with 16% and 30% respectively. Danneskiold et al. [40] found a decline in shoulder flexion and extension joint moment capacity of both 19% in elderly aged 70-79, which is less compared to Murgia et al. [42]. Elbow flexion joint moment capacity (29%) declines more rapidly compared to extension (23%), and the same effect is visible in wrist flexion (17%) and extension (9%) [41].

Although it is difficult to compare the capacity measured in literature with the task demand in this study due to the angle the capacity is measured in, the angular velocity and the participant group, some comparisons can be made. Wrist extension, elbow flexion, shoulder adduction, and shoulder abduction joint moments in both AR and TP strategies are relatively small compared to the joint moment capacity in literature. Age related decline in shoulder external rotation joint moment is greater compared to internal rotation. The joint moment capacity was already lower in external rotation in healthy young adults, this could be a reason to choose TP instead of AR, but only in combination with an other objective to compensate for. Otherwise one would choose NA over TP. Also, elbow extension declines with 23% in elderly people, and could result in TP as a compensation strategy instead of AR. In our capacity measures it can be seen that in AR the capacity limits are reached with respect to the elbow (Appendix F). However, it only serves as a relative percentage compared to the other strategies. The angle and velocity with which the capacity is measured is different compared to the velocity and angles of the STS movement. Shoulder and elbow loading are significantly lower in TP compared to AR, but due to the different magnitudes this has to be further investigated.

4.6 Limitations

Residual actuators have to be applied to correct for dynamic inconsistency between the estimated model accelerations and the measured GRFs. Marker measurement error, inconsistency in the scaled model, and inertial parameters can cause these inconsistencies [24]. Residual forces and moments have to be checked to make sure these are reasonable. Residual forces and moments were larger (50N and 170Nm) than the OpenSim threshold values (25N and 75Nm). Our residuals are more comparable to literature (75N and 100Nm) [26]. The residuals reported in

literature are measured with the arms crossed in front of the body with the upper limb joints locked during the simulations. We have had full movement in the upper limb, therefore our residual moments are higher. Caruthers et al [26] expected that the lack of interaction between the seat and the thighs to be a reason of the large residuals. However, we included a force plate on the seat and this did not lower the residuals. The seat force plate did not have a large influence on our results. The OpenSim threshold values for the residuals were determined using gait, which is a completely different movement from STS. The models used to establish the threshold values did not have arms and multiple DoF like our model [24]. To validate that our results did not rely on the residual actuators we checked the SO and ID calculated joint moments (Appendix C: Eqn 2,11,4,12, 6,and 13) and this illustrated that our muscle forces are consistent with the joint moment determined with the GRFs (Figure7).

Secondly, the model used in this thesis was limited. It was validated for high knee and hip flexion movements, but not specifically for the STS movement. The current model lacks flexibility in the spine, as a result of just one joint in the back of our model. A model validated for the STS movement and including lumbar joints was developed in OpenSim 3, but could not be used in OpenSim 4 and was therefore not used [26]. However, the results of the validated STS model and the results in this thesis were comparable [26]. This thesis was supposed to include an upper limb muscle analysis, but there was no full body model available including both arms with muscles, including the lower limb. Developing a model ourselves ended up being outside the scope of this study and therefore a model including a torque actuated upper limb was used.

Lastly, the force plate data was a limitation in this thesis. The armrest data of two participant lacked the ML component. To our knowledge this was the first study measuring the force in three directions. The difference between the peak resultant force with and without ML component is only 7.9e-04N/BW and is not significant. Therefore the results would probably not have been different without missing the ML component of two participants, thus it is not necessary to measure the ML component. Also, participants had to be excluded due to unreliable or missing force plate data. This caused a small participant group for this thesis. As a result TP kinetic data was available of only 6 participants, which is considered a small sample size. Some differences between AR and NA were not significant for six participants, but were significant when including 9 participants, this shows the relevance of increasing the sample size. However, it was in line with other simulation-based studies [26; 43]. Since fifty participants had completed the experiments, we have the possibility to include more participants in our simulations in future research.

4.7 Recommendations

In future research we will use or develop a model with all lumbar joints to increase flexibility in the spine and a muscle actuated upper limb, and torso to be able to do a full body muscle force analysis in all three STS strategies. Upper limb and back muscle force analysis can complement to the research whether TP is also used as compensation for muscular capacity. Furthermore the reason for the lower lumbar extension joint moment in TP compared to NA can be analysed with the muscle actuated torso.

Furthermore, it is recommended to include all participants and investigate a relation between muscle force, position of hand placement on the thigh (moment arm), and external force on the hand. We would have expected a relationship between these variables. Nevertheless, there was no relation visible at all except for the FES-I score. Also, the prevalence of TP is over 50% in elderly people in STW trials [8]. Therefore the biomechanics of TP in the STW trials should be

analysed in future research.

Lastly, our initial simulations were done before adjusting the maximal isometric force. The optimisation criterion which was used is activation based. A high maximum isometric force leads to a lower cost on the cost function compared to a lower maximum isometric force. At first an analysis was done by only decreasing the vastus lateralis muscle force, resulting in a muscle force decrease from approximately 3300N to 1300N. The rectus femoris, vastus lateralis and vastus medialis muscle force increased. However, when also decreasing these muscles the vastus lateralis increased again, thus the muscle activation is very sensitive for their peak isometric force. Due to the sensitivity to peak isometric forces, it is recommended to do a sensitivity analysis. Also in the to be developed models.

5 Conclusion

- The lumbar extension joint moment is lower in TP compared to NA, but higher compared to AR. Furthermore, shoulder and elbow loading are lower in TP compared to AR.
- AR upper limb joint moments were significantly larger in shoulder external rotation, elbow extension, and wrist flexion compared to TP. Also, dominant shoulder abduction moment was higher in AR compared to TP.
- Lower limb muscle forces were not significantly lower in TP compared to NA. Therefore, compensation for muscular capacity in the lower limb is not the reason for standing up with TP.
- We can conclude that TP is not used to lower energy usage, or to increase velocity.
- It is likely that stability and pain avoidance are movement objectives on which TP is based.
- We suggest that TP is used to unload the lower back to reduce pain or to compensate for age-related decline in abdominal muscle force, but this could also be accomplished with AR. However, AR upper limb loading is higher compared to TP. TP is used to unload the back and upper limb joints.
- We would advise elderly people with a lack of stability, skeletal capacity, and/or low capacity in the upper limb to stand up using TP. Also, when no armrests are available and pain in the lower back is present, TP would be advised.

References

[1] C. Statline, "Bevolking; geslacht, leeftijd en burgerlijke staat, 1 januari," *Laatst bewerkt op*, vol. 17, 2018.

[2] UnitedNations, "Ageing," *https://www.un.org/en/sections/issues-depth/ageing/*, 2019.

[3] A. Clegg, J. Young, S. Iliffe, M. O. Rikkert, and K. Rockwood, "Frailty in elderly people," *The lancet*, vol. 381, no. 9868, pp. 752–762, 2013.

[4] A. S. I. D. W. M. . I. L. Resnik, L, "Perspectives on use of mobility aids in a diverse population of seniors: Implications for intervention." *Disability and Health Journal*, pp. 77–85, 2009.

[5] E. van der Kruk, A. K. Silverman, L. Koizia, P. Reilly, M. Fertleman, and A. M. Bull, "Age-related compensation: Neuromusculoskeletal capacity, reserve movement objectives." 2021.

[6] E. van der Kruk, A. K. Silverman, P. Reilly, and A. M. Bull, "Compensation due to age-related decline in sit-to-stand and sit-to-walk." 2021.

[7] E. van der Kruk and A. M. Bull, "Rising from a seated position: future directions for an ageing population," 2021.

[8] D.-S. Komaris, C. Govind, A. Murphy, A. Ewen, and P. Riches, "Identification of movement strategies during the sit-to-walk movement in patients with knee osteoarthritis," *Journal of applied biomechanics*, vol. 34, no. 2, pp. 96–103, 2018.

[9] Orthoload, "Loading of orthopeadic implants." [Online]. Available: https://orthoload.com/

[10] D. B. Rolfson, S. R. Majumdar, R. T. Tsuyuki, A. Tahir, and K. Rockwood, "Validity and reliability of the edmonton frail scale," *Age and ageing*, vol. 35, no. 5, pp. 526–529, 2006.

[11] G. I. Kempen, L. Yardley, J. C. Van Haastregt, G. R. Zijlstra, N. Beyer, K. Hauer, and C. Todd, "The short fes-i: a shortened version of the falls efficacy scale-international to assess fear of falling," *Age and ageing*, vol. 37, no. 1, pp. 45–50, 2008.

[12] R. C. Oldfield *et al.*, "The assessment and analysis of handedness: the edinburgh inventory," *Neuropsychologia*, vol. 9, no. 1, pp. 97–113, 1971.

[13] A. Electronics, "Load cell - 50kg, disc (tas606)." [Online]. Available: https://www.antratek.nl/load-cell-200kg-disc-tas606-3691

[14] W. Rose, "Electromyogram analysis. mathematics and signal processing for biomechanics," 2014.

[15] H. Sedghamiz, "Automatic activity detection in noisy signals with hilbert transfrom," Copy right April 2013, Edited March 2014.

[16] A. Seth, J. L. Hicks, T. K. Uchida, A. Habib, C. L. Dembia, J. J. Dunne, C. F. Ong, M. S. DeMers, A. Rajagopal, M. Millard *et al.*, "Opensim: Simulating musculoskeletal dynamics and neuromuscular control to study human and animal movement," *PLoS computational biology*, vol. 14, no. 7, p. e1006223, 2018.

[17] S. L. Delp, F. C. Anderson, A. S. Arnold, P. Loan, A. Habib, C. T. John, E. Guendelman, and D. G. Thelen, "Opensim: open-source software to create and analyze dynamic simulations of movement," *IEEE transactions on biomedical engineering*, vol. 54, no. 11, pp. 1940–1950, 2007.

[18] A. K. Lai, A. S. Arnold, and J. M. Wakeling, "Why are antagonist muscles co-activated in my simulation? a musculoskeletal model for analysing human locomotor tasks," *Annals of biomedical engineering*, vol. 45, no. 12, pp. 2762–2774, 2017.

[19] A. Rajagopal, C. L. Dembia, M. S. DeMers, D. D. Delp, J. L. Hicks, and S. L. Delp, "Full-body musculoskeletal model for muscle-driven simulation of human gait," *IEEE transactions on biomedical engineering*, vol. 63, no. 10, pp. 2068–2079, 2016.

[20] S. R. Ward, C. M. Eng, L. H. Smallwood, and R. L. Lieber, "Are current measurements of lower extremity muscle architecture accurate?" *Clinical orthopaedics and related research*, vol. 467, no. 4, pp. 1074–1082, 2009.

[21] G. G. Handsfield, C. H. Meyer, J. M. Hart, M. F. Abel, and S. S. Blemker, "Relationships of 35 lower limb muscles to height and body mass quantified using mri," *Journal of biomechanics*, vol. 47, no. 3, pp. 631–638, 2014.

[22] E. M. Arnold, S. R. Ward, R. L. Lieber, and S. L. Delp, "A model of the lower limb for analysis of human movement," *Annals of biomedical engineering*, vol. 38, no. 2, pp. 269–279, 2010.

[23] J. Walker, D. Sue, N. Miles-Elkousy, G. Ford, and H. Trevelyan, "Active mobility of the extremities in older subjects," *Physical therapy*, vol. 64, no. 6, pp. 919–923, 1984.

[24] H. J, "Simulation with opensim - best practices."

[25] S. R. Hamner, A. Seth, and S. L. Delp, "Muscle contributions to propulsion and support during running," *Journal of biomechanics*, vol. 43, no. 14, pp. 2709–2716, 2010.

[26] E. J. Caruthers, J. A. Thompson, A. M. Chaudhari, L. C. Schmitt, T. M. Best, K. R. Saul, and R. A. Siston, "Muscle forces and their contributions to vertical and horizontal acceleration of the center of mass during sit-to-stand transfer in young, healthy adults," *Journal of applied biomechanics*, vol. 32, no. 5, pp. 487–503, 2016.

[27] S. Olejnik and J. Algina, "Generalized eta and omega squared statistics: measures of effect size for some common research designs." *Psychological methods*, vol. 8, no. 4, p. 434, 2003.

[28] M. K. Mak, O. Levin, J. Mizrahi, and C. W. Hui-Chan, "Joint torques during sit-to-stand in healthy subjects and people with parkinson's disease," *Clinical Biomechanics*, vol. 18, no. 3, pp. 197–206, 2003.

[29] P. Manckoundia, F. Mourey, P. Pfitzenmeyer, and C. Papaxanthis, "Comparison of motor strategies in sit-to-stand and back-to-sit motions between healthy and alzheimer's disease elderly subjects," *Neuroscience*, vol. 137, no. 2, pp. 385–392, 2006.

[30] S. Smith, "Quantifying musculoskeletal reserve in the elderly," 2017.

[31] S. Yoshioka, A. Nagano, D. C. Hay, and S. Fukashiro, "Peak hip and knee joint moments during a sit-to-stand movement are invariant to the change of seat height within the range of low to normal seat height," *Biomedical engineering online*, vol. 13, no. 1, pp. 1–13, 2014.

[32] S. J. Lee, R. Mehta-Desai, K. Oh, J. Sanford, and B. I. Prilutsky, "Effects of bilateral swing-away grab bars on the biomechanics of stand-to-sit and sit-to-stand toilet transfers," *Disability and Rehabilitation: Assistive Technology*, vol. 14, no. 3, pp. 292–300, 2019.

[33] U. P. ARBORELIUS, P. Wretenberg, and F. LINDBERG, "The effects of armrests and high seat heights on lower-limb joint load and muscular activity during sitting and rising," *Ergonomics*, vol. 35, no. 11, pp. 1377–1391, 1992.

[34] R. G. Burdett, R. Habasevich, J. Pisciotta, and S. R. Simon, "Biomechanical comparison of rising from two types of chairs," *Physical Therapy*, vol. 65, no. 8, pp. 1177–1183, 1985.

[35] C. Anglin, U. Wyss, and D. Pichora, "Glenohumeral contact forces," *Proceedings of the Institution of Mechanical Engineers, Part H: Journal of Engineering in Medicine*, vol. 214, no. 6, pp. 637–644, 2000.

[36] M. Ellis, B. Seedhom, and V. Wright, "Forces in the knee joint whilst rising from a seated position," *Journal of biomedical engineering*, vol. 6, no. 2, pp. 113–120, 1984.

[37] V. Shia, T. Y. Moore, P. Holmes, R. Bajcsy, and R. Vasudevan, "Stability basin estimates fall risk from observed kinematics, demonstrated on the sit-to-stand task," *Journal of biomechanics*, vol. 72, pp. 37–45, 2018.

[38] E. van der Kruk, L. Koizia, P. Reilly, M. Fertleman, and A. M. Bull, "Why do older adults move in a different way than young adults while standing up?, manuscript in submission," 2021.

[39] T. Abe, M. Sakamaki, T. Yasuda, M. G. Bemben, M. Kondo, Y. Kawakami, and T. Fukunaga, "Age-related, site-specific muscle loss in 1507 japanese men and women aged 20 to 95 years," *Journal of sports science & medicine*, vol. 10, no. 1, p. 145, 2011.

[40] B. Danneskiold-Samsøe, E. Bartels, P. Bülow, H. Lund, A. Stockmarr, C. Holm, I. Wätjen, M. Appleyard, and H. Bliddal, "Isokinetic and isometric muscle strength in a healthy population with special reference to age and gender," *Acta physiologica*, vol. 197, pp. 1–68, 2009.

[41] T. Harbo, J. Brincks, and H. Andersen, "Maximal isokinetic and isometric muscle strength of major muscle groups related to age, body mass, height, and sex in 178 healthy subjects," *European journal of applied physiology*, vol. 112, no. 1, pp. 267–275, 2012.

[42] A. Murgia, T. Hortobágyi, A. Wijnen, L. Bruin, R. Diercks, and R. Dekker, "Effects of age and sex on shoulder biomechanics and relative effort during functional tasks," *Journal of biomechanics*, vol. 81, pp. 132–139, 2018.

[43] M. M. van der Krogt, S. L. Delp, and M. H. Schwartz, "How robust is human gait to muscle weakness?" *Gait & posture*, vol. 36, no. 1, pp. 113–119, 2012.

Appendices

Appendix A. EMG and Marker Positions

Table 9: Anatomical locations of reflective markers. Total number of markers = 84

Segment	Markers	Nr.	Anatomical location
Thorax	C7	1	7th cervical vertebra
	T8	2	8th thoracic vertebra
	IJ	3	Sternum jugular notch
	MA	4	Sternum manubrium
	PX	5	Sternum xiphoid process
Pelvis	RASIS	6	Right anterior superior iliac spine
	LASIS	7	Left anterior superior iliac spine
	RPSIS	8	Right posterior superior iliac spine
	LPSIS	9	Left posterior superior iliac spine
	P1,P2,P3	10	Cluster of three markers placed on the pelvis
Clavicle	LA	11	Left Acromioclavicular joint
	RA	12	Right Acromioclavicular joint
	SC	13	Sternoclavicular joint
Scapula	S1,S2,S3	14	Scapula trackers (3 markers) placed on both scapula spines
Humerus	HU1,HU2,HU3,HU4	15	Cluster of four markers placed on the upper arm
	LE	16	Lateral epicondyle
	ME	17	Medial epicondyle
Forearm	U1,U2,U3,U4	18	Cluster of four markers placed on the forearm
	US	19	Ulnar styloid
	RS	20	Radial styloid
Hand	H1,H2,H3	21	Cluster of three markers placed on the back of the hand
Foot	FM2	22	Head of the second metatarsal
	FCC	23	Calcaneus
	FMT	24	Tuberosity of the fifth metatarsal
	TF	25	Additional marker placed on the foot
	FAM	26	Apex of the lateral malleolus
	TAM	27	Apex of the medial malleolus
Shank	C1,C2,C3,C4	28	Cluster of four markers placed on the calf segment
Knee	FLE	29	Lateral femoral epicondyle
	FME	30	Medial femoral epicondyle
Thigh	T1,T2,T3, T4	31	Cluster of four markers placed on the thigh segment

Table 10: EMG sensors placed on the muscles of each participant.

Sensor nr.	Abb.	Muscle
Left		
1	SOL_L	Left Soleus
2	GAS_L	Left Medial Gastrocnemius
3	TA_L	Left Tibialis anterior
4	HAM_L	Left Biceps femoris long head
9	VAS_L	Left Vastus Lateralis
10	GLU_L	Left Gluteus maximus
11	RF_L	Left Rectus Femoris
12	HAB_L	Left Gluteus Medius
Right		
5	SOL_R	Right Soleus
6	GAS_R	Right Medial Gastrocnemius
7	TA_R	Right Tibialis anterior
8	HAM_R	Right Biceps femoris long head
13	VAS_R	Right Vastus Lateralis
14	GLU_R	Right Gluteus maximus
15	RF_R	Right Rectus Femoris
16	HAB_R	Right Gluteus Medius

Appendix B. Capacity Measures

Task Measures

a. Timed-up-and-Go
Before the STS and STW movements were measured a timed-up-and-go (TUG) test was performed. This was done using a normal chair without armrests and the participant had to stand up, walk 3 meters towards an object, go around it and return seated on the chair. Participants were timed and recorded with a normal camera.

b. Sit-to-walk After the TUG test, participants were instrumented with markers (Table 9) and 16 electromyography (EMG) sensors, to be able to track the full body motion and activity of the lower limb muscles. The EMG sensors were placed on muscle groups (Table 10) according to European guidelines to be able to track the activity of these muscles. The seat height was adjusted to knee height approximately. Before the different conditions were measured a static and dynamic trial was recorded. The first trials were sit-to-walk (STW) trials at a self selected speed and strategy. Participants had to rise from the instrumented chair and walk to an object 3 meters away from the chair, touch the object and return to the seat. The second condition was the same as the first but now as fast as possible. No instructions, except for speed in the second condition, were given in the first two conditions and both were performed five times.

c. Sit-to-stand In the second part, three different arm strategies were tested in STS: standing up with the use of armrests (AR), with the use of a thigh/knee push-off (TP) and without using the arms (NA). All three conditions were performed three times and standing up with the use of

a thigh push-off was followed by twice performing STW with a thigh push-off. All participants were able to execute all the tasks. Participants were equipped with self-made force gloves during the TP technique to be able to measure the reaction force of the thigh.

Capacity Measures

a. Isokinetic strength measures
To determine maximum peak isokinetic joint moment strength measurements were done on the Cybex Humac CSMI dynamometer for the dominant and nondominant side. The measurements were done for the hip, ankle, knee and elbow joints for flexion and extension at two angular velocities (60°/s and 90°/s). During the measurements parts of the body were secured to make sure the strength was performed by the measured joint. The joint was in line with the axis of the apparatus. Hip flexion and extension was measured in supine position from 90° flexion to 0° and back to 90° flexion with the contralateral leg with 0° hip flexion and 90° knee flexion. Knee flexion and extension was measured in sitting position from 90° flexion to 5°, to prevent overextension. Ankle dorsi- and plantarflexion was measured in supine position from 5° dorsiflexion to 5° plantarflexion with the ipsilateral hip and knee slightly bent. The elbow joint was measured from 0° to 90° flexion in supine position. Every new condition started with one test trial followed by three repetitions per condition. The maximum peak isokinetic joint moment was determined of the three repetitions for each condition. The joint moments were corrected for bodyweight (BW).

b. Handgrip strength(HGS)
Handgrip strength was measured with a Jamar hand-held dynamometer. It has been proven that handgrip strength is a useful tool for prediction of movement limitations. Strength was measured on the dominant and nondominant hand in a sitting position with feet of the ground. Participants were encouraged by the investigators to squeeze the dynamometer as hard as possible. Three trials were conducted on each side and the highest value was taken as the maximum hand grip strength on each side.

c. Balance
Balance was measured while standing on one force plate on the ground. Participants were asked to stand as still as possible for 30 seconds or until they lost their balance. A second time participants had to close their eyes and do the same for 30 seconds. The feet were close together such that the medial malleoli were (almost) touching and their arms were crossed in front of their chest. Both trials were recorded with the Vicon Motion Capture system.

d. Proprioception
Participants were seated on a bench with both legs not touching the ground. Knees and hips were bend approximately 90°. Participants were asked to lift their left or right foot until full knee extension until the researcher told them to stop. The knee was flexed with an angle between 0° and 90° flexion and the participant was asked to keep this position for approximately 5 seconds. Then the participant was asked to release the angle and let the foot hang freely. Then the participant was asked to replicate the previous test angle. The angles were randomly chosen by the researcher. The contralateral leg hung freely. After ten times, the participant had to switch leg. This was recorded with the Vicon Motion Capture system.

e. Join Range of Motion (JROM)
Joint ranges of motion were measured for the hip and ankle joint on the Cybex Humac CSMI dynamometer. Hip measurements were in supine position and participants were asked to pull their leg towards their chest with the help of their arms. The contralateral leg had a fully extended hip and a 90° flexed knee. Ankle measurements were also in supine position, comparable to the isokinetic strength measurement position. The researcher moved their ankle in maximum dorsi- and plantarflexion until the participant indicated they reached their limit.

f. Nerve Conduction Study (NCS)
To study the electrical activity in the nerves a nerve conduction study was conducted. Slight electrical pulses were given to the nerve to estimate the velocity of the nerves and to estimate the maximum excitation of the muscle. The peroneal, tibial and median nerve are stimulated at both sides of the bodies. Muscle responses were measured using electrodes on the skin at the abductor digiti minimi muscle, the gastrocnemius muscle and the thenar muscle respectively. The current increased until the plateau phase occurred and the current was multiplied by 1.2, at this current three pulses were given directly after one another to be sure the plateau phase was reached and the H-reflex had disappeared. At this intensity the nerve was stimulated every second to find ten F-waves.

Appendix C. Inverse Dynamics and Static Optimisation Equations

Foot

$$\sum F_f = F_a + F_g + F_{grf} = m_f \cdot a_f \tag{1}$$

$$\sum M_f = M_a + M_{F,a} = \frac{d}{dt}\left(I_f \cdot \omega_f\right) \tag{2}$$

Where F_{grf} is the ground reaction force acting at the center of pressure (COP) of the foot. F_g is the gravitational force acting on the center of mass (COM) of this segment and F_a is the force acting in the ankle joint center. The sum of the forces should add up to the acceleration of the COM of the ankle, $m_f \cdot a_f$. M_a is the moment in the ankle joint, $M_{F,a}$ is the moment comprised by the ankle joint force ($M_{F,a}$=$r_{a,g}F_a$), where $r_{a,g}$ is the moment arm from COM of the foot to the ankle joint center. The sum of the moments in the foot should add up to the change in angular momentum of the foot around the COM, where ω_f is the angular velocity and I is the moment of inertia.

Shank

$$\sum F_s = -F_a + F_k + F_g = m_s \cdot a_s \tag{3}$$

$$\sum M_s = -M_a + M_k + M_{Fa,s} + M_{Fk,s} = \left(\frac{d}{dt} I_s \cdot \omega_s\right) \tag{4}$$

Where F_k is the force acting in the knee joint, F_a is the opposite of the force acting in the ankle joint, F_g is the gravitational force acting on the shank. The sum of the forces should equal the acceleration of the COM of the knee, $m_s \cdot a_s$. M_a is the opposite to the ankle moment, M_k is the moment acting in the knee joint, $M_{Fa,\,s}$ and $M_{Fk,\,s}$ are the moments induced by the forces in the ankle and knee joints respectively, with their moment arms running from ankle joint center to COM of the shank and from knee joint center to COM of the shank. The moments add up to the angular momentum of the COM of the shank.

Thigh

$$\sum F_t = -F_k + F_h + F_g = m_t \cdot a_t \tag{5}$$

$$\sum M_t = -M_k + M_h + M_{Fk,t} + M_{Fh,t} = \frac{d}{dt}\left(I_t \cdot \omega_t\right) \tag{6}$$

Where F_k is the force acting in the knee joint (opposite to the force in the shank), F_h is the force acting in the hip joint, F_g is the gravitational force acting on the thigh. The sum of the forces should equal the acceleration of the COM of the hip. M_k is the opposite to the knee moment, M_h is the moment acting in the hip joint, $M_{F\,k,\,t}$ and $M_{F\,h,\,t}$ are the moments induced by the forces in the knee and hip joints respectively, with their moment arms running from knee joint center to COM of the thigh and from hip joint center to COM of the thigh. The moments add up to the angular momentum of the COM of the thigh.

Pelvis

$$\sum F_p = -F_H^l - F_H^r + F_L + F_g = m_p \cdot a_p \tag{7}$$

$$\sum M_p = -M_H^l - M_H^r - M_{Fh,p}^l - M_{Fh,p}^r + M_L + M_{Fl,p} = \frac{d}{dt}\left(I_p \cdot \omega_p\right) \tag{8}$$

Where F_H is the force acting in the hip joint on the left and right side, F_L is the force acting at the lumbar joint, F_g is the gravitational force acting in the COM of the pelvis. The sum of the forces should add up to the acceleration of the COM of the pelvis. $M_H{}^l$ and $M_H{}^r$ are

the moments opposite of the hip moments, $M_{F\ h,\ p}$ and $M_{F\ l,\ p}$ are the moments induced by the forces in the hip and lumbar joints respectively, with their moment arms running from hip joint center to COM of the pelvis and from lumbar joint center to COM of the pelvis. The moments add up to the angular momentum of the COM of the pelvis.

Head, Arms, Torso

$$\sum F_{hat} = -F_L + F_g = m_{hat} \cdot a_{hat} \tag{9}$$

$$\sum M_{hat} = -M_L - M_{Fl,hat} = \frac{d}{dt} \left(I_{hat} \cdot \omega_{hat} \right) \tag{10}$$

Where F_L is the force acting in the lumbar joint, F_g is the gravitational force of this segment. This should be equal to the acceleration of the COM of the head,arms, and torso. M_L is the moment opposite of the lumbar moment, $M_{F\ l,\ hat}$ is the moment induced by the forces in the lumbar joints respectively, with their moment arms running from lumbar joint center to COM of the HAT. The moments add up to the angular momentum of the COM of HAT.

Ankle

$$M_{ankle} = F_{pf} \cdot r_{pf} - F_{df} \cdot r_{df} \tag{11}$$

Where F_{pf} and F_{df} is the force produced by the plantar and dorsi flexors and r_{pf} and r_{df} are the moment arms of the muscle to the ankle joint center.

Knee

$$M_{knee} = F_{kf} \cdot r_{kf} - F_{ke} \cdot r_{ke} \tag{12}$$

Where F_{kf} and F_{ke} is the force produced by the knee flexors and knee extensors respectively, and r_{kf} and r_{ke} are the moment arms of the muscle respective to the knee joint center.

Hip

$$M_{hip} = F_{kf} \cdot r_{kf} - F_{ke} \cdot r_{ke} \tag{13}$$

Where F_{hf} and F_{he} is the force produced by the hip flexors and hip extensors respectively, and r_{hf} and r_{he} are the moment arms of the muscle respective to the hip joint center.

Appendix D. Joint Moments in Phases

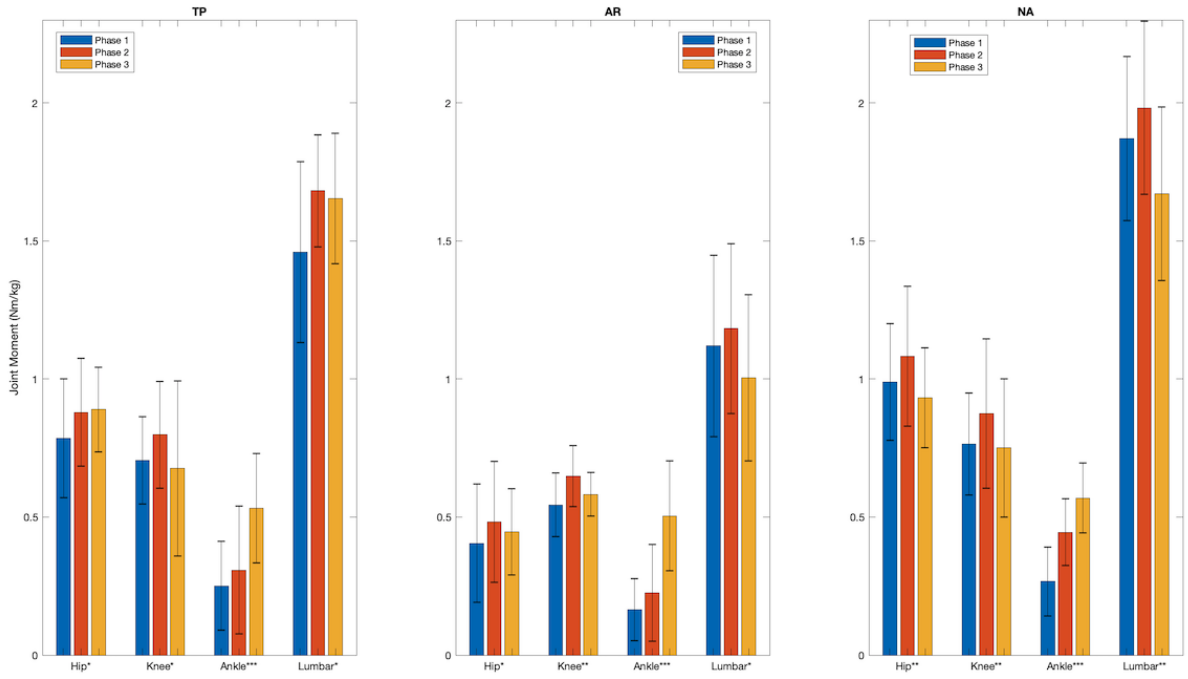

Figure 12: Joint moments in Nm/kg of all techniques separately with the difference in phases. An asterisk (*) indicates significance between phases.

Appendix E. Muscle Forces in Phases

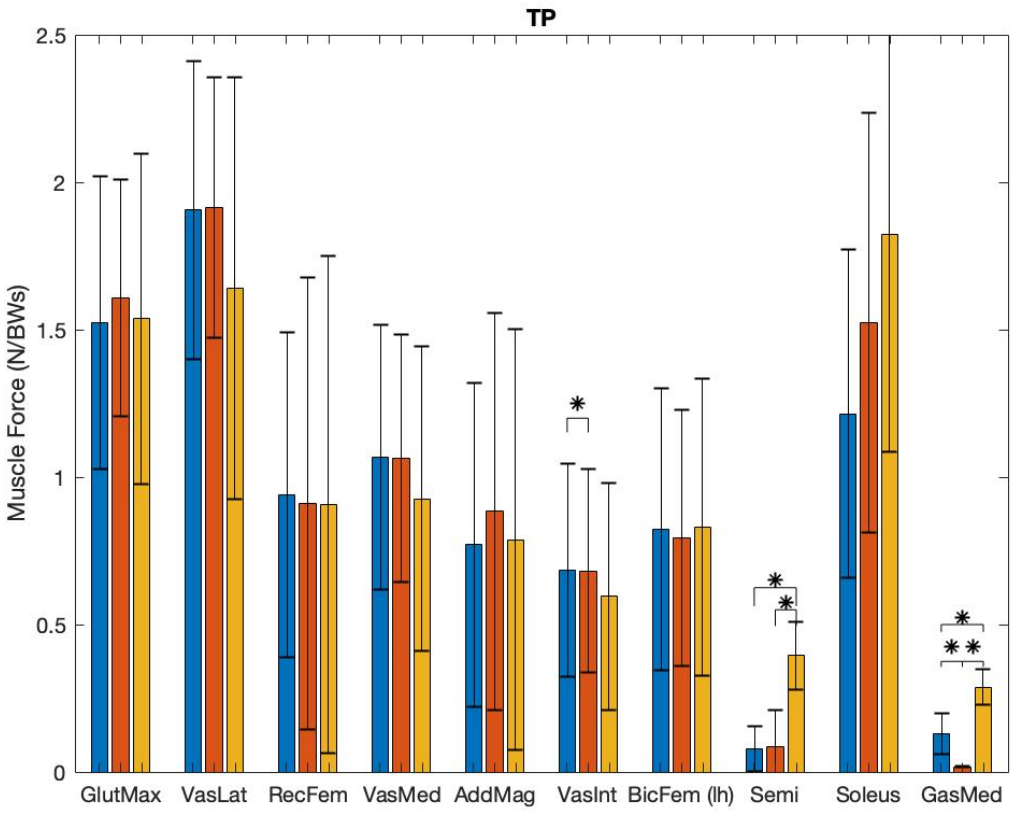

Figure 13: The muscle forces in TP in three different phases. The asterisk (*) indicates significant difference between the respective phases ($p<0.05$).

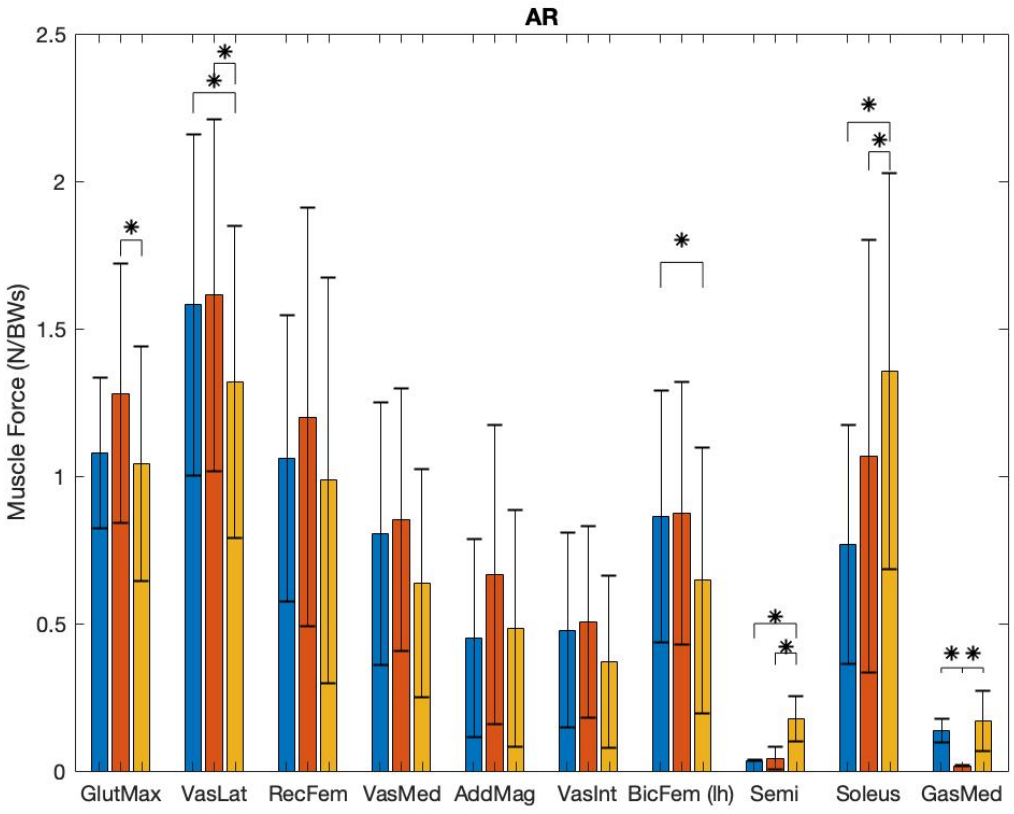

Figure 14: The muscle forces in AR in three different phases. The asterisk (*) indicates significant difference between the respective phases ($p<0.05$).

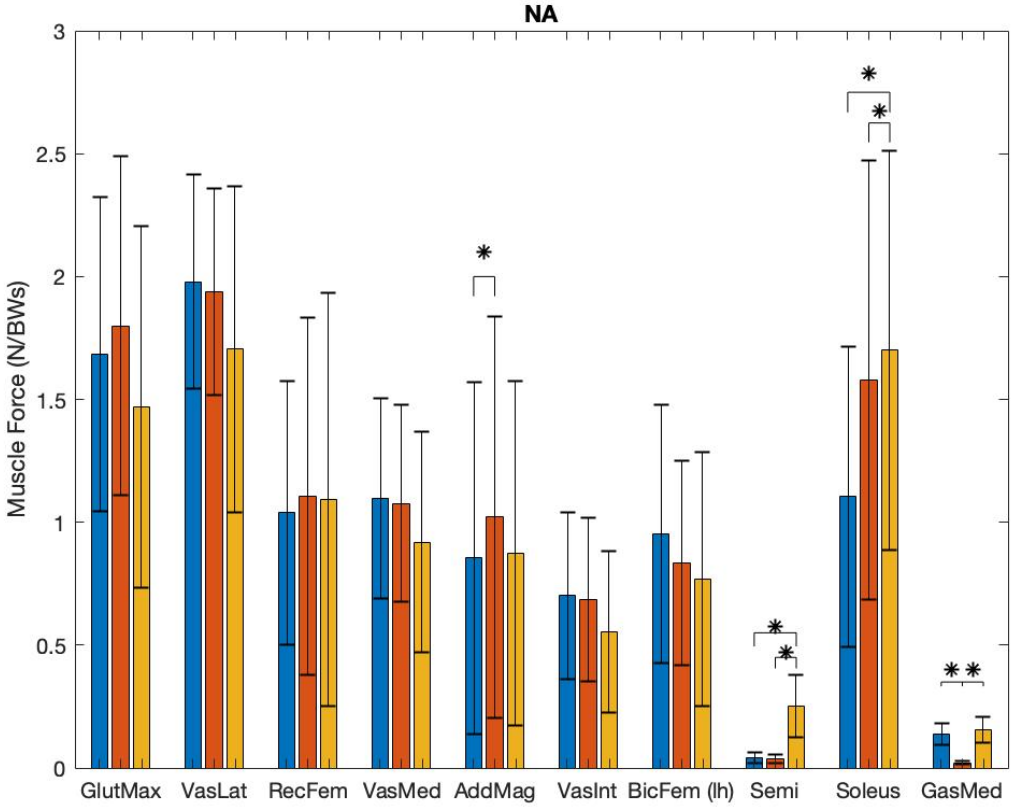

Figure 15: The muscle forces in NA in three different phases. The asterisk (*) indicates significant difference between the respective phases ($p<0.05$).

Appendix F. Capacity Tables

Table 11: TP capacity that is being used in TP for all participants as a percentage of the maximal peak isokinetic joint moment strength measures (%). The ankle was measured at a velocity of 60 degrees per second and the other joints at 90 degrees per second.

	Elbow Flexion		Elbow Extension		Knee		Ankle		Hip	
TP	D	ND	D	ND	D	ND	D	ND	D	ND
P2219	17	14	10	12	81	270	511	369	168	233
P2220	9	11	1	0	72	66	333	331	145	98
P2236	11	12	3	3	56	54	329	285	223	205
P2237	13	13	5	15	48	63	538	654	304	214
P2239	16	33	0	0	72	79	463	533	168	149
P2249	31	7	3	10	53	76	186	239	173	179

Table 12: AR capacity that is being used in AR for all participants as a percentage of the maximal peak isokinetic joint moment strength measures (%). The ankle was measured at a velocity of 60 degrees per second and the other joints at 90 degrees per second.

	Elbow Flexion		Elbow Extension		Knee		Ankle		Hip	
AR	D	ND	D	ND	D	ND	D	ND	D	ND
P2219	18	27	54	67	51	214	595	407	81	126
P2220	9	13	119	22	69	51	226	308	97	56
P2235	13	14	54	74	92	66	298	215	210	127
P2236	13	14	105	96	44	46	357	319	111	134
P2237	28	11	74	78	48	65	176	153	174	53
P2239	23	26	71	54	67	73	233	391	89	114
P2249	27	8	48	46	33	57	178	220	113	90
P2250	19	12	64	67	28	49	111	138	49	49

Table 13: NA capacity that is being used in NA for all participants as a percentage of the maximal peak isokinetic joint moment strength measures (%). The ankle was measured at a velocity of 60 degrees per second and the other joints at 90 degrees per second.

	Elbow Flexion		Elbow Extension		Knee		Ankle		Hip	
NA	D	ND	D	ND	D	ND	D	ND	D	ND
P2219	10	12	1	2	87	305	567	371	201	222
P2220	9	9	1	0	69	66	248	340	137	107
P2235	14	12	1	1	119	83	212	228	197	189
P2236	13	15	5	7	53	52	311	284	208	198
P2237	23	23	3	4	66	53	362	506	274	233
P2239	17	17	3	2	84	90	248	558	102	170
P2249	9	10	3	2	54	85	140	265	116	156
P2250	14	12	3	2	54	94	117	147	89	133

Appendix G. Results Tables Including Nine Participants

Table 14: Lower limb peak joint torques in three different conditions in elderly men. Peak joint moments are represented in Nm/kg.

	TP		AR		NA	
	(D)	(ND)	(D)	(ND)	(D)	(ND)
Hip	-1.03 ± 0.17[a]	-0.9 ± 0.09[a]	-0.64 ± 0.23[a,b]	-0.56 ± 0.2[a,b]	-0.98 ± 0.29[b]	-1.03 ± 0.21[b]
Knee	-0.78 ± 0.22[a]	-0.69 ± 0.09[a]	-0.67 ± 0.2[a,b]	-0.63 ± 0.12[a,b]	-0.9 ± 0.22[b]	-0.84 ± 0.27[b]
Ankle	-0.64 ± 0.15	-0.56 ± 0.09	-0.49 ± 0.19	-0.46 ± 0.15	-0.49 ± 0.16	-0.54 ± 0.1
Lumbar	1.74 ± 0.25[a,c]		1.21 ± 0.27[a,b]		2.02 ± 0.26[b,c]	

[a]: Significant difference between TP and AR.
[b]: Significant difference between AR and NA.
[c]: Significant difference between TP and NA.

Table 15: Upper limb peak joint torques in three different STS conditions. Peak joint moments are represented in Nm/kg.

	TP		AR		NA	
	(D)	(ND)	(D)	(ND)	(D)	(ND)
Arm Flex	0.29 ± 0.16 [b]	0.31 ± 0.2[b]	0.15 ± 0.09	0.23 ± 0.12	0.08 ± 0.05[b]	0.08 ± 0.04[b]
Arm Ext	-0.04 ± 0.02	-0.04 ± 0.02[a]	-0.35 ± 0.46	-0.15 ± 0.08[a]	-0.04 ± 0.03	-0.04 ± 0.03
Arm Exrot	0.01 ± 0.01[a]	0.01 ± 0.01[a]	0.19 ± 0.18[a]	0.12 ± 0.05[a]	0.01 ± 0.01	0.01 ± 0.01
Arm Inrot	-0.13 ± 0.07[a,b]	-0.21 ± 0.13[a,b]	-0.04 ± 0.01[a]	-0.03[a]0.01	-0.02 ± 0.01[b]	-0.02 ± 0.01[b]
Arm Abd	-0.04 ± 0.02[a]	-0.07 ± 0.03	-0.1 ± 0.04[a]	-0.08 ± 0.02	-0.03 ± 0.03	-0.03 ± 0.03
Elbow Ext	-0.01 ± 0.02[a,b]	-0.03 ± 0.03[a,b]	-0.35 ± 0.17[a]	-0.29 ± 0.09[a]	0.01 ± 0.01[b]	0.01 ± 0.01[b]
Wrist Flex	0 ± 0[a]	0 ± 0[a]	0.09 ± 0.1[a]	0.04 ± 0.03[a]	0 ± 0	0 ± 0

[a]: Significant difference between TP and AR.
[b]: Significant difference between TP and NA.

Table 16: Muscle forces with most contribution to the standing up movements in N/BW.

Muscle	TP		AR		NA	
	(D)	(ND)	(D)	(ND)	(D)	(ND)
BicFem (lh)	0.96 ± 0.51	0.89 ± 0.49[a]	1.19 ± 0.79	0.95 ± 0.86[a,b]	1.41 ± 0.77	1.26 ± 0.89[b]
GasMed	0.3 ± 0.07	0.3 ± 0.1	0.18 ± 0.08	0.22 ± 0.07	0.19 ± 0.07	0.2 ± 0.05
Iliacus	0.22 ± 0.12	0.26 ± 0.14	0.2 ± 0.05	0.25 ± 0.08	0.2 ± 0.08	0.21 ± 0.07
Psoas	0.23 ± 0.08	0.21 ± 0.1	0.25 ± 0.09	0.28 ± 0.09	0.37 ± 0.29	0.28 ± 0.12
RecFem	1.08 ± 0.72[a]	0.9 ± 0.42	1.53 ± 1.03[a]	1.2 ± 0.98	1.8±1	1.35 ± 0.82
Semimem	0.4 ± 0.12	0.34 ± 0.08	0.23 ± 0.2	0.21 ± 0.15	0.6 ± 0.78	0.26 ± 0.11
Soleus	1.83 ± 0.74	1.51 ± 0.38	1.31 ± 0.56[b]	1.2 ± 0.4[b]	1.64 ± 0.72[b]	1.68 ± 0.33[b]
TibAnt	0.46 ± 0.28	0.3 ± 0.14	0.36 ± 0.18[b]	0.32 ± 0.12	0.47 ± 0.19[b]	0.38 ± 0.16
TibPost	0.56 ± 0.38	0.42 ± 0.18	0.53 ± 0.2[b]	0.5 ± 0.21[b]	0.66 ± 0.19[b]	0.62 ± 0.25[b]
VasInt	0.69 ± 0.35[a]	0.62 ± 0.26[a]	0.62 ± 0.42[a,b]	0.57 ± 0.42[a,b]	1 ± 0.49[b]	0.93 ± 0.52[b]
VasLat	1.95 ± 0.45[a]	2.06 ± 0.38[a]	2.04 ± 0.92[a,b]	2.01 ± 0.9[a,b]	2.52 ± 0.82[b]	2.49 ± 0.8[b]
VasMed	1.08 ± 0.43[a]	1.06 ± 0.34	1.04 ± 0.61[a,b]	0.98 ± 0.63[b]	1.51 ± 0.64[b]	1.45 ± 0.66[b]
Glmax	1.71 ± 0.46[a]	1.57 ± 0.4[a]	1.54 ± 0.73[a]	1.23 ± 0.6[a,b]	2.05 ± 0.62	1.93 ± 0.73[b]
Glmed	0.49 ± 0.25	0.53 ± 0.25	0.39 ± 0.2	0.4 ± 0.25[b]	0.4 ± 0.17	0.52 ± 0.23b
AddMag	0.93 ± 0.71	0.72 ± 0.37[a]	0.75 ± 0.68[a,b]	0.54 ± 0.46[a,b]	1.39 ± 0.81[b]	1.19 ± 0.19[b]
Ham	1.09 ± 0.47	1.06 ± 0.44[a]	1.28 ± 0.9	1.07 ± 0.92[a,b]	1.78 ± 1.13	1.38 ± 0.84[b]
Quad	4.59 ± 1.87	4.5 ± 1.32[a]	5.06 ± 2.76	4.61 ± 2.71[a,b]	6.57 ± 2.58b	6.03 ± 2.46[b]

[a]: Significant difference between TP and AR.
[b]: Significant difference between AR and NA.
[c]: Significant difference between TP and NA.

Appendix H. All Participant ID Inputs

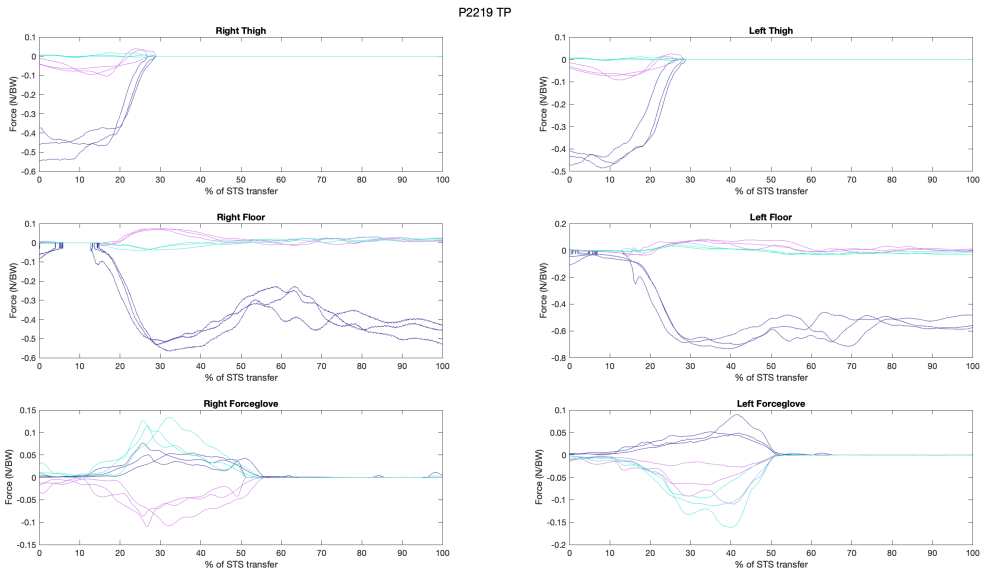

Figure 16: External Forces applied to the model in TP in N/BW.

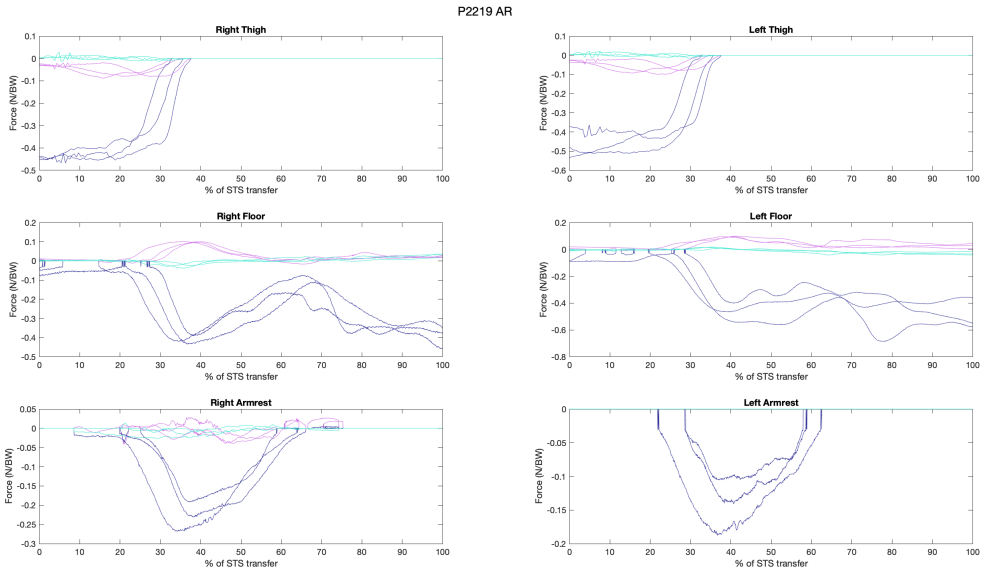

Figure 17: External Forces applied to the model in AR in N/BW.

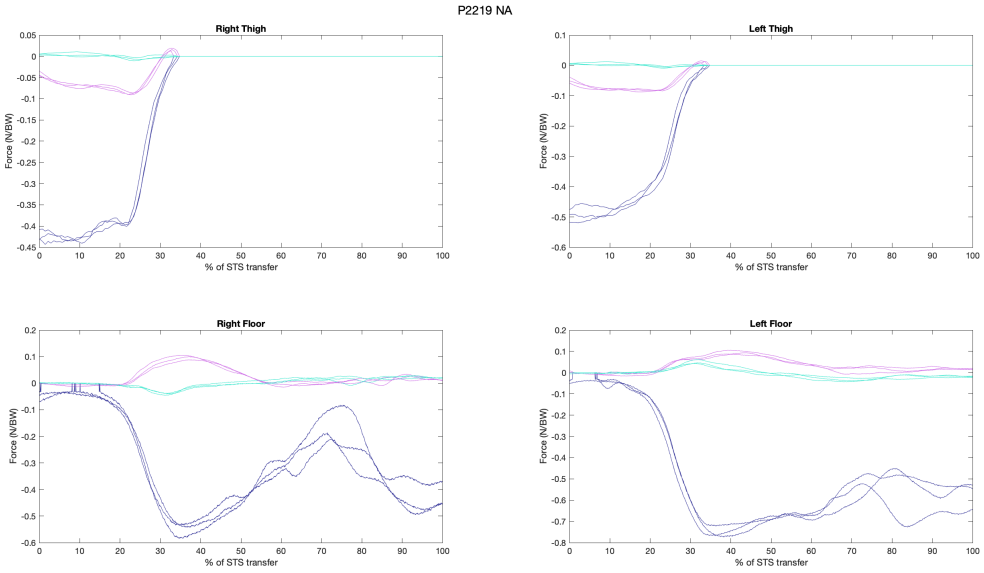

Figure 18: External Forces applied to the model in NA in N/BW.

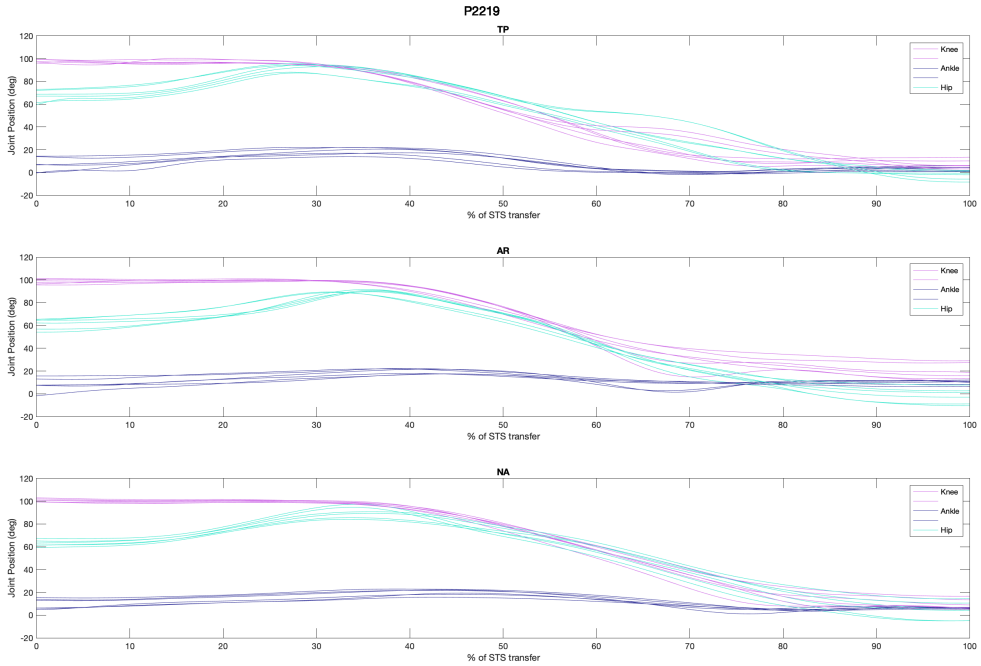

Figure 19: Joint Positions of the knee, hip, and ankle joint in the three different conditions

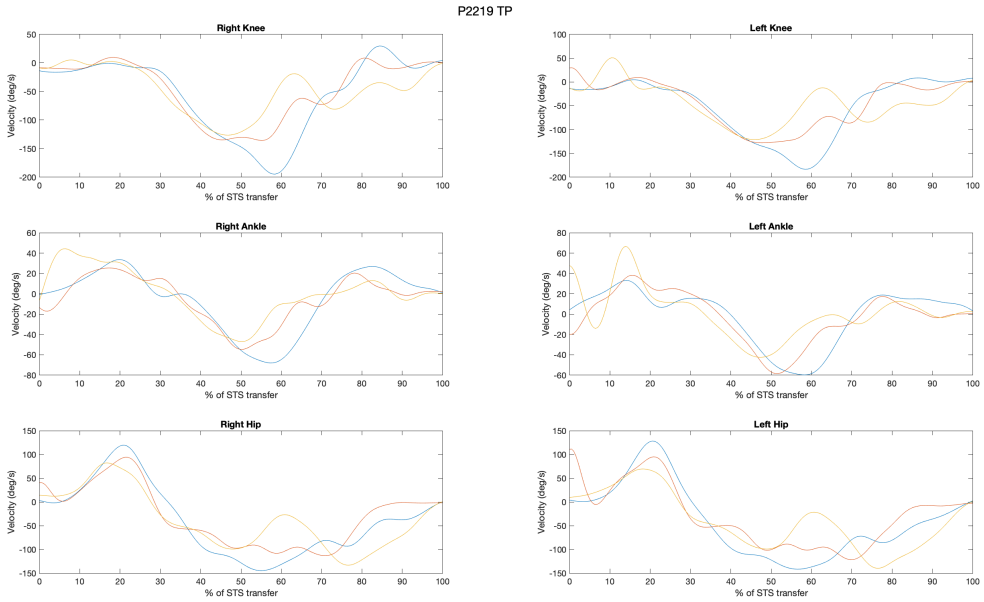

Figure 20: Joint velocities of the hip, knee and ankle joint in TP.

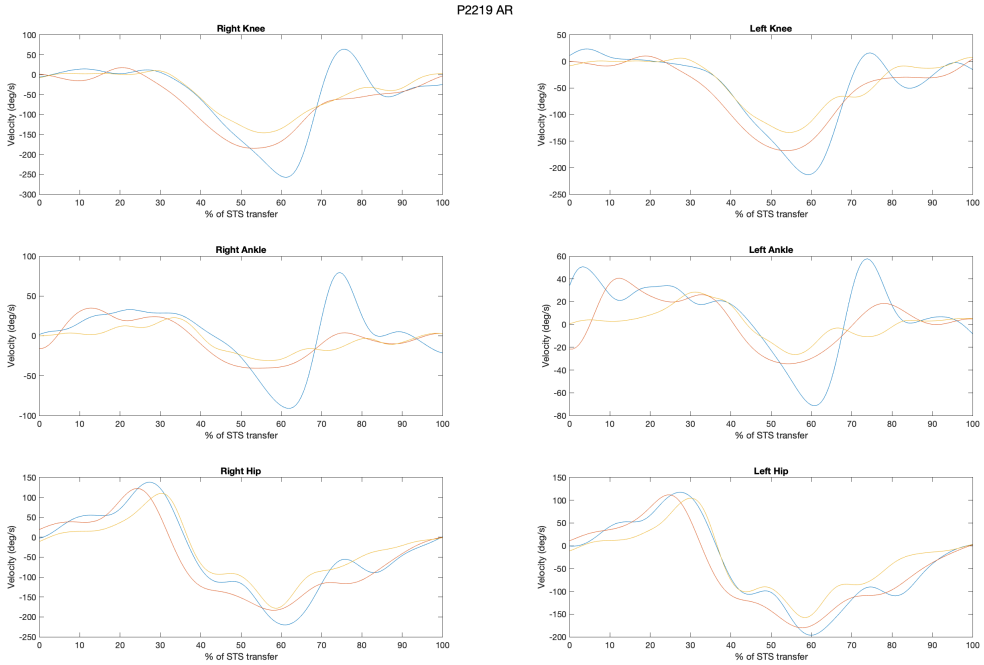

Figure 21: Joint velocities of the hip, knee, and ankle joint in AR.

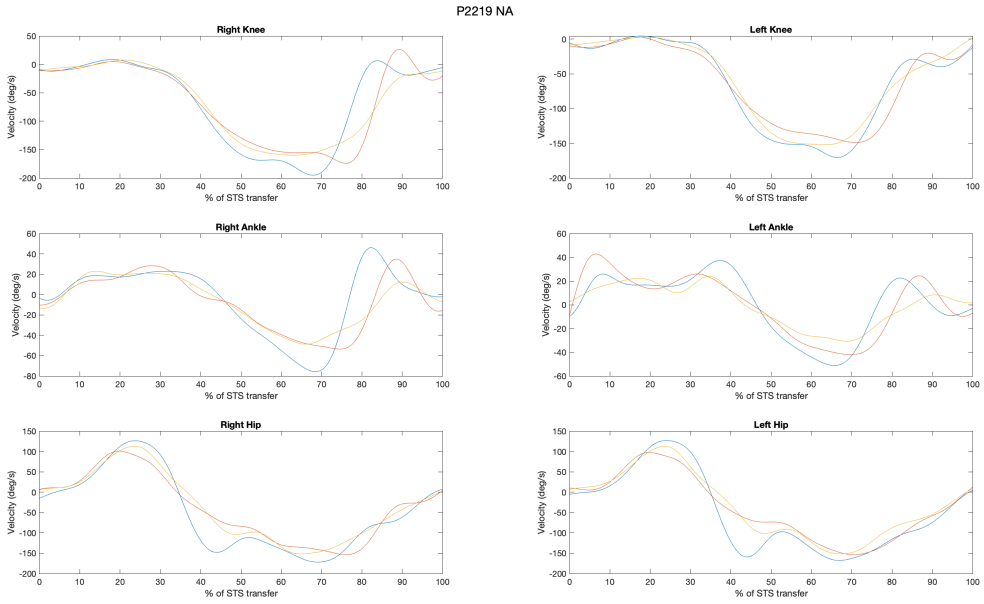

Figure 22: Joint velocities of the hip, knee and ankle joint in NA.

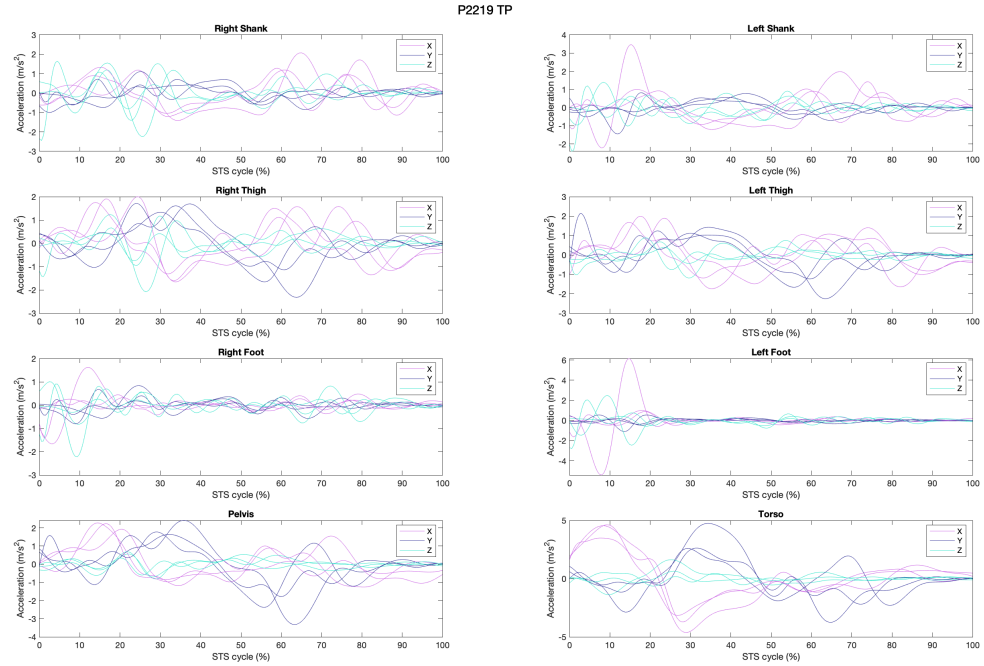

Figure 23: The segment accelerations in m/s^2 in TP.

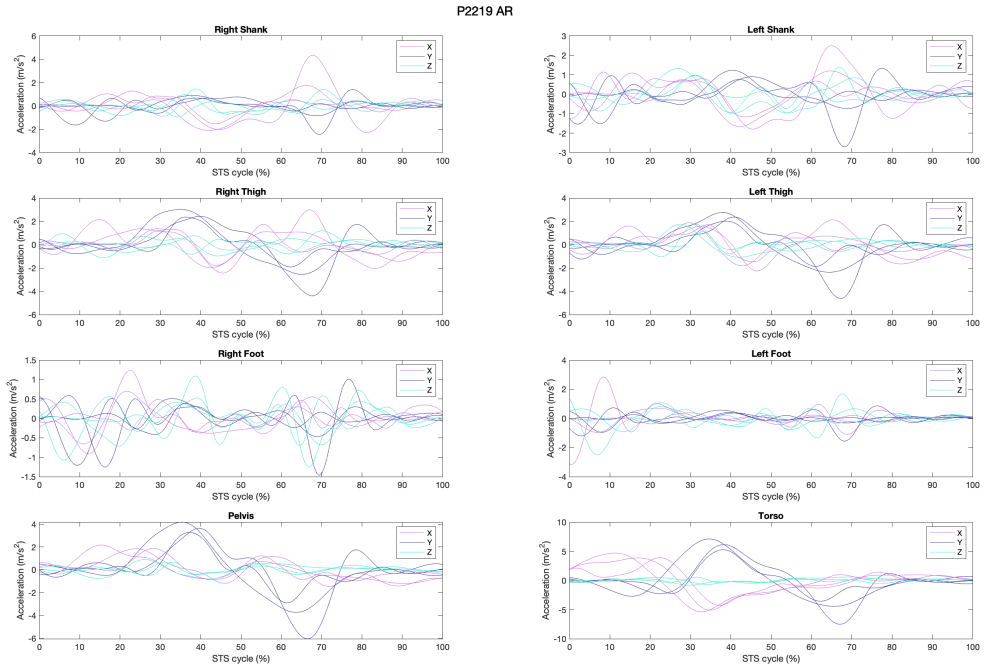

Figure 24: The segment accelerations in m/s^2 in AR.

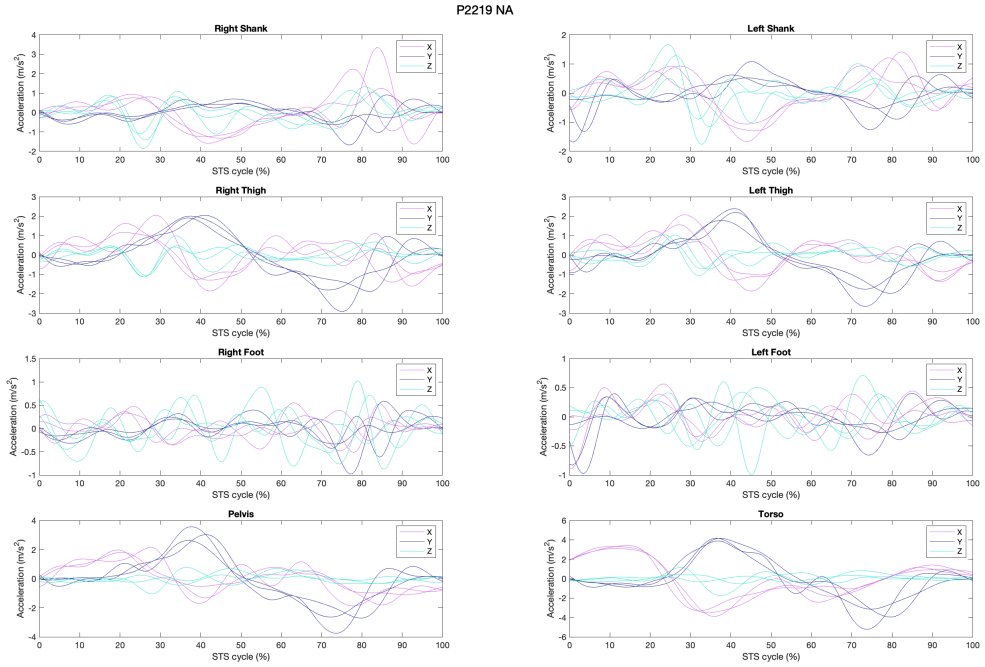

Figure 25: The segment accelerations in m/s^2 in NA.

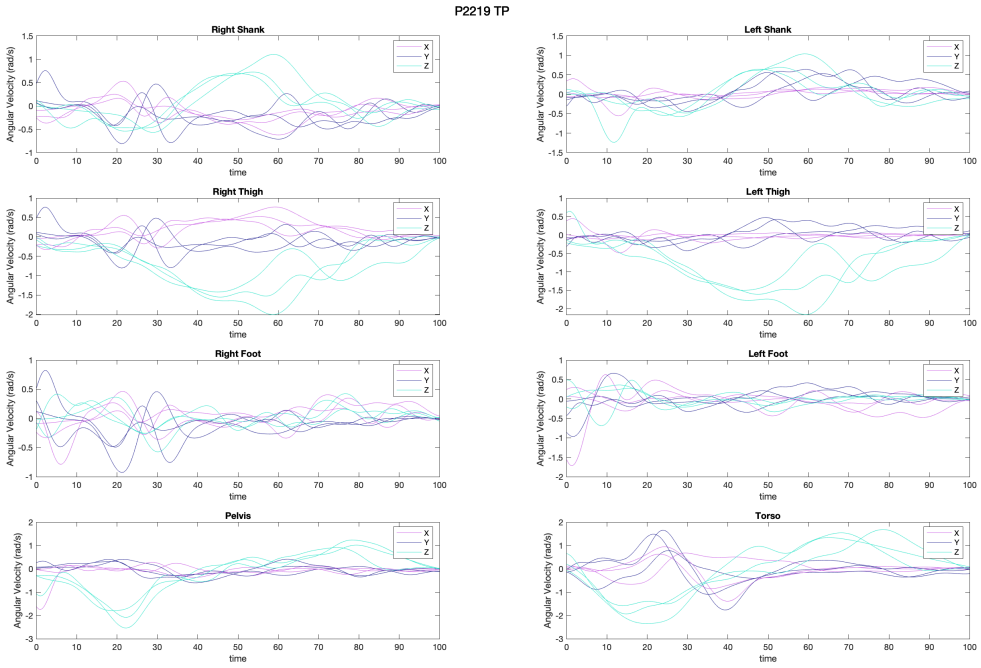

Figure 26: The segment angular velocity in radians per second in TP.

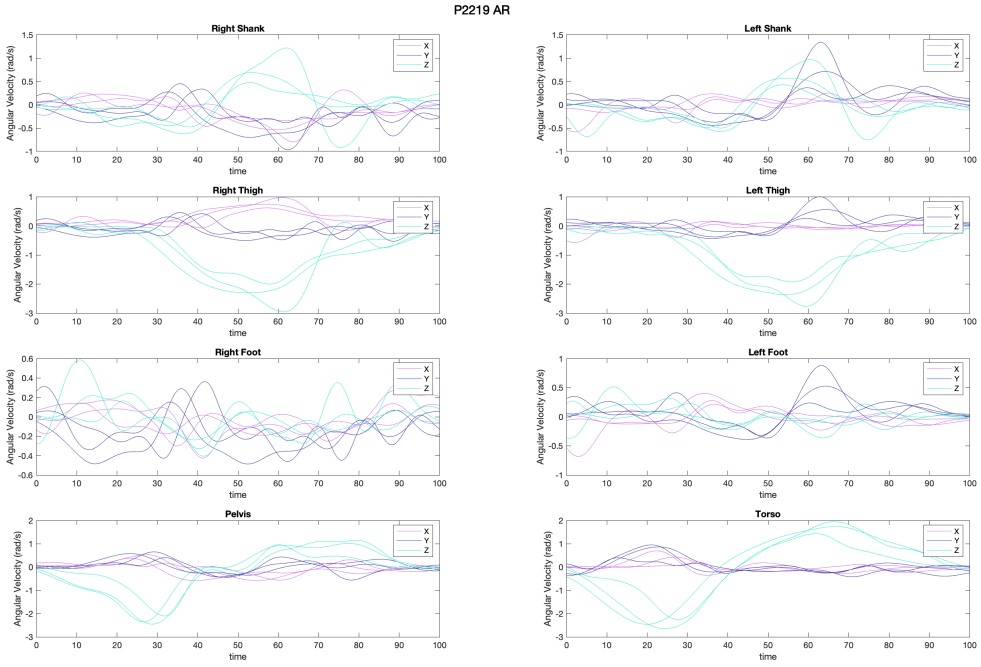

Figure 27: The segment angular velocity in radians per second in AR.

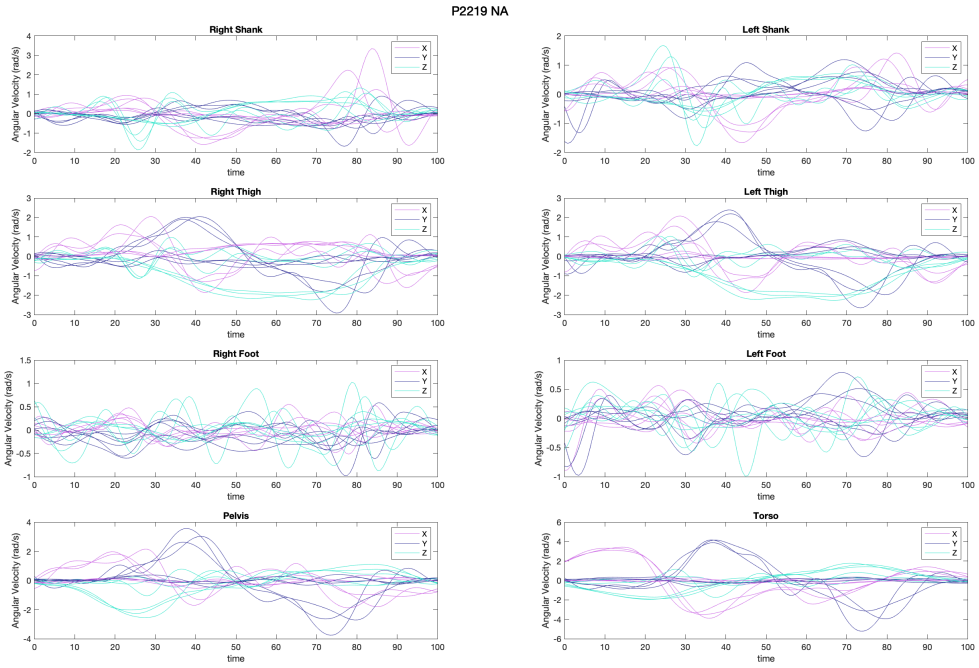

Figure 28: The segment angular velocity in radians per second in NA.

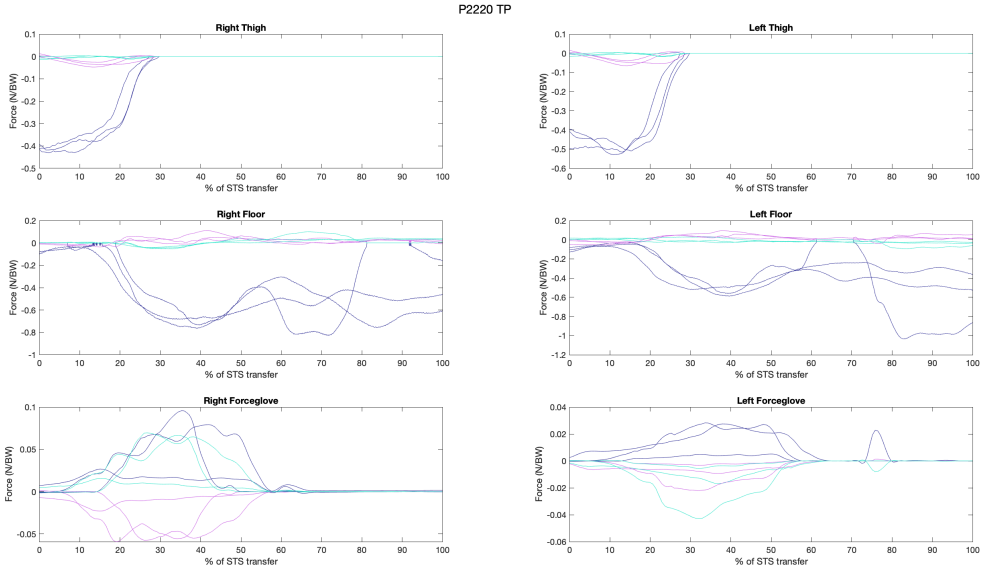

Figure 29: External Forces applied to the model in TP.

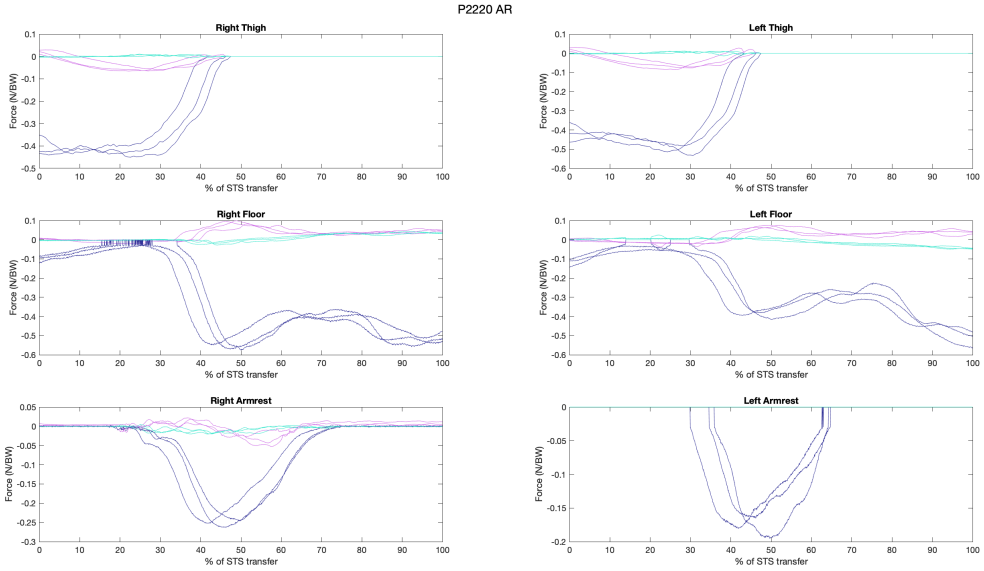

Figure 30: External Forces applied to the model in AR.

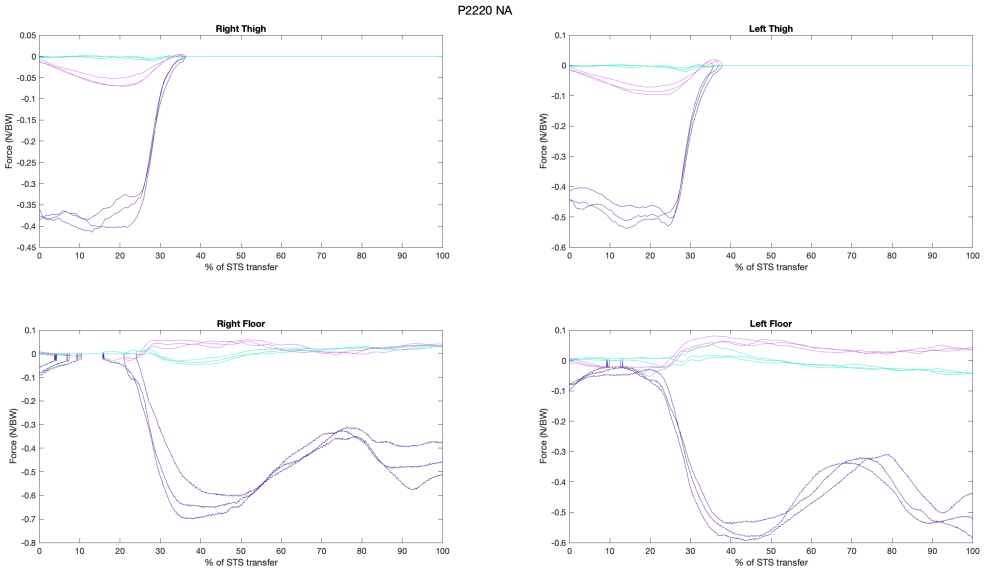

Figure 31: External Forces applied to the model in NA.

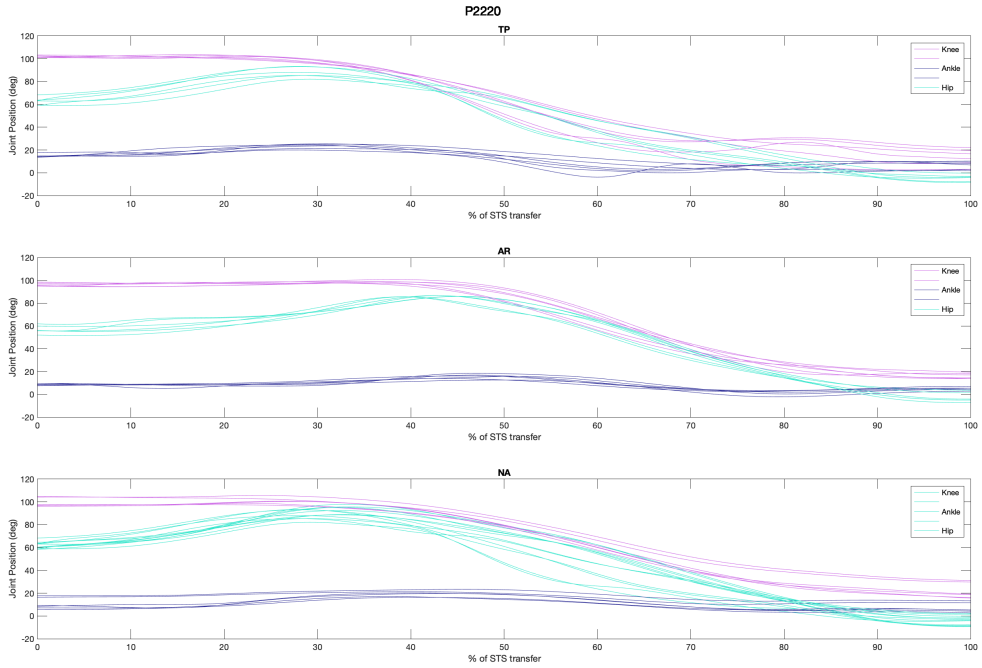

Figure 32: Joint Positions of the knee, hip, and ankle joint in the three different conditions

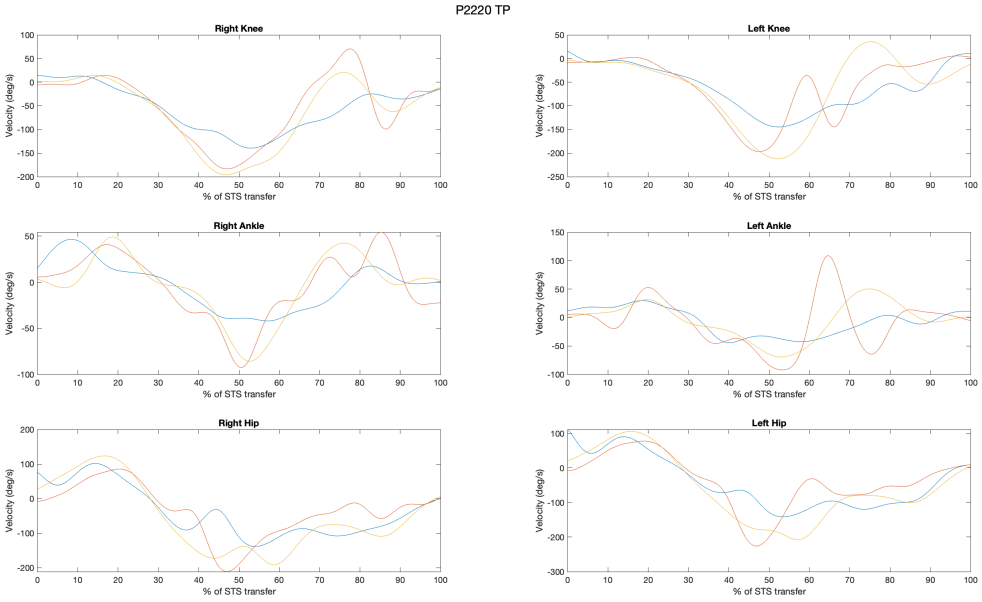

Figure 33: Joint velocities of the hip, knee and ankle joint in TP.

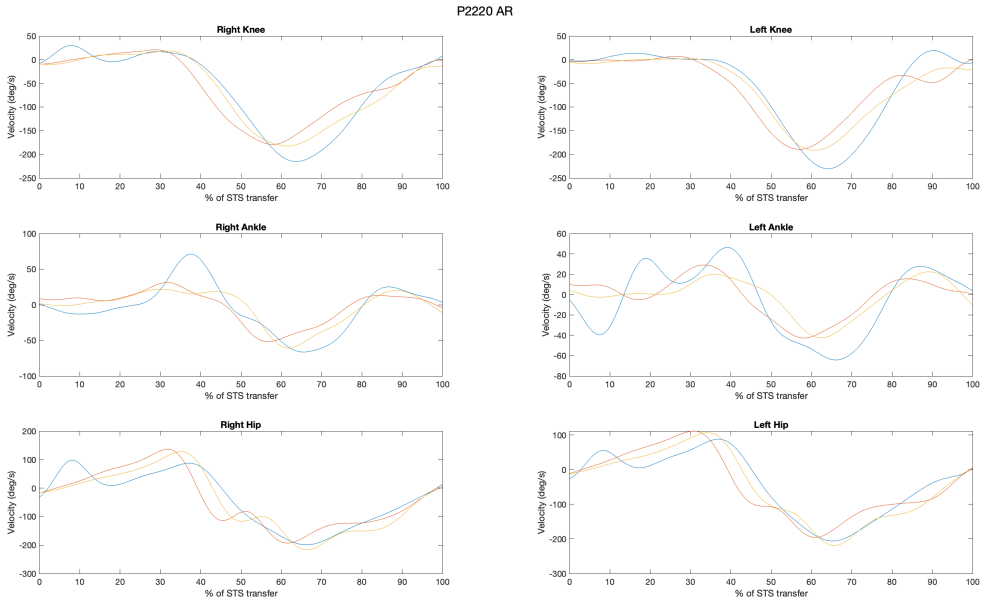

Figure 34: Joint velocities of the hip, knee and ankle joint in AR.

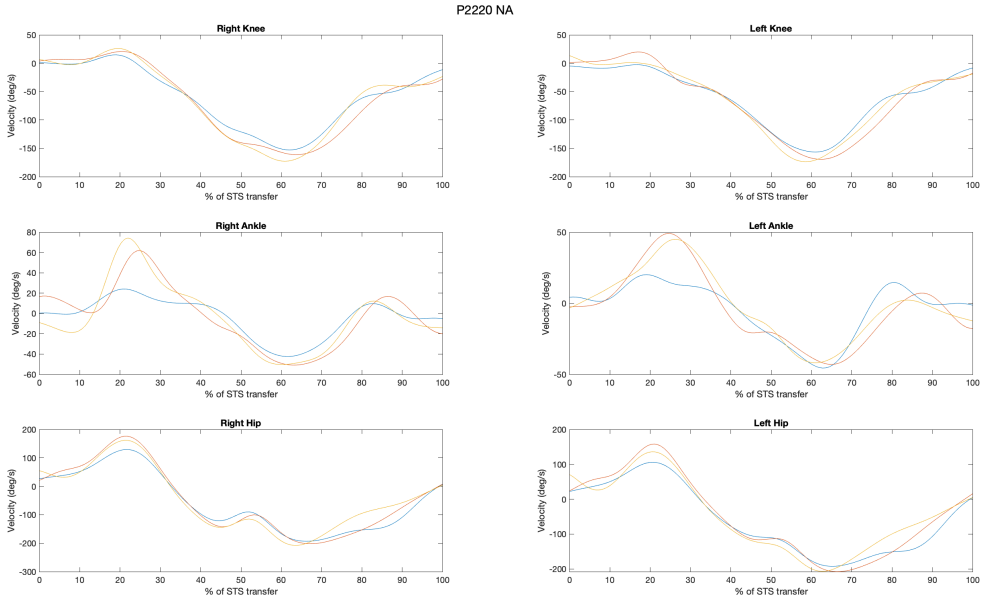

Figure 35: Joint velocities of the hip, knee and ankle joint in NA.

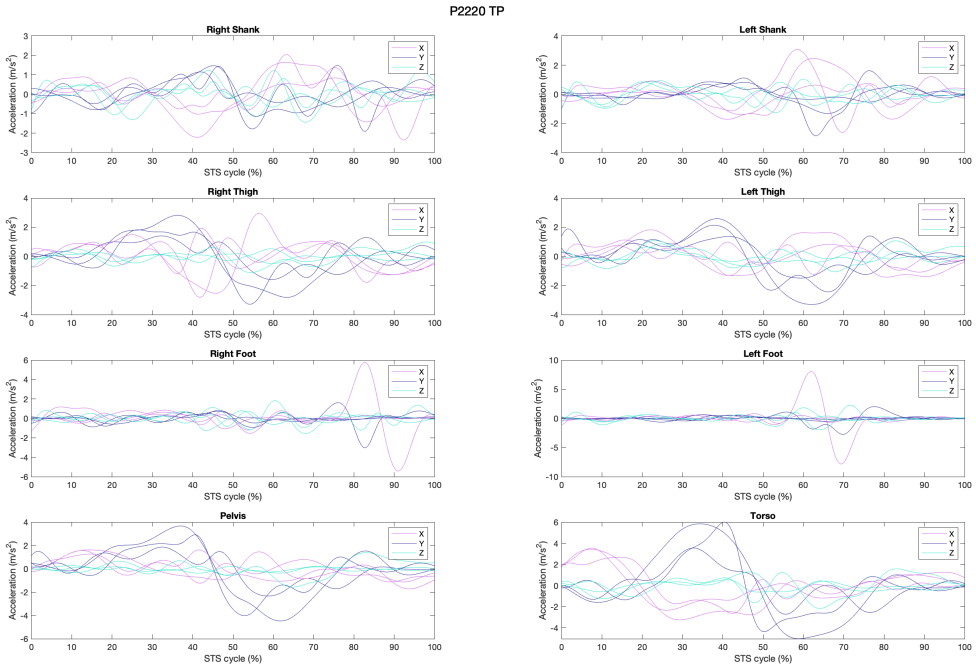

Figure 36: The segment accelerations in m/s^2 in TP.

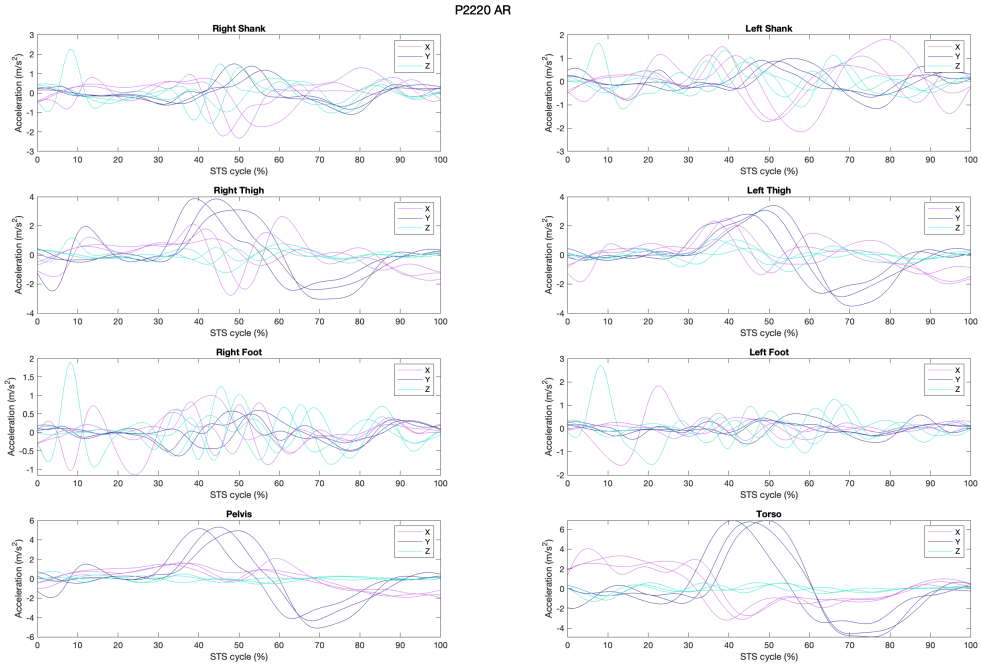

Figure 37: The segment accelerations in m/s^2 in AR.

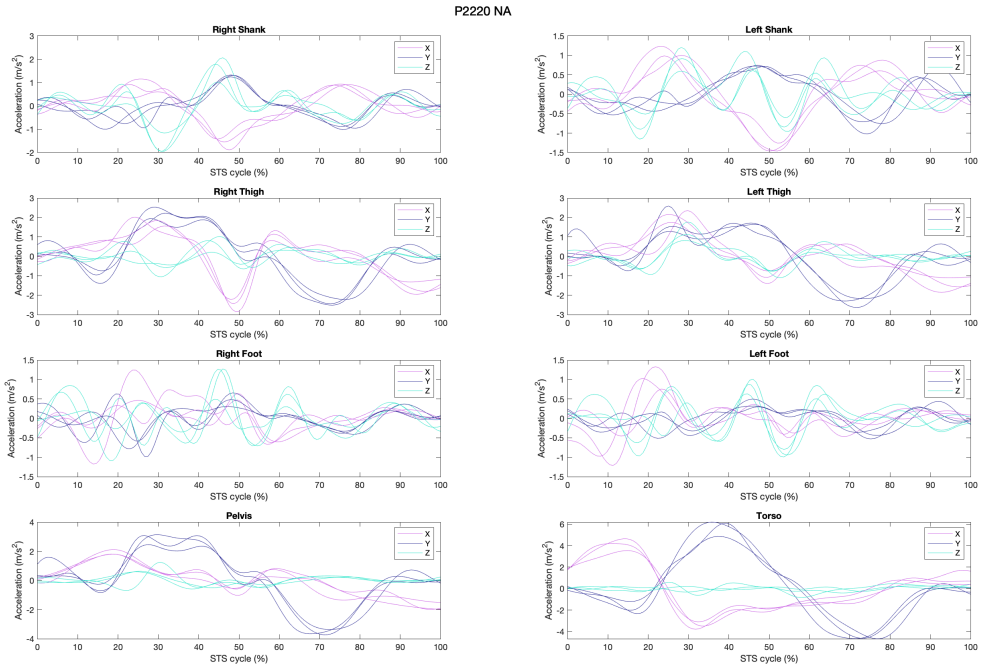

Figure 38: The segment accelerations in m/s^2 in NA.

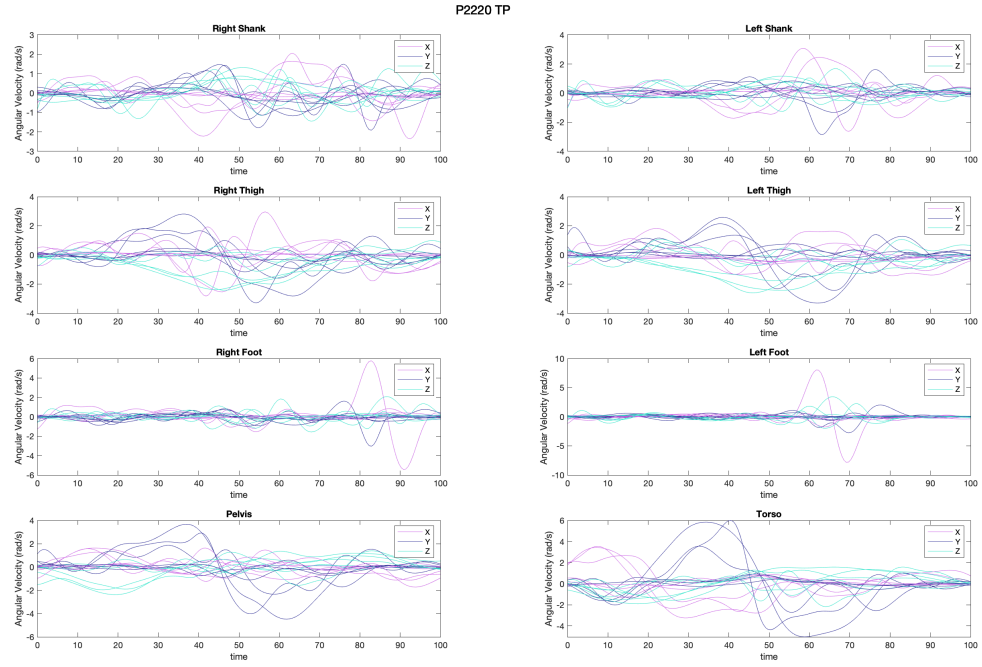

Figure 39: The segment angular velocity in radians per second in TP.

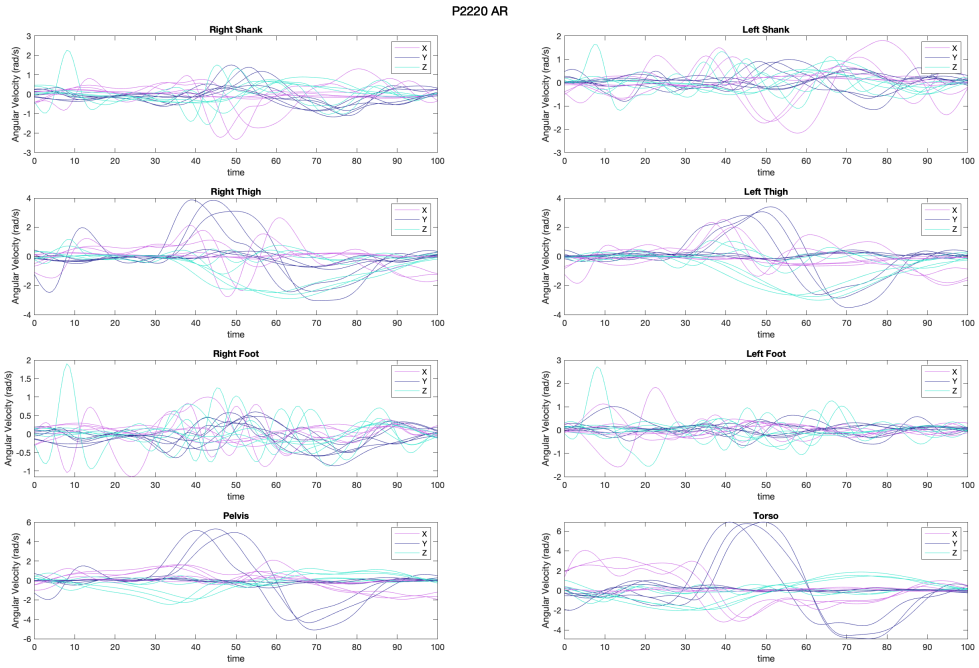

Figure 40: The segment angular velocity in radians per second in AR.

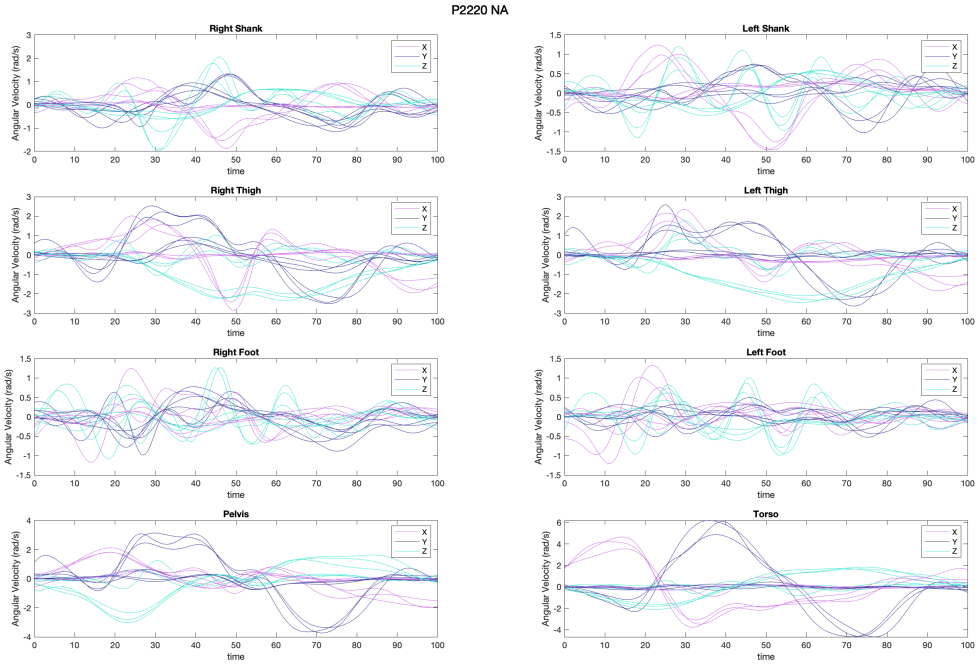

Figure 41: The segment angular velocity in radians per second in NA.

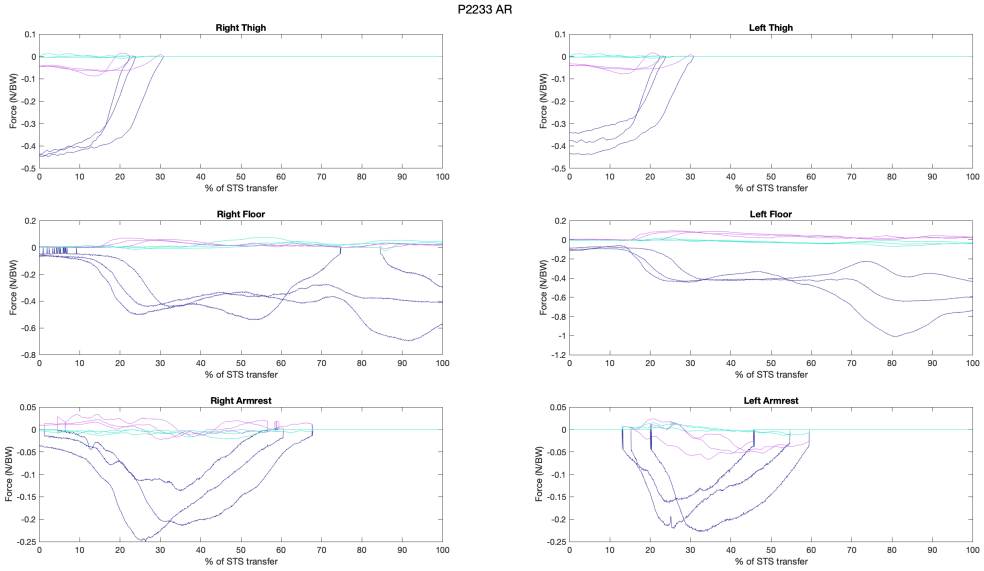

Figure 42: External Forces applied to the model in AR in N/BW.

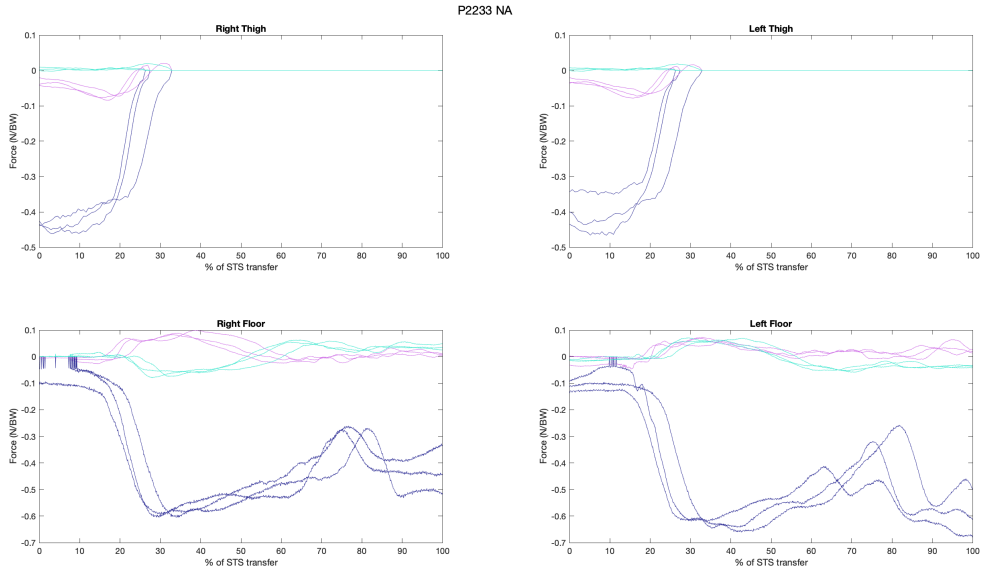

Figure 43: External Forces applied to the model in NA in N/BW.

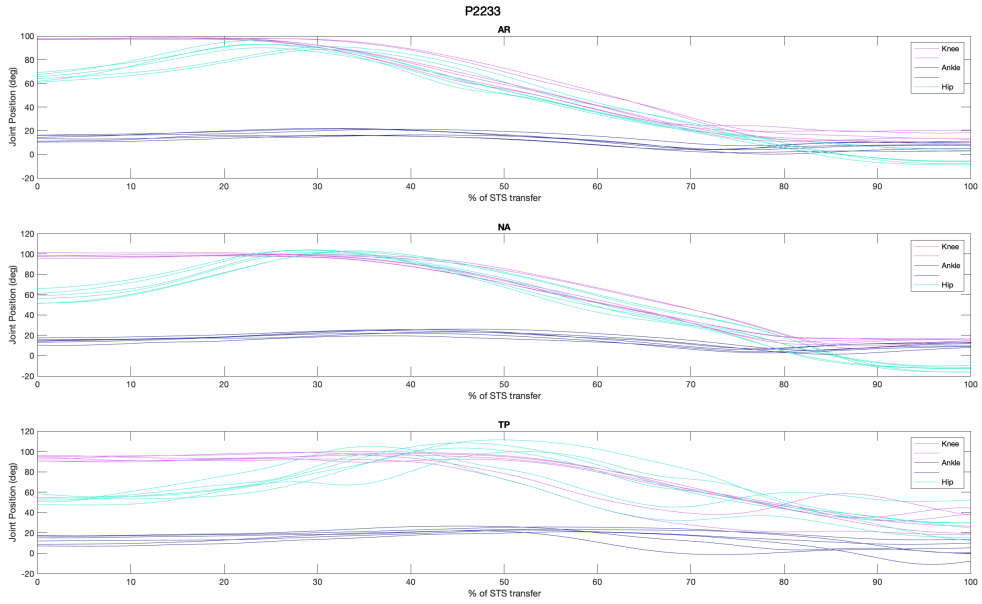

Figure 44: Joint Positions of the knee, hip, and ankle joint in the three different conditions

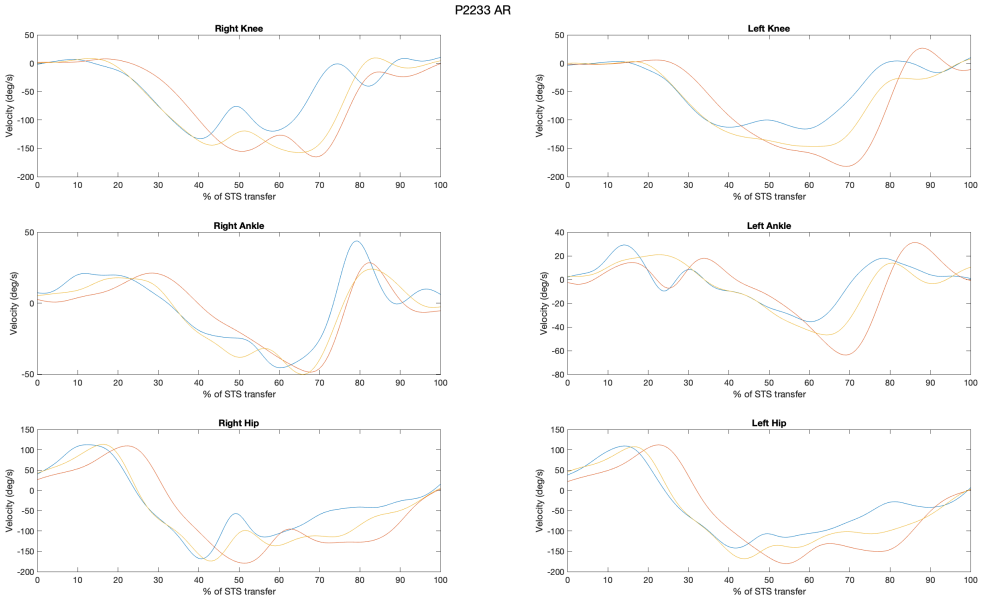

Figure 45: Joint velocities of the hip, knee and ankle joint in AR.

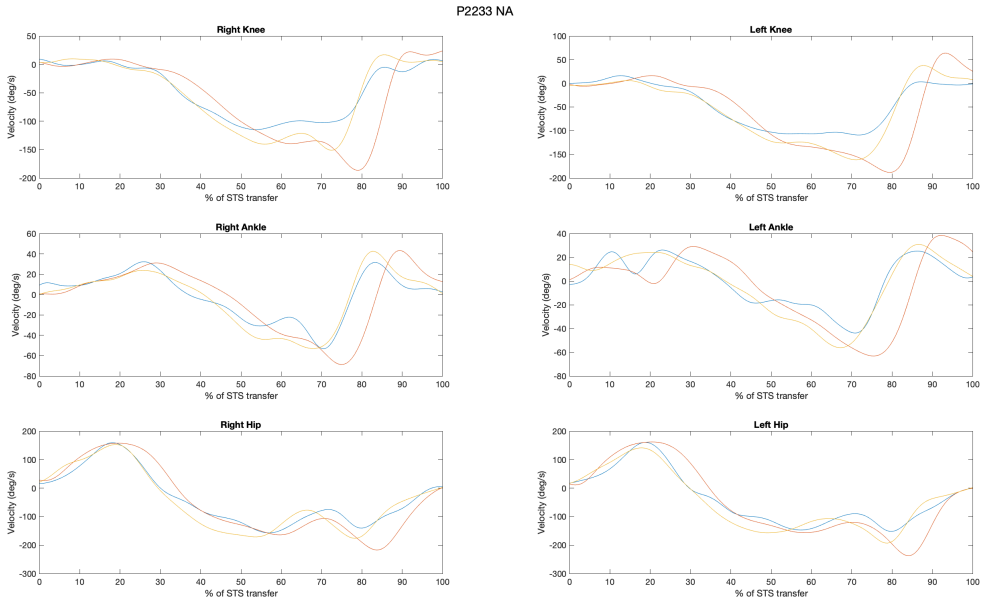

Figure 46: Joint velocities of the hip, knee and ankle joint in NA.

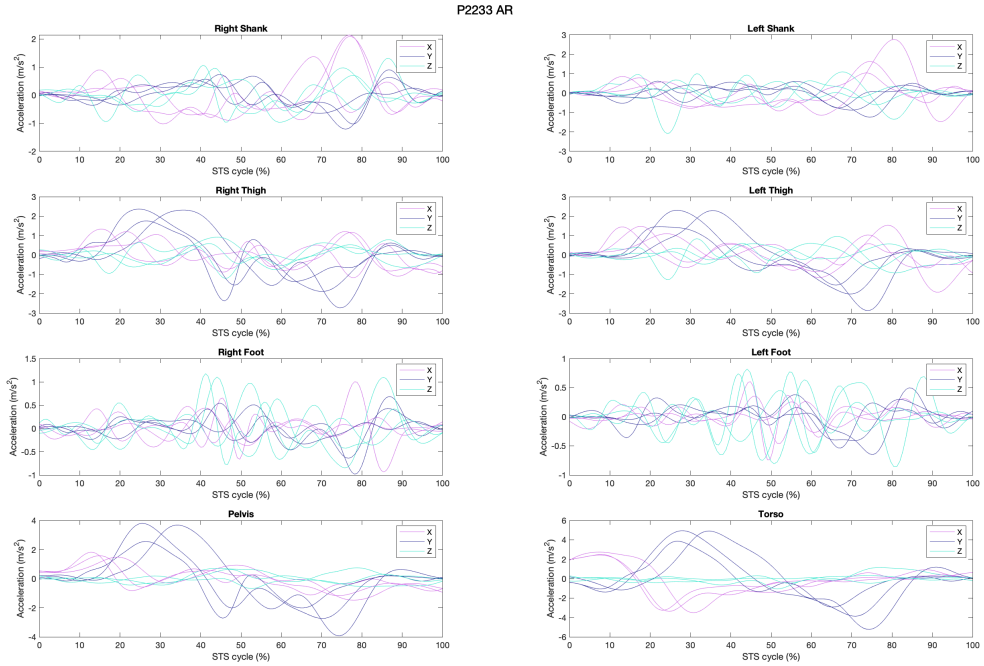

Figure 47: The segment accelerations in m/s^2 in AR.

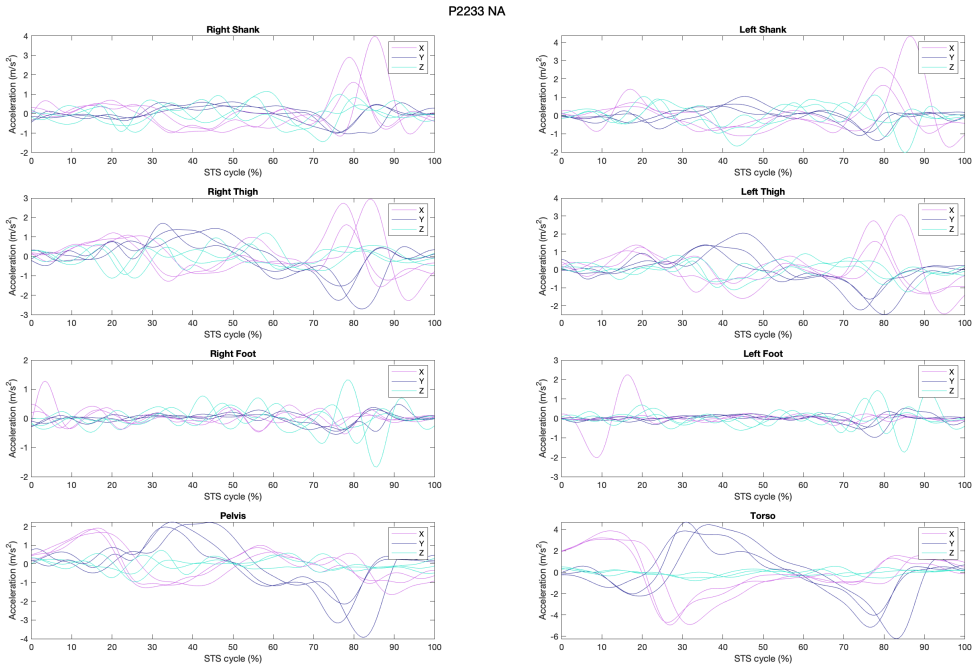

Figure 48: The segment accelerations in m/s^2 in NA.

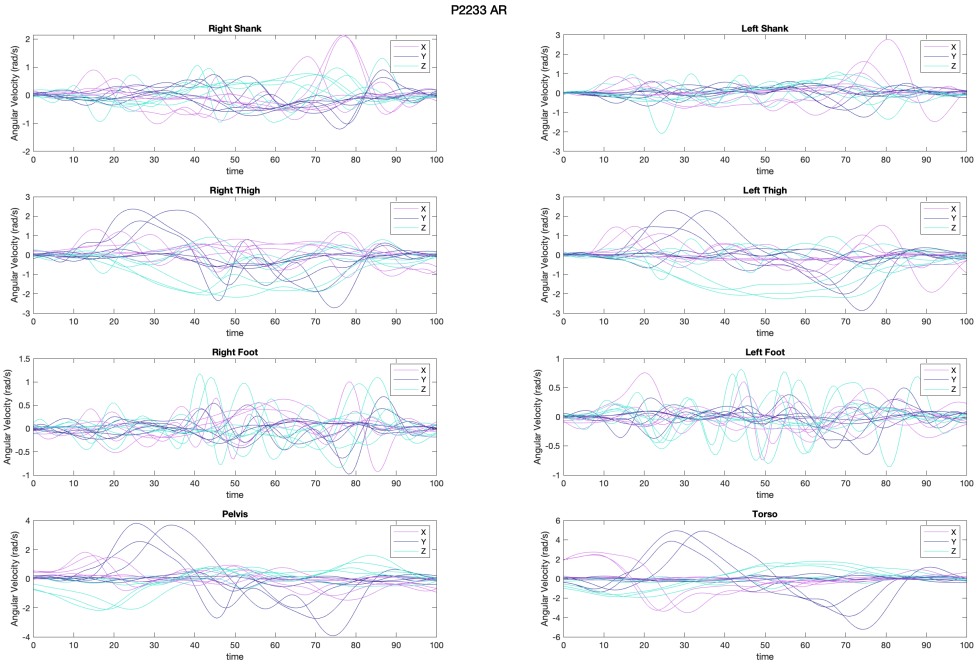

Figure 49: The segment angular velocity in radians per second in AR.

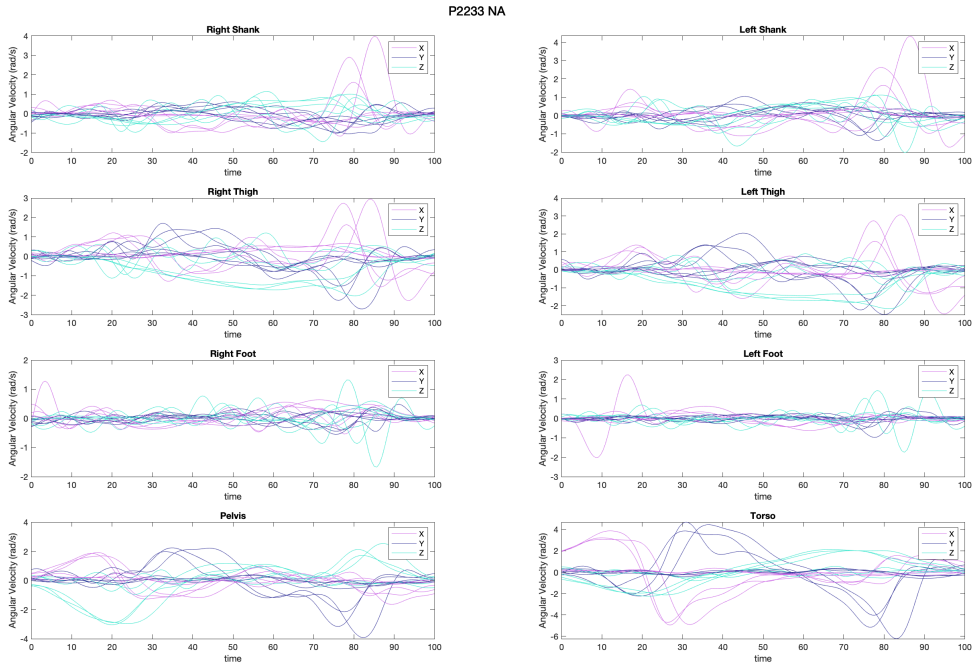

Figure 50: The segment angular velocity in radians per second in NA.

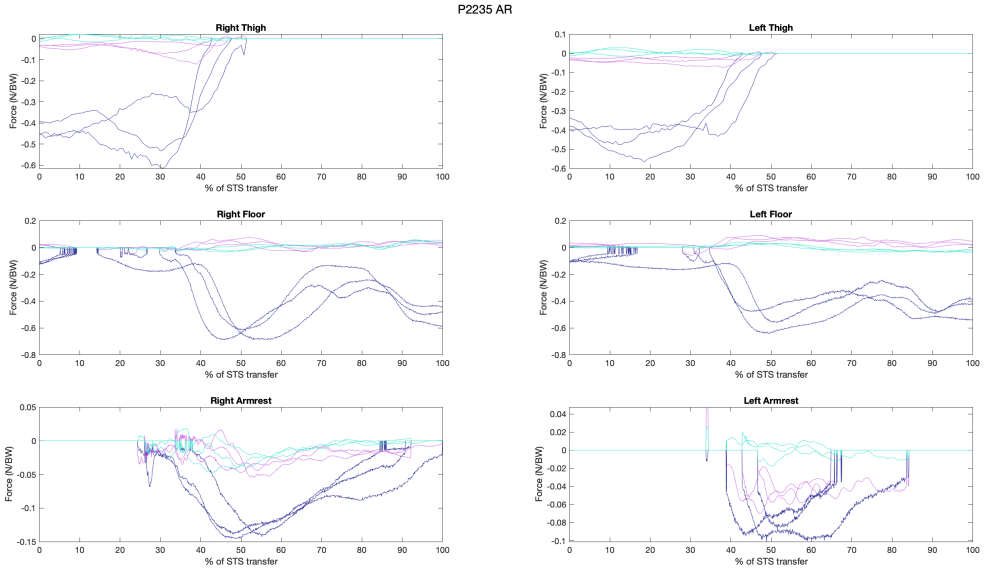

Figure 51: External Forces applied to the model in AR in N/BW.

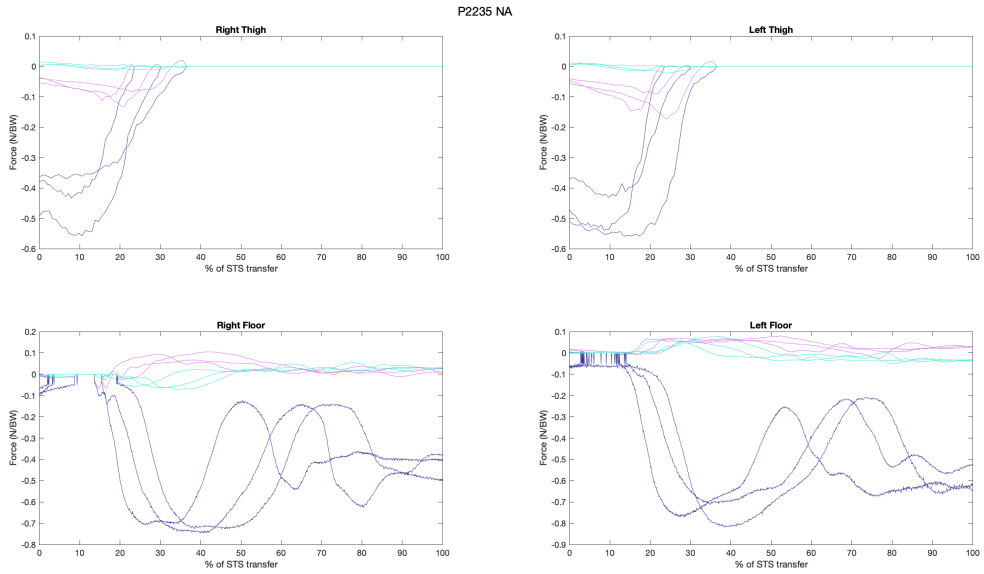

Figure 52: External Forces applied to the model in NA in N/BW.

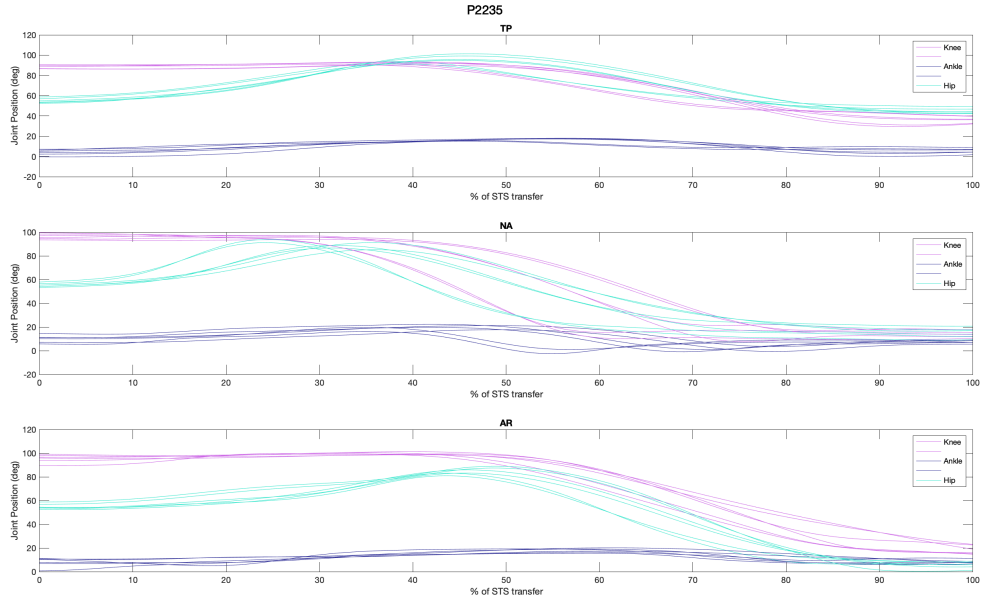

Figure 53: Joint Positions of the knee, hip, and ankle joint in the three different conditions

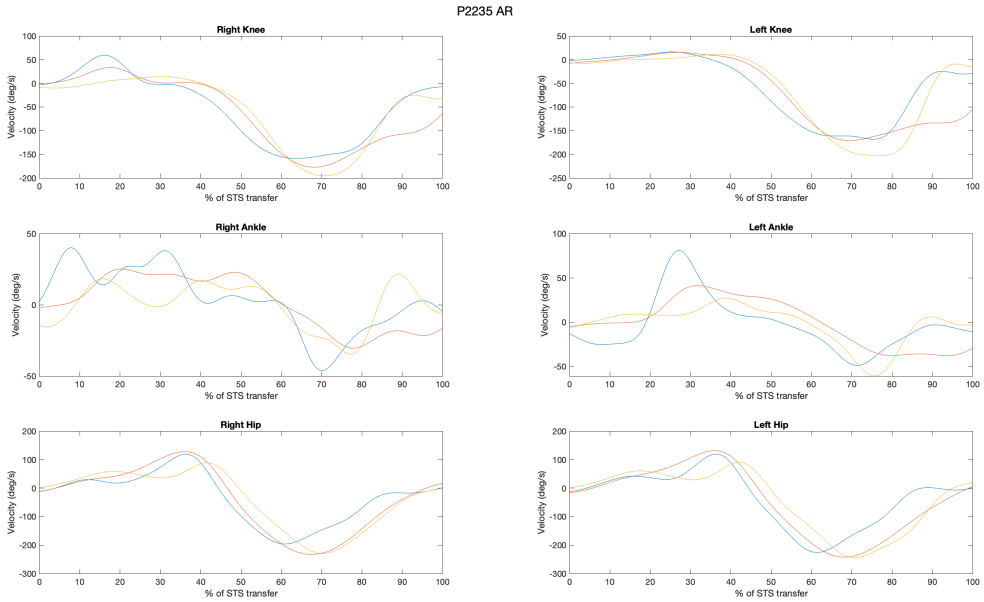

Figure 54: Joint velocities of the hip, knee and ankle joint in AR.

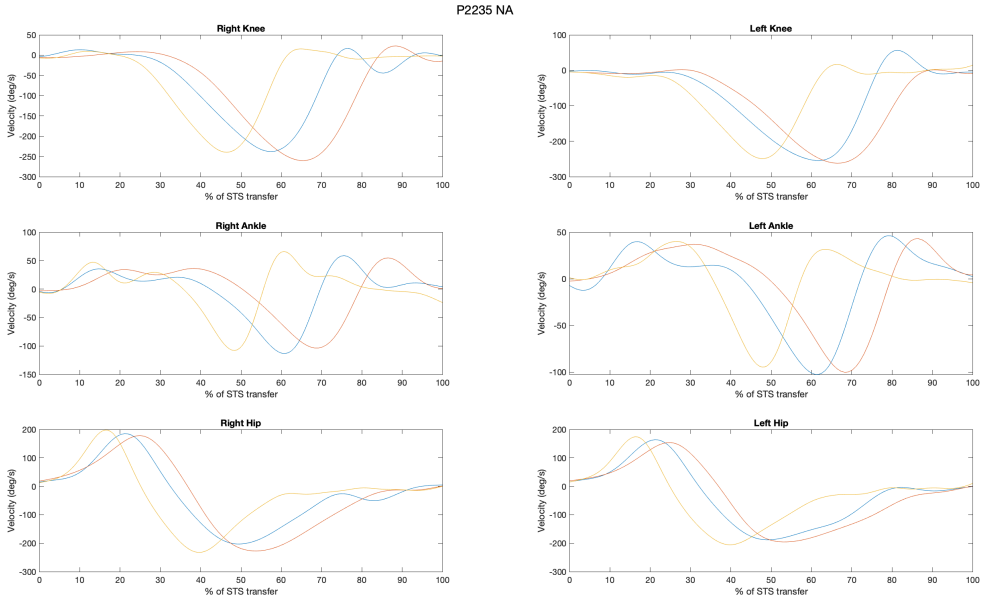

Figure 55: Joint velocities of the hip, knee and ankle joint in NA.

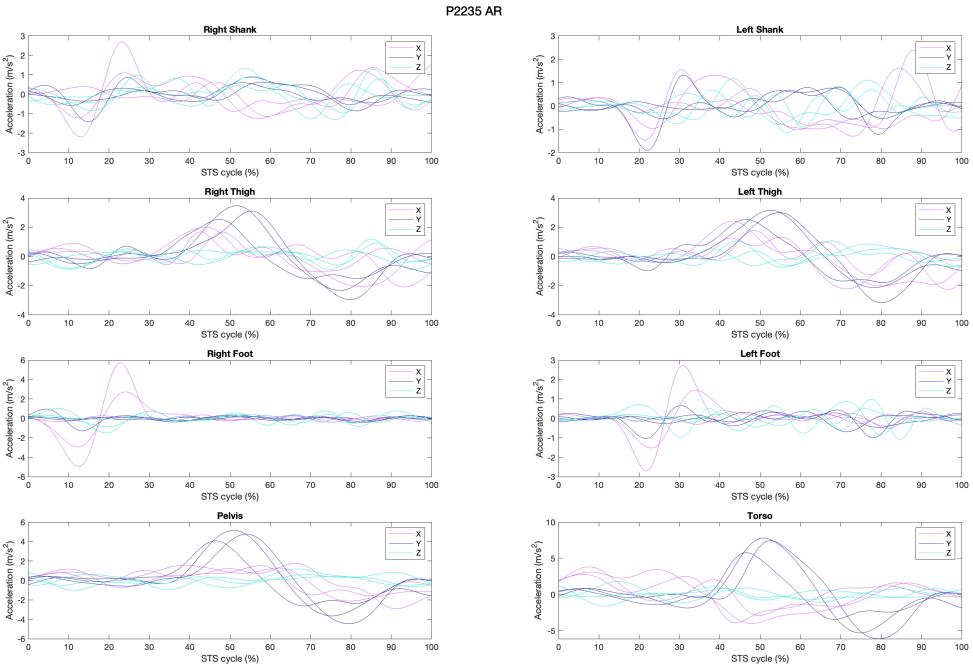

Figure 56: The segment accelerations in m/s^2 in AR.

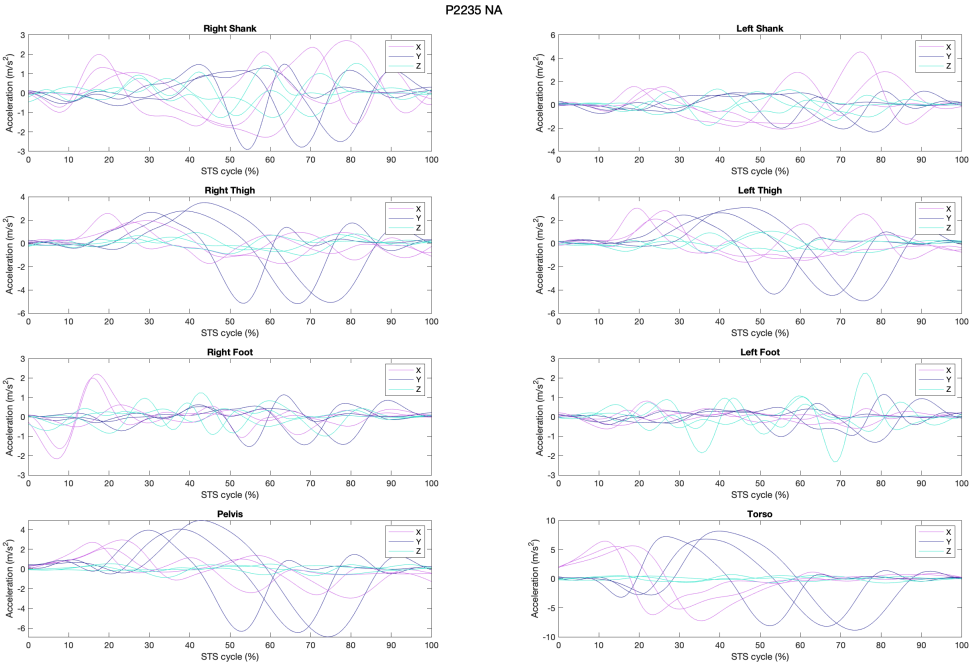

Figure 57: The segment accelerations in m/s^2 in NA.

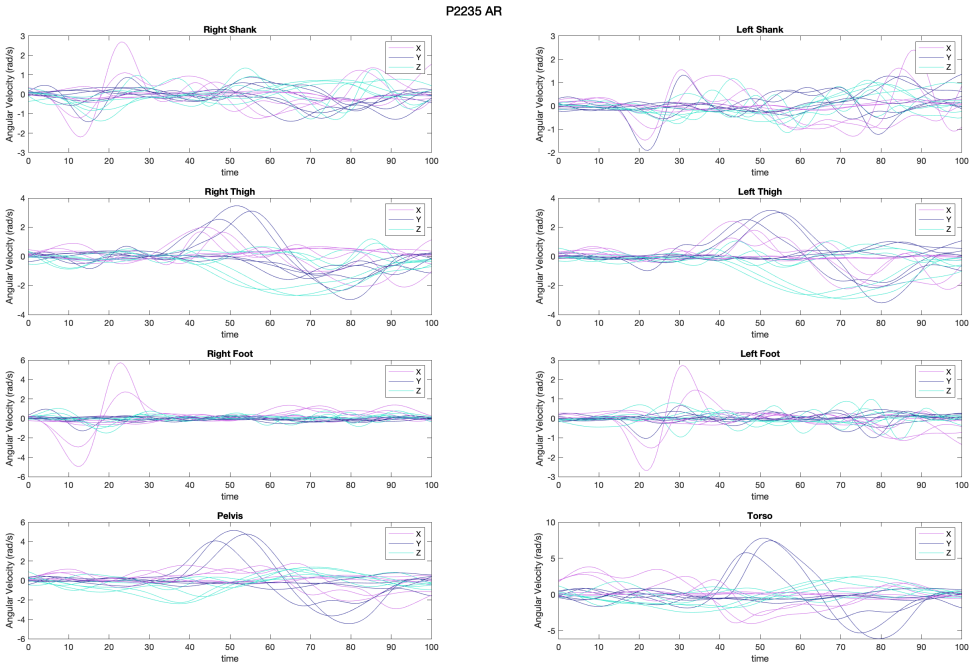

Figure 58: The segment angular velocity in radians per second in AR.

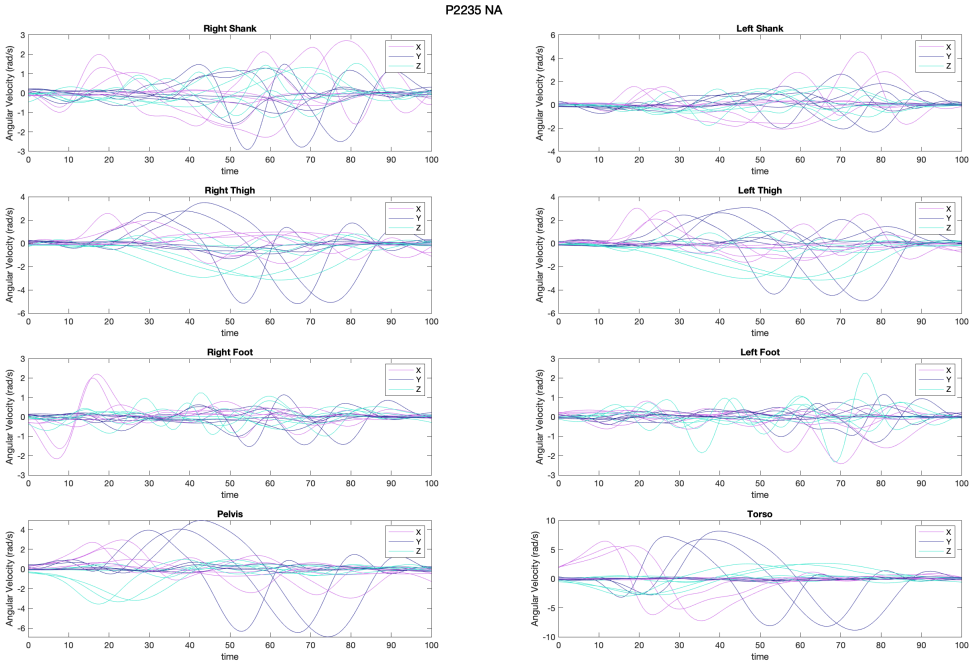

Figure 59: The segment angular velocity in radians per second in NA.

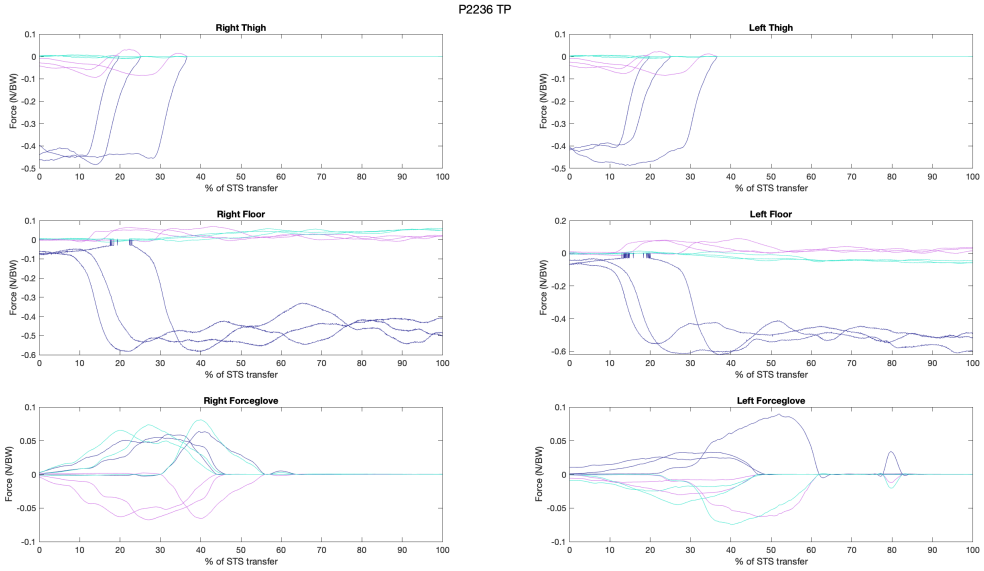

Figure 60: External Forces applied to the model in TP in N/BW.

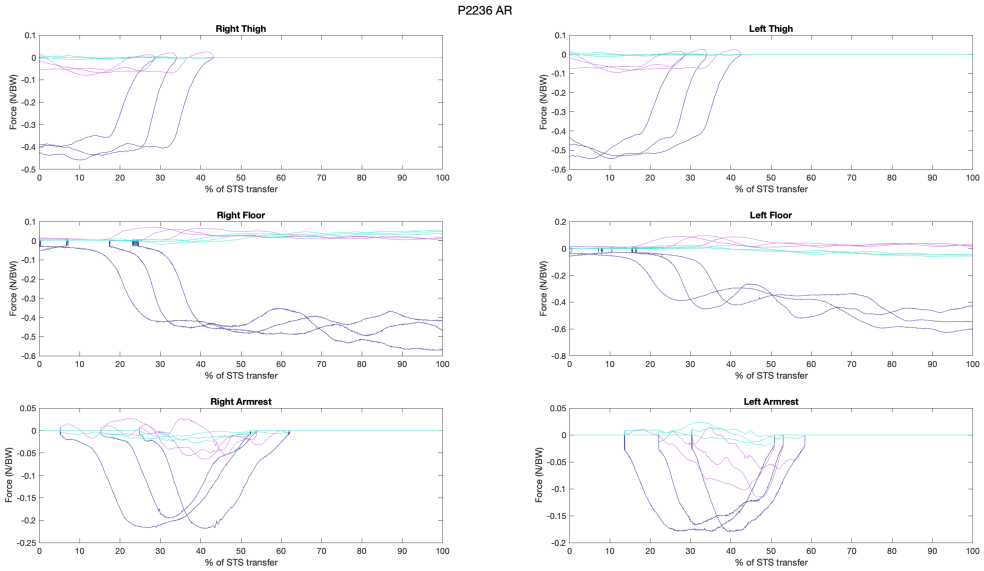

Figure 61: External Forces applied to the model in AR in N/BW.

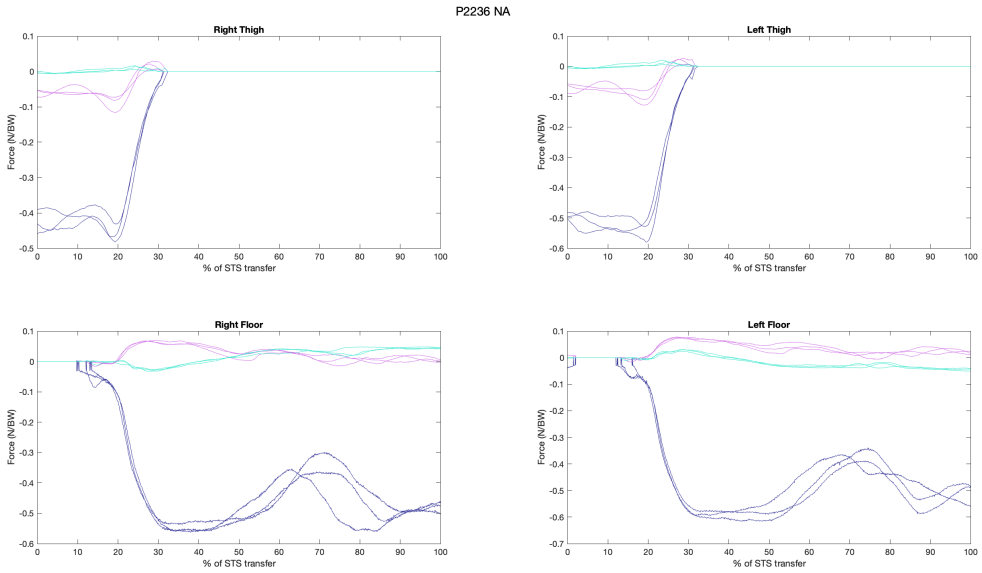

Figure 62: External Forces applied to the model in NA in N/BW.

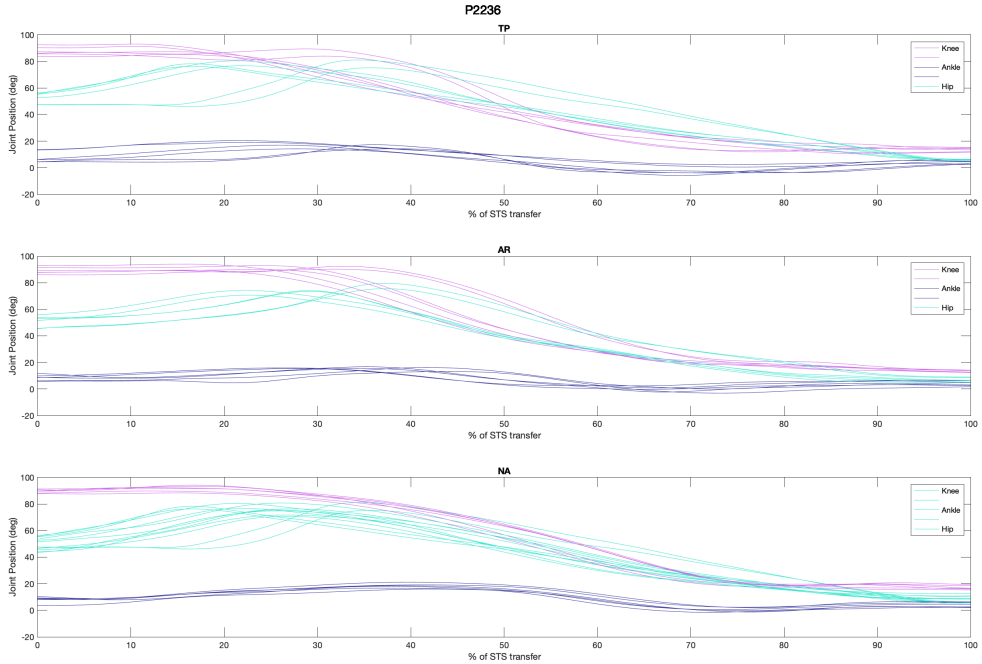

Figure 63: Joint Positions of the knee, hip, and ankle joint in the three different conditions

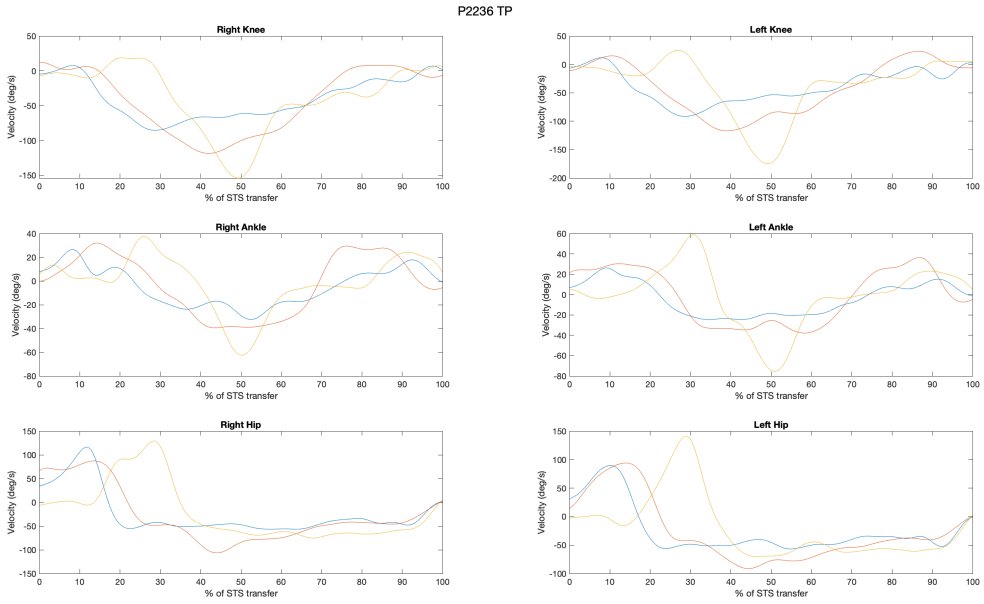

Figure 64: Joint velocities of the hip, knee and ankle joint in TP.

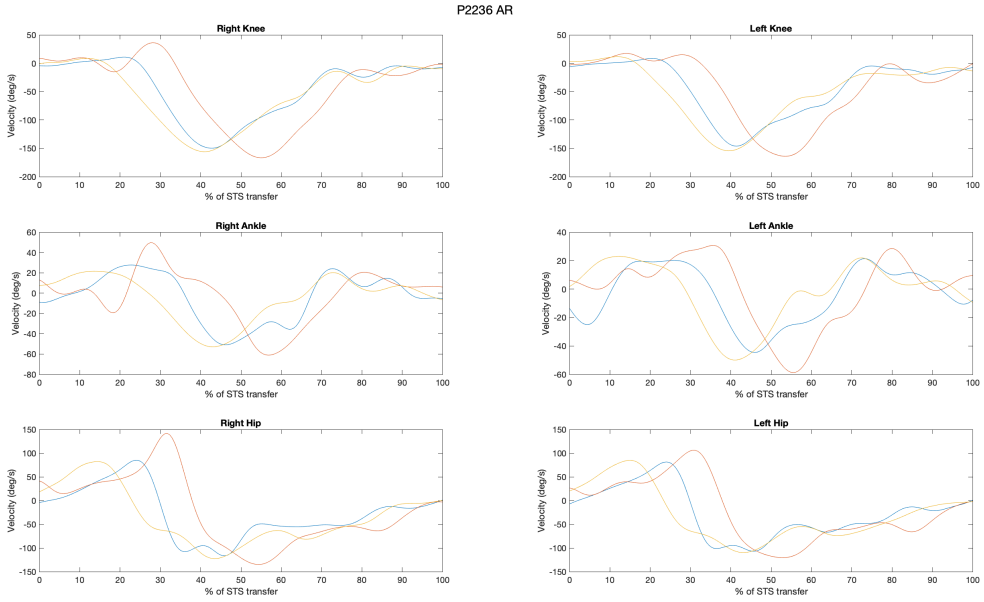

Figure 65: Joint velocities of the hip, knee and ankle joint in AR.

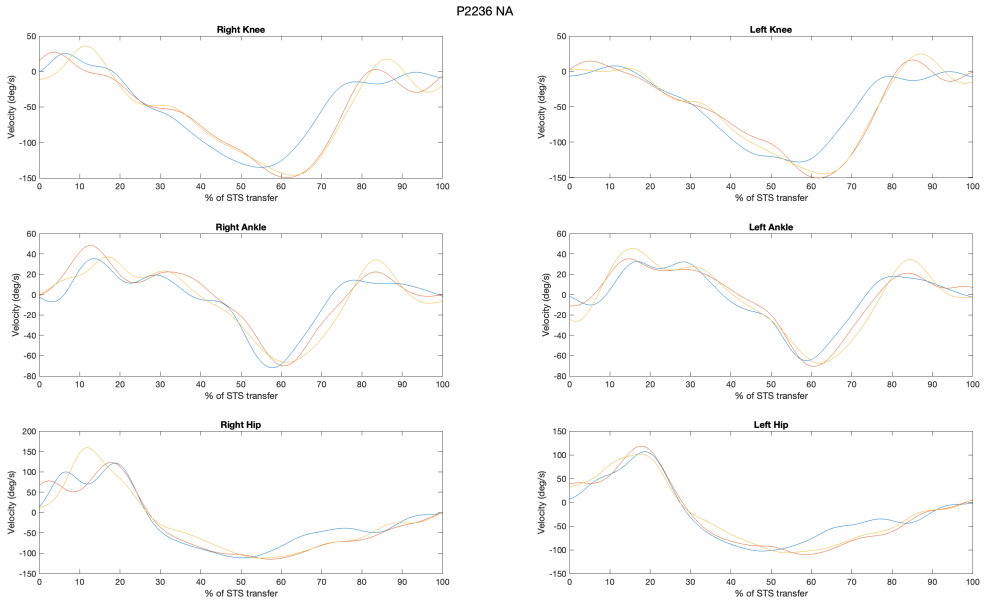

Figure 66: Joint velocities of the hip, knee and ankle joint in NA.

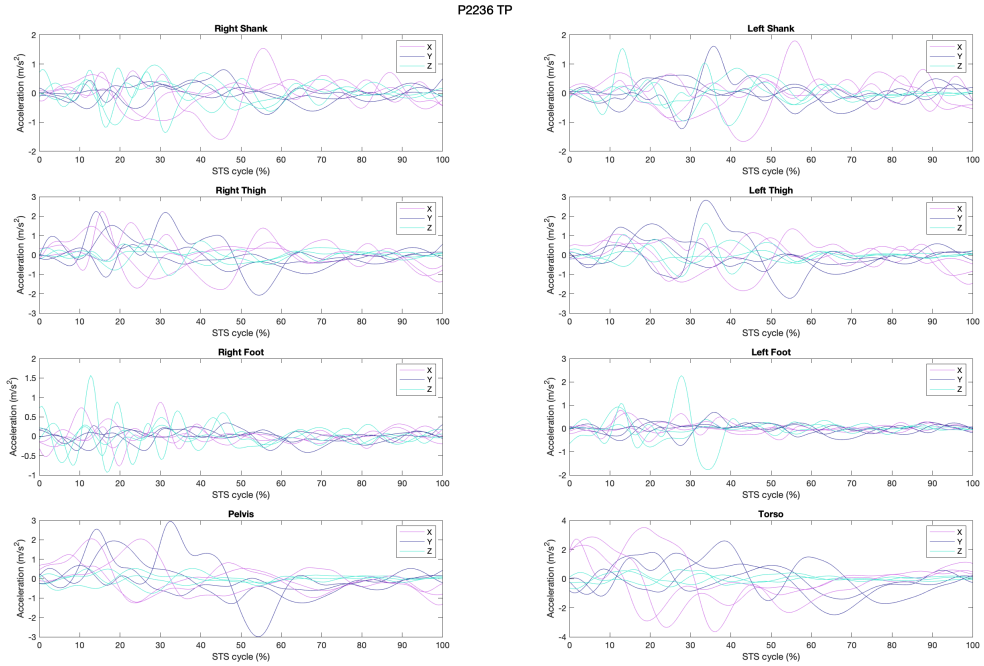

Figure 67: The segment accelerations in m/s^2 in TP.

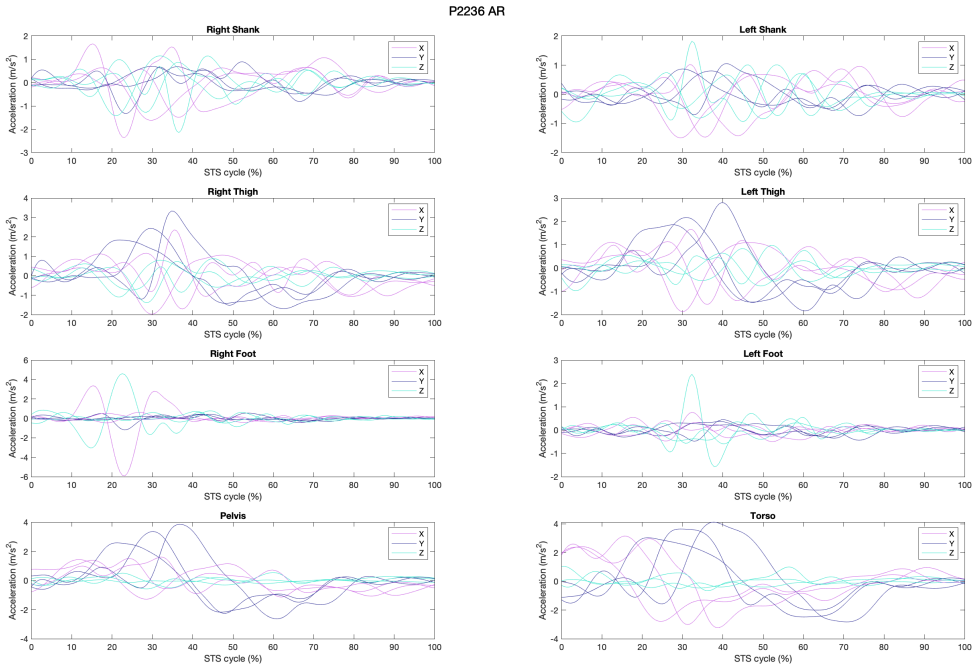

Figure 68: The segment accelerations in m/s^2 in AR.

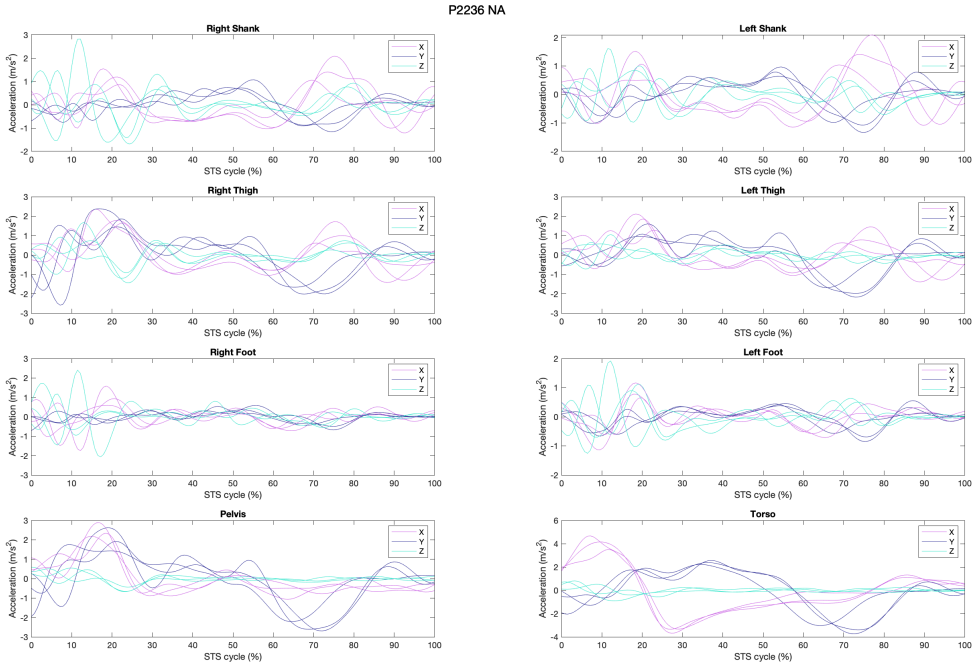

Figure 69: The segment accelerations in m/s^2 in NA.

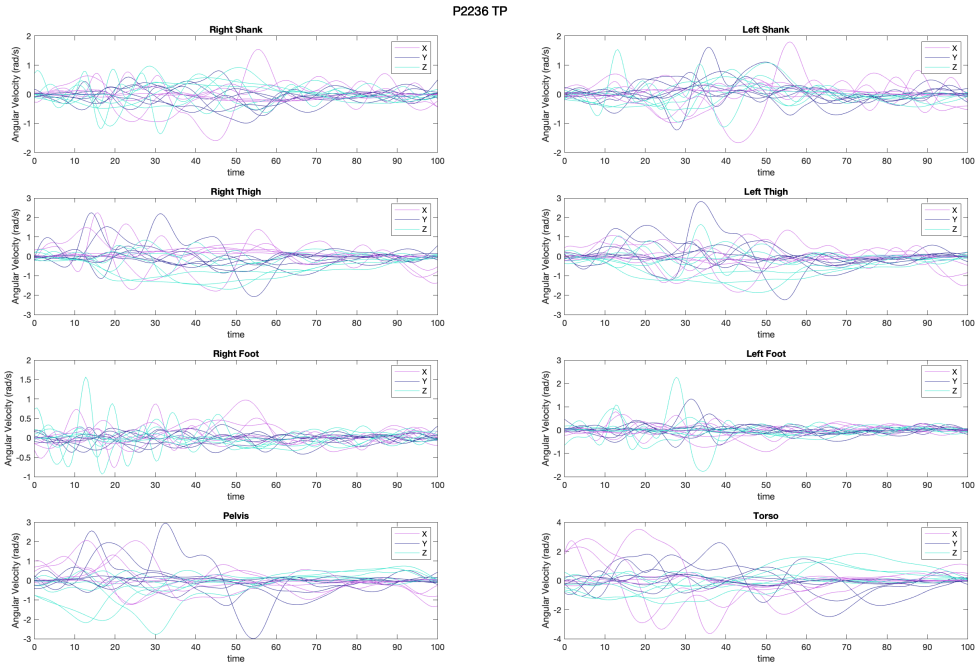

Figure 70: The segment angular velocity in radians per second in TP.

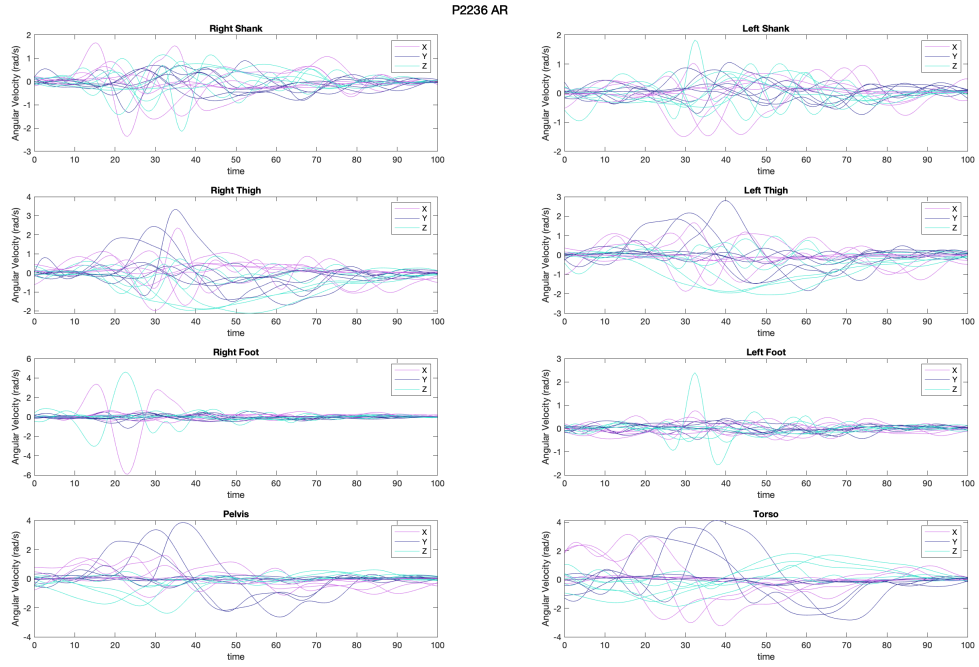

Figure 71: The segment angular velocity in radians per second in AR.

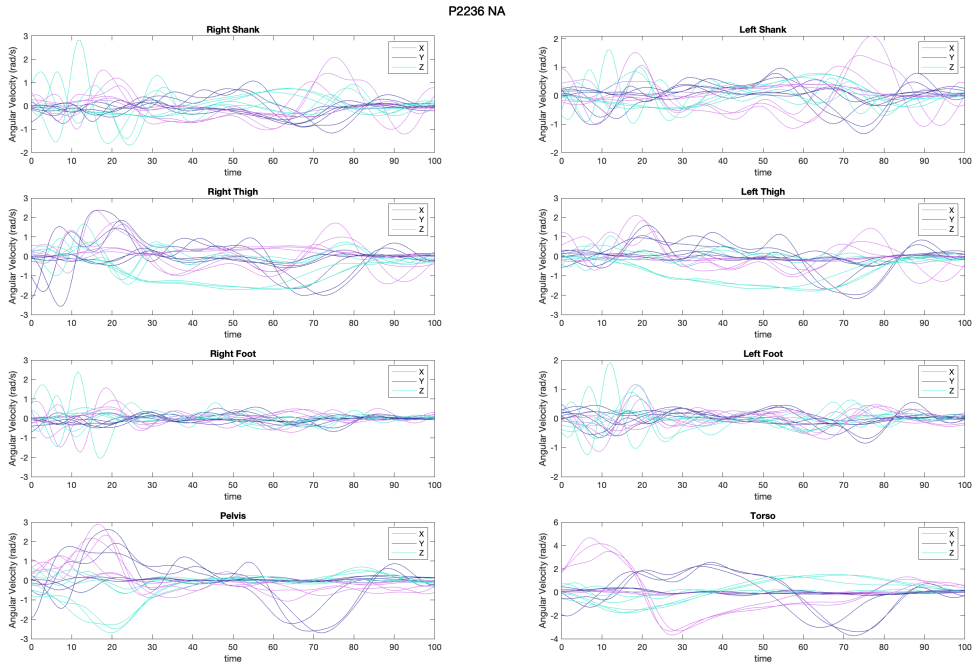

Figure 72: The segment angular velocity in radians per second in NA.

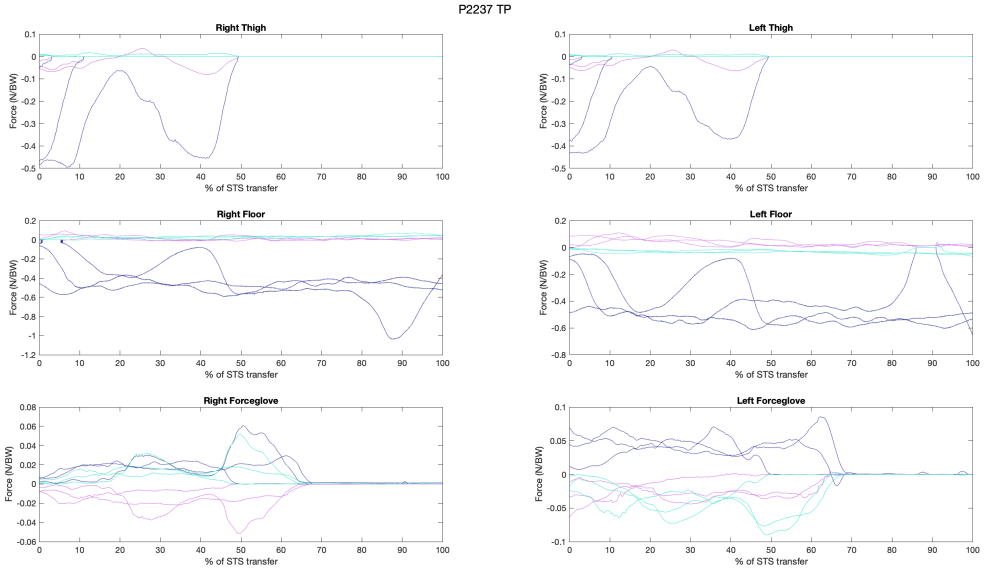

Figure 73: External Forces applied to the model in TP in N/BW.

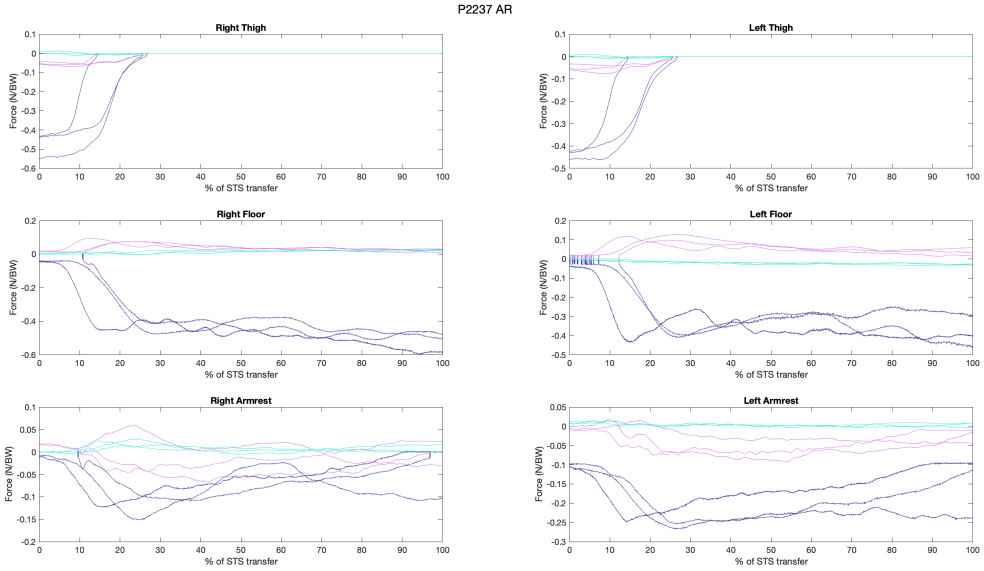

Figure 74: External Forces applied to the model in AR in N/BW.

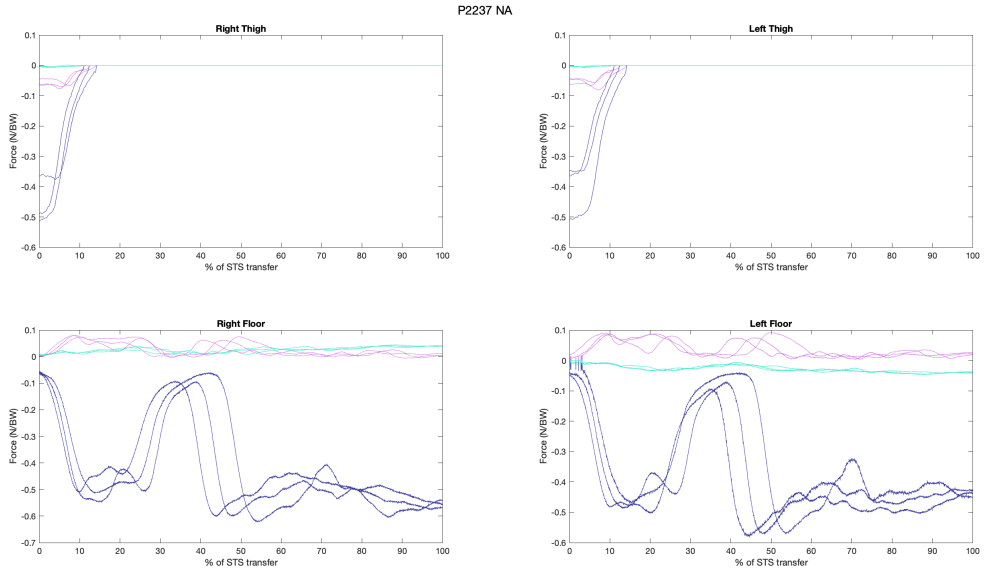

Figure 75: External Forces applied to the model in NA in N/BW.

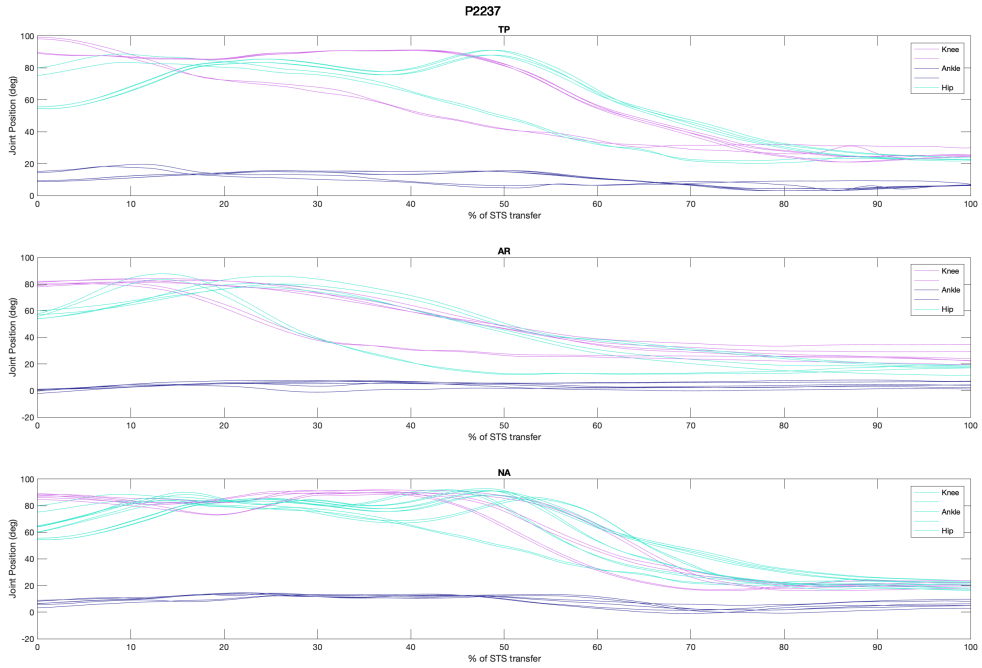

Figure 76: Joint Positions of the knee, hip, and ankle joint in the three different conditions

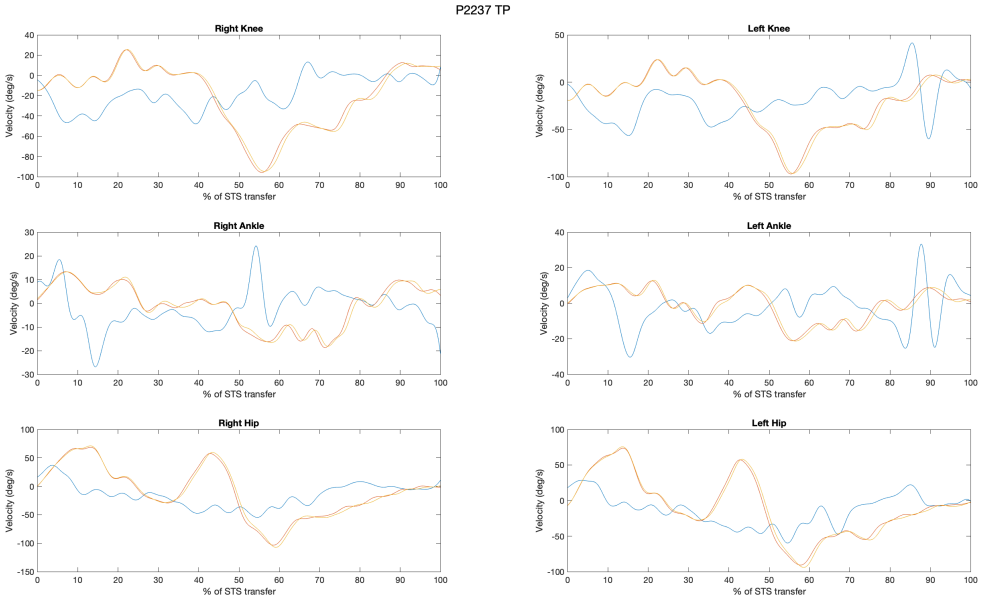

Figure 77: Joint velocities of the hip, knee and ankle joint in TP.

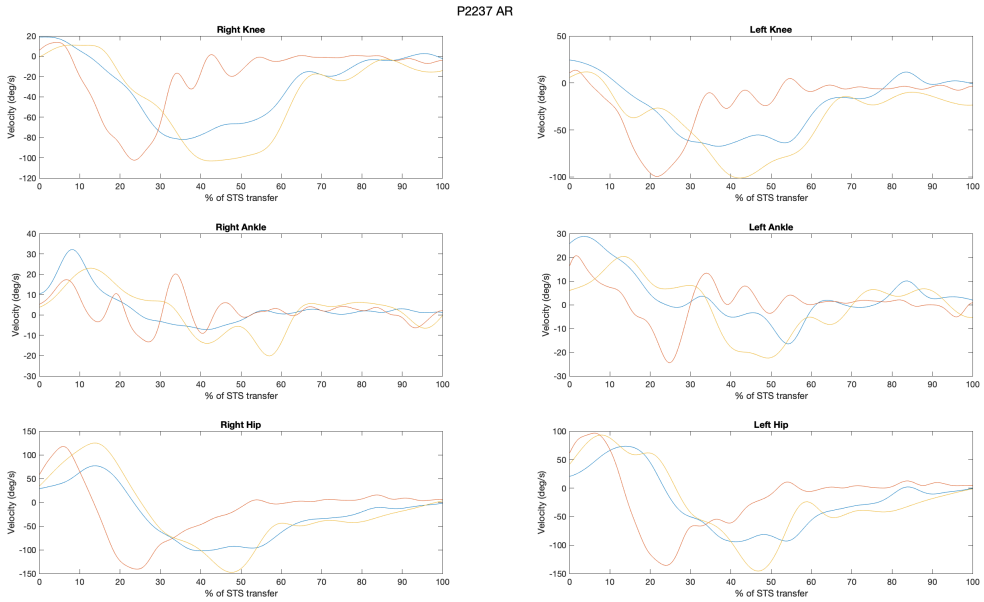

Figure 78: Joint velocities of the hip, knee and ankle joint in AR.

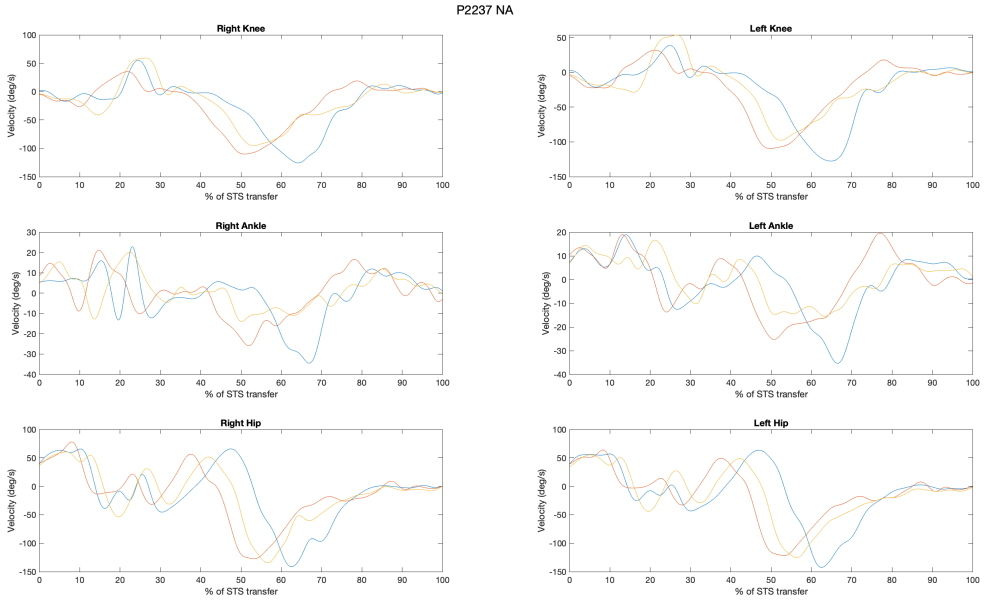

Figure 79: Joint velocities of the hip, knee and ankle joint in NA.

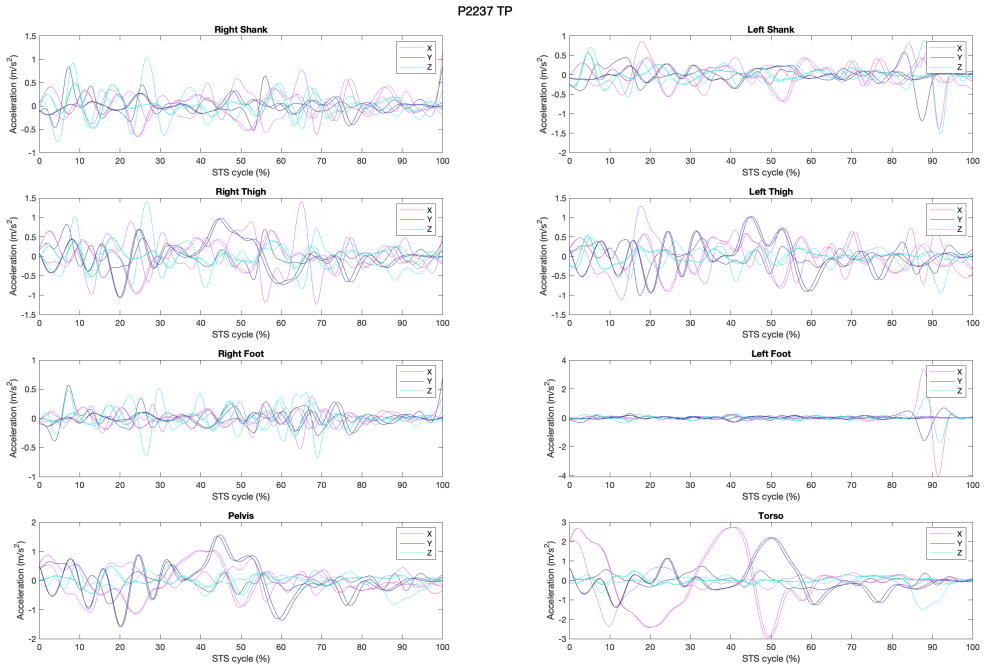

Figure 80: The segment accelerations in m/s^2 in TP.

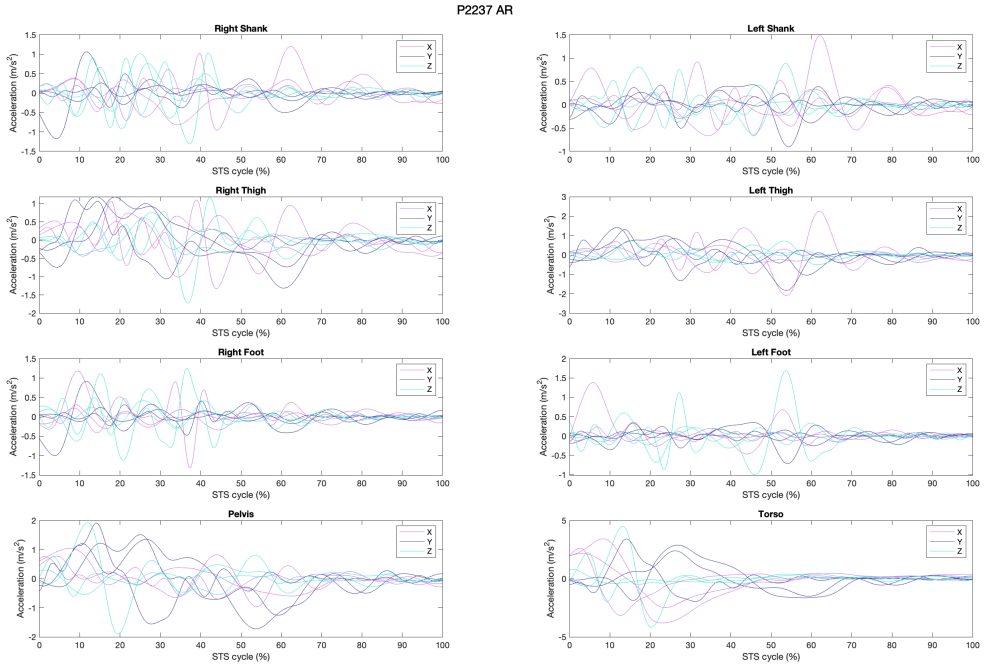

Figure 81: The segment accelerations in m/s^2 in AR.

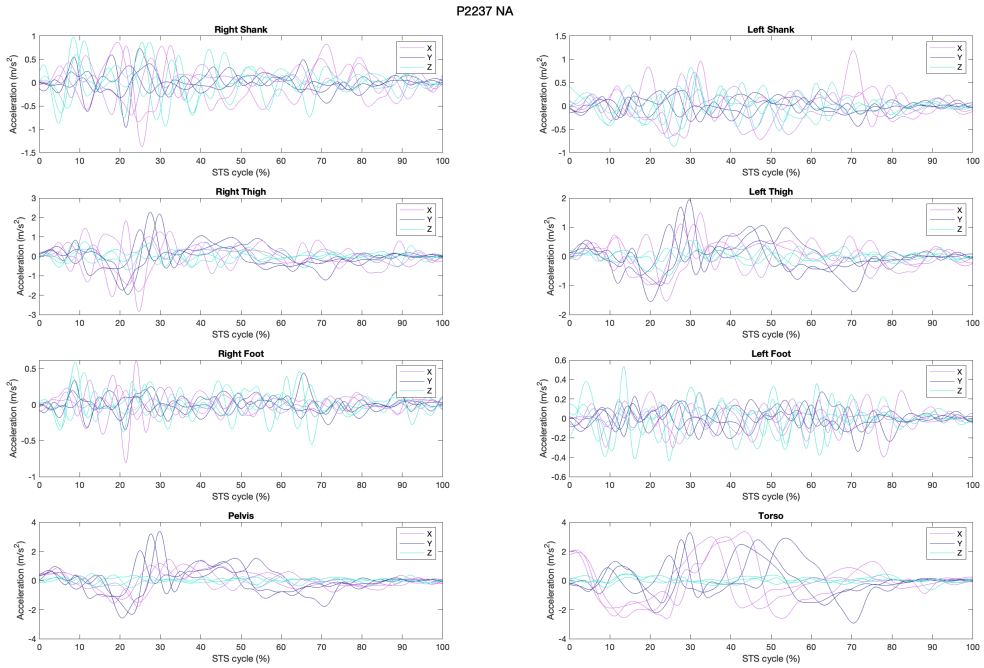

Figure 82: The segment accelerations in m/s^2 in NA.

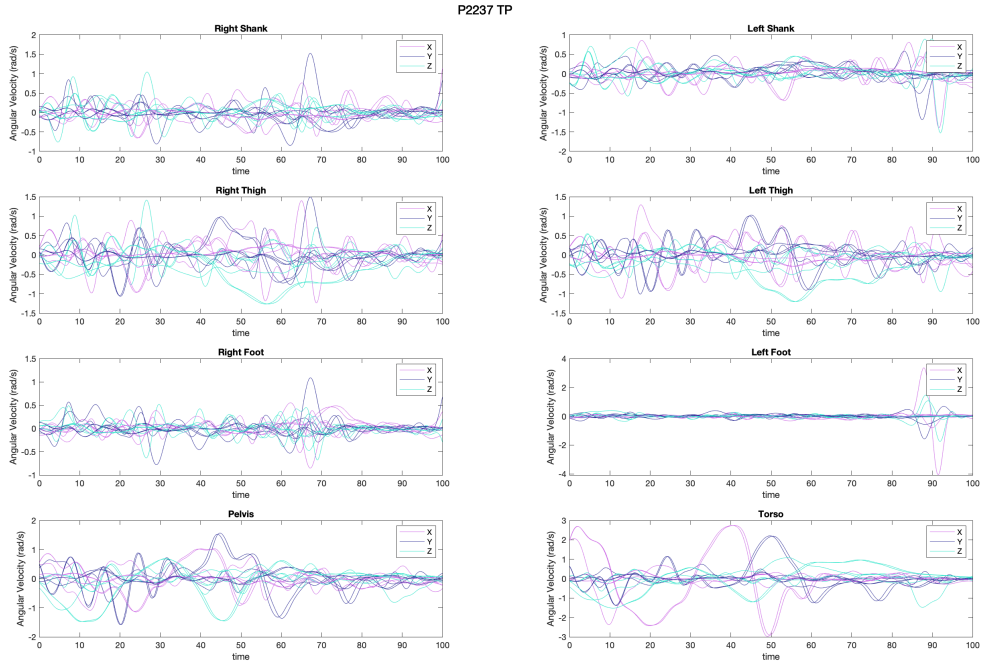

Figure 83: The segment angular velocity in radians per second in TP.

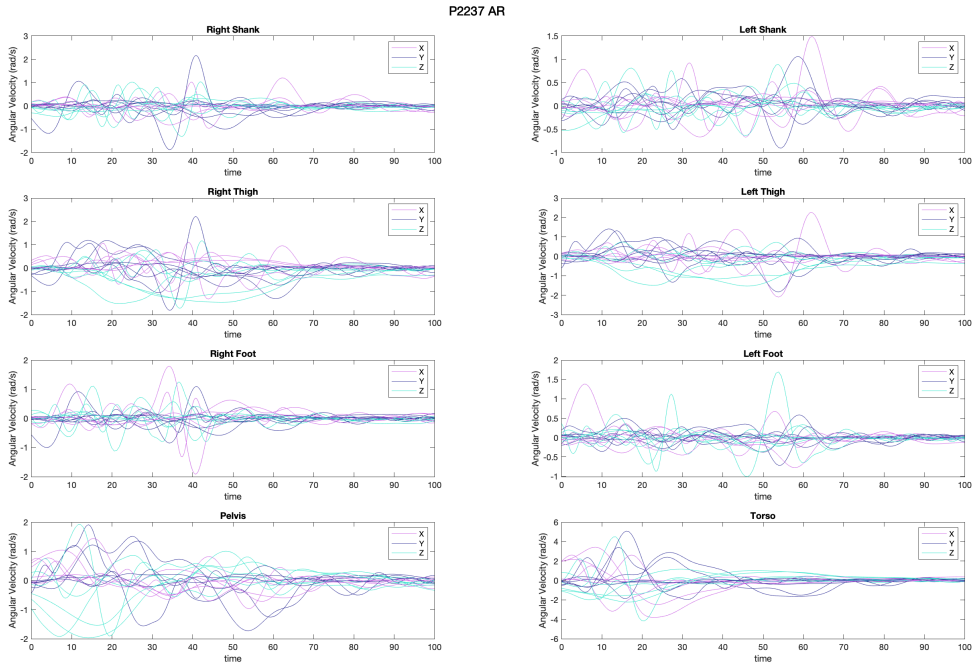

Figure 84: The segment angular velocity in radians per second in AR.

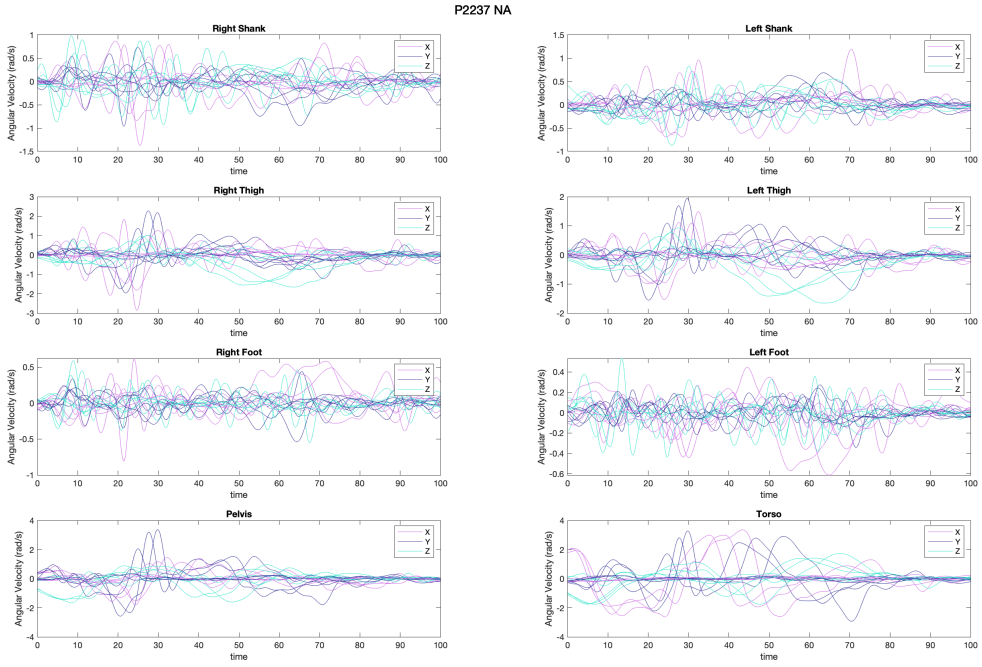

Figure 85: The segment angular velocity in radians per second in NA.

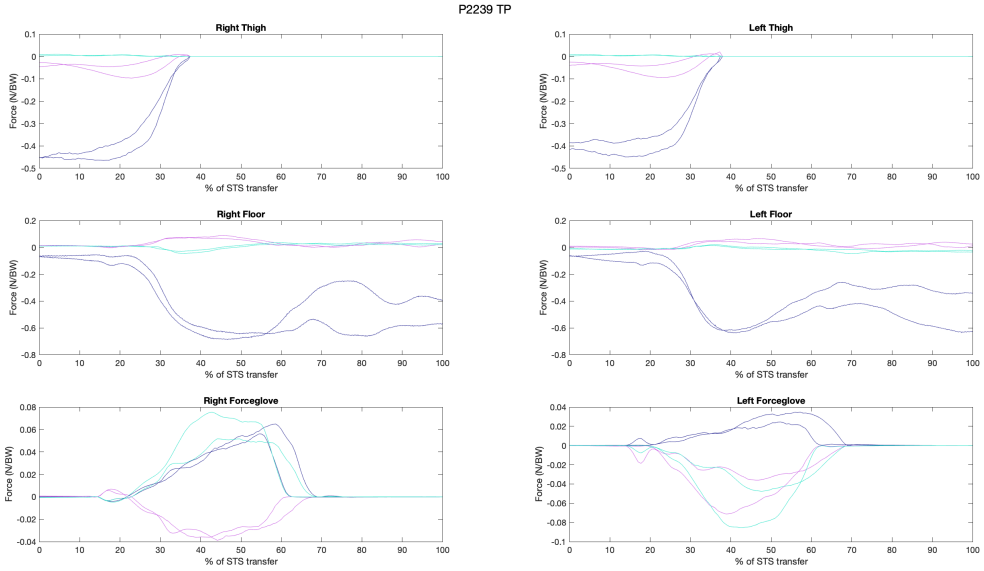

Figure 86: External Forces applied to the model in TP in N/BW.

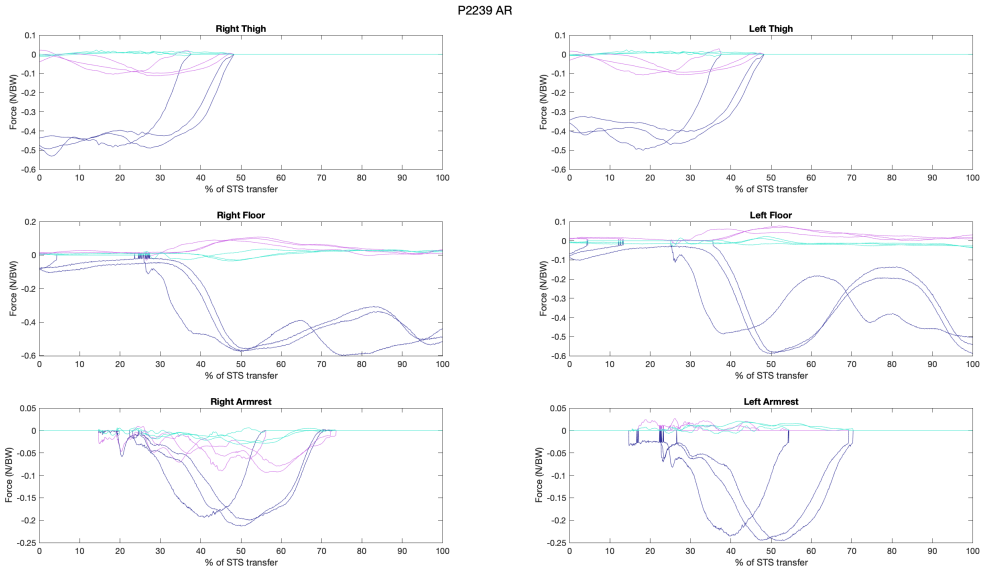

Figure 87: External Forces applied to the model in AR in N/BW.

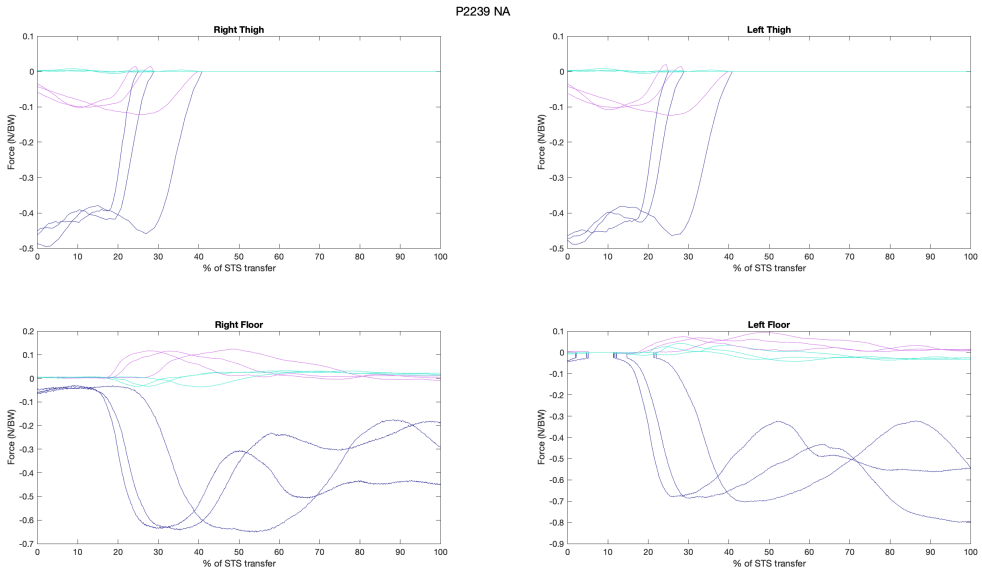

Figure 88: External Forces applied to the model in NA in N/BW.

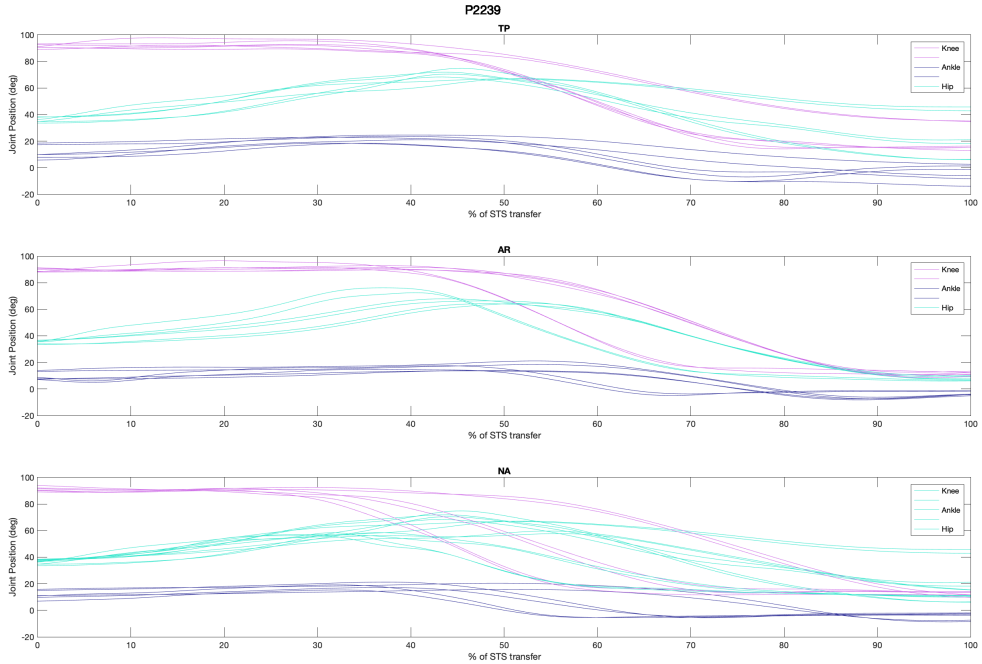

Figure 89: Joint Positions of the knee, hip, and ankle joint in the three different conditions

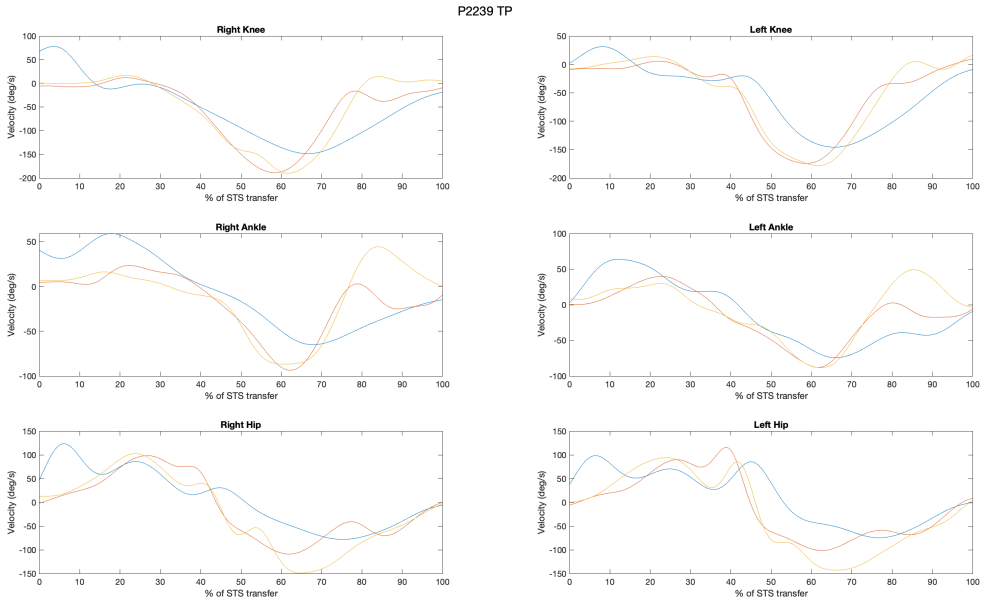

Figure 90: Joint velocities of the hip, knee and ankle joint in TP.

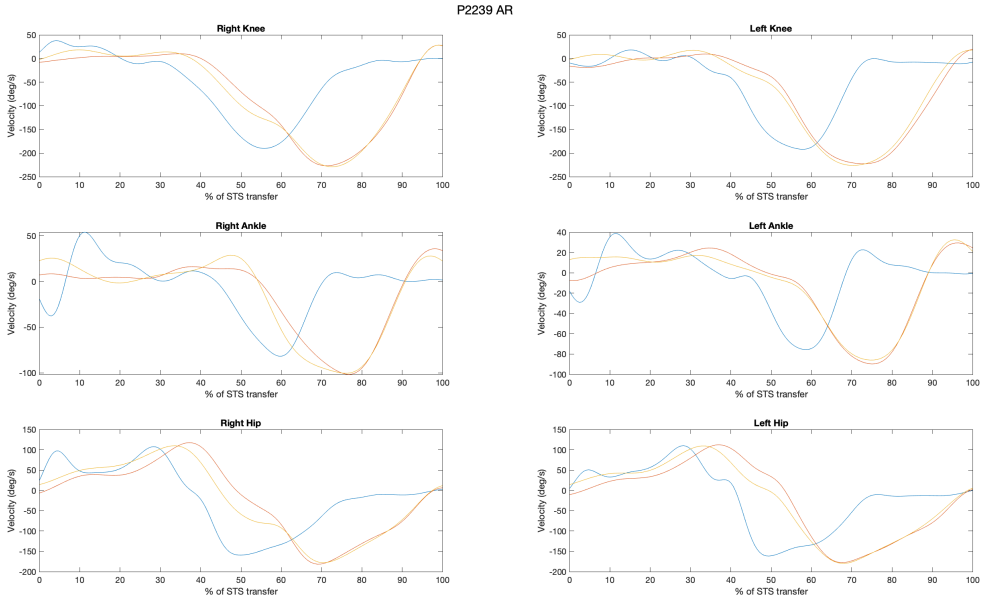

Figure 91: Joint velocities of the hip, knee and ankle joint in AR.

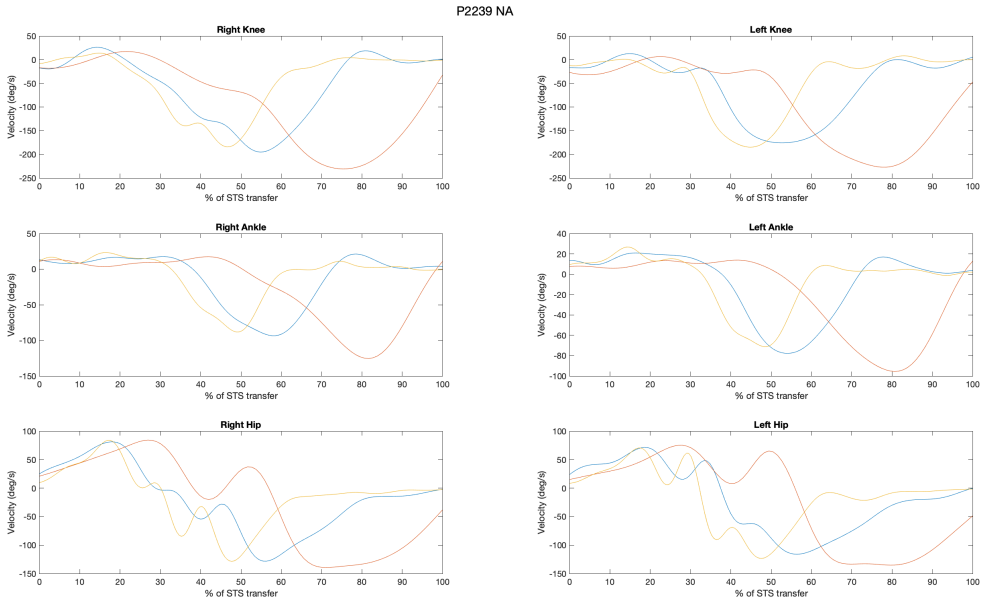

Figure 92: Joint velocities of the hip, knee and ankle joint in NA.

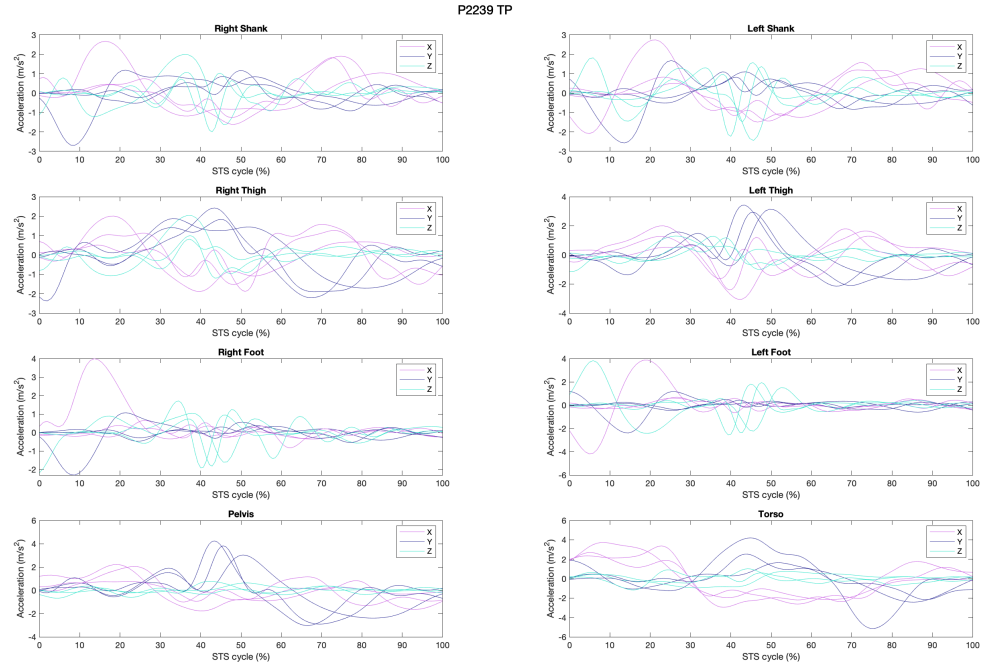

Figure 93: The segment accelerations in m/s^2 in TP.

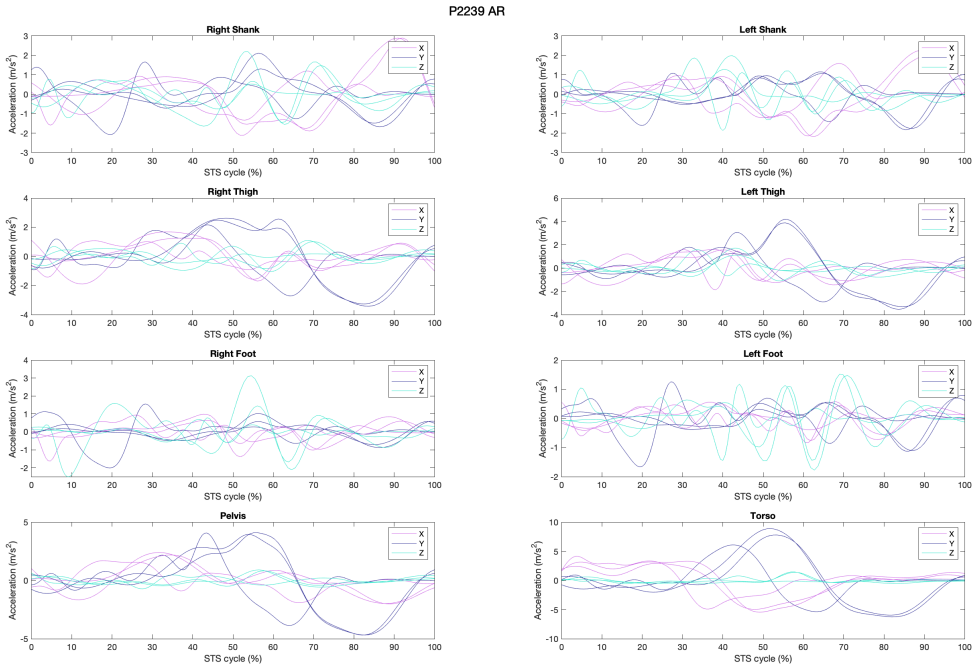

Figure 94: The segment accelerations in m/s^2 in AR.

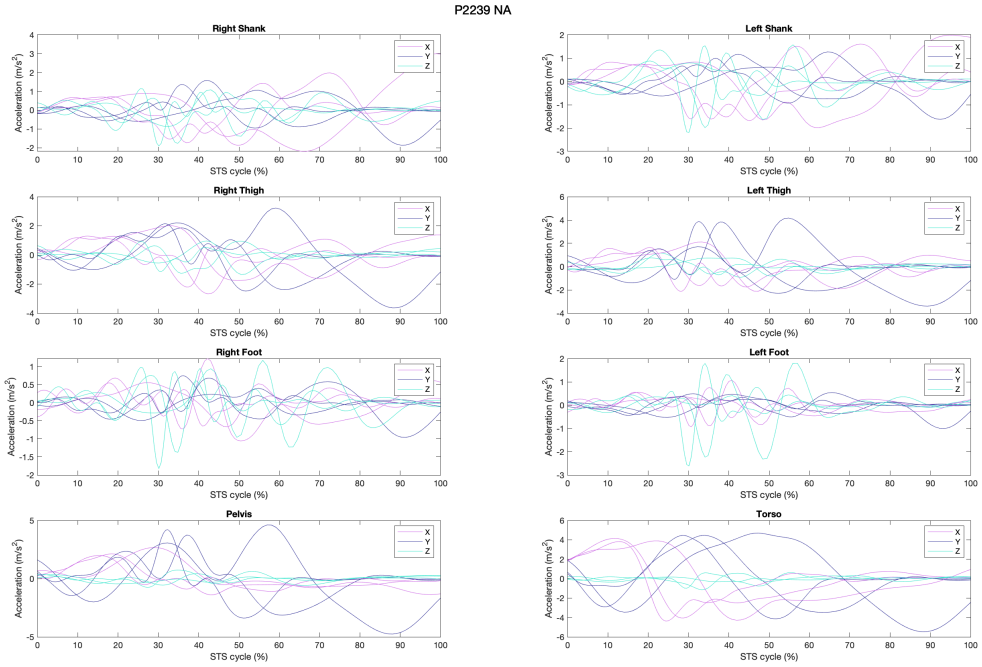

Figure 95: The segment accelerations in m/s^2 in NA.

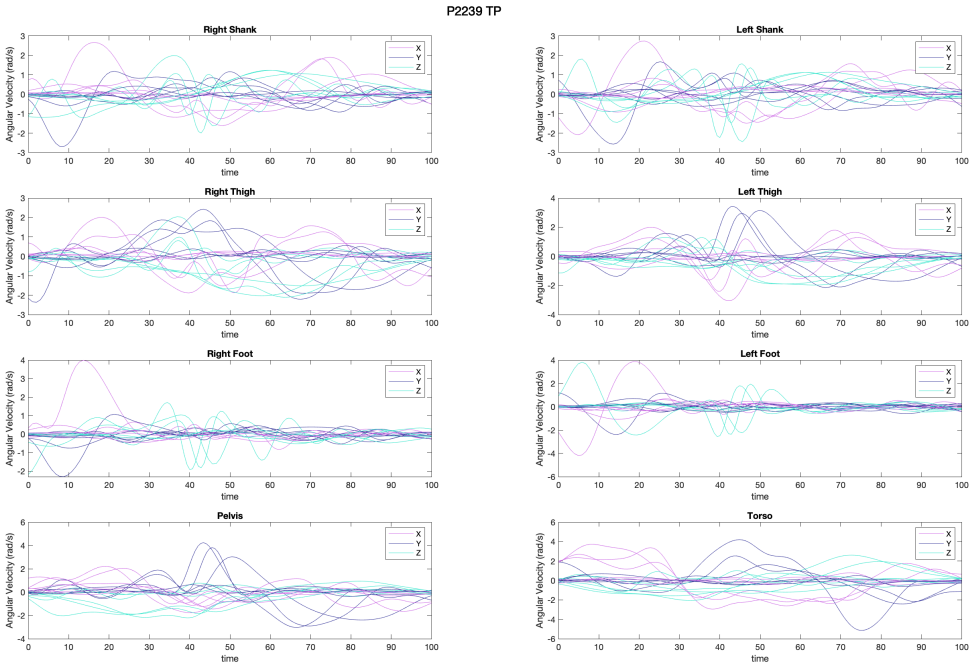

Figure 96: The segment angular velocity in radians per second in TP.

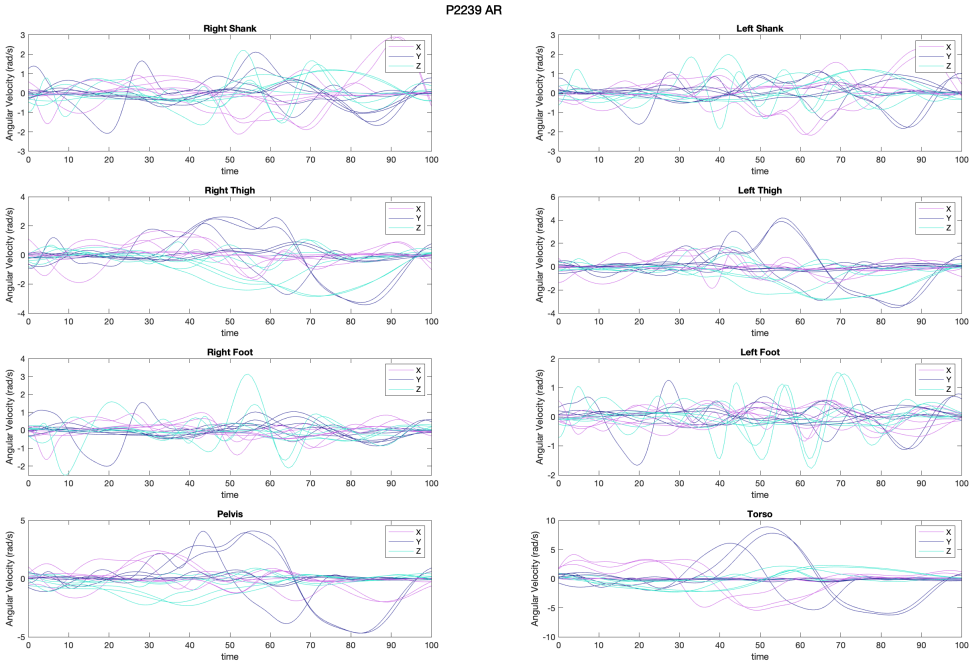

Figure 97: The segment angular velocity in radians per second in AR.

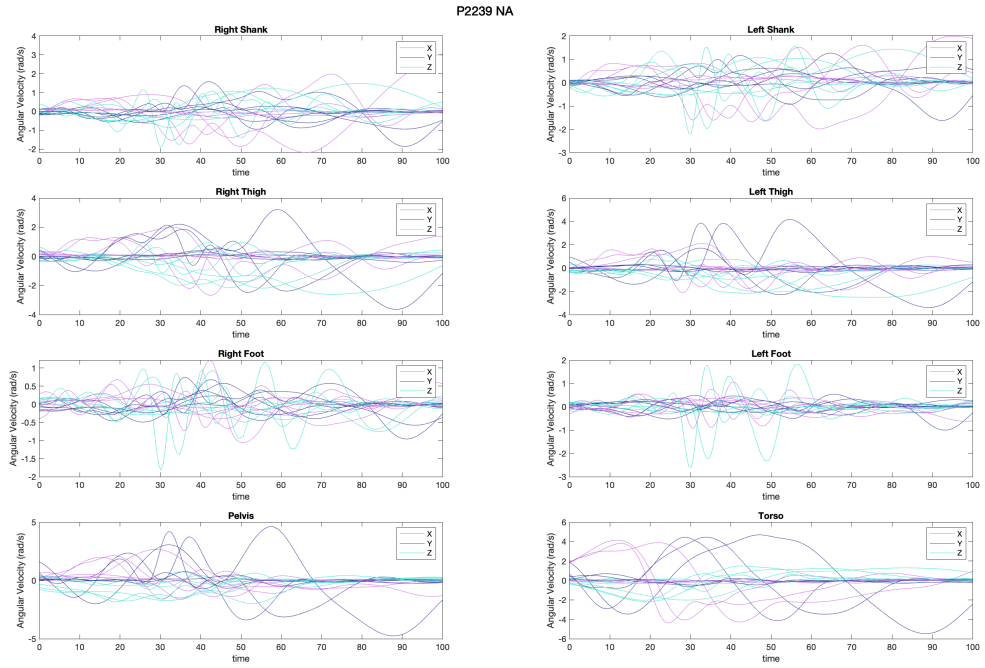

Figure 98: The segment angular velocity in radians per second in NA.

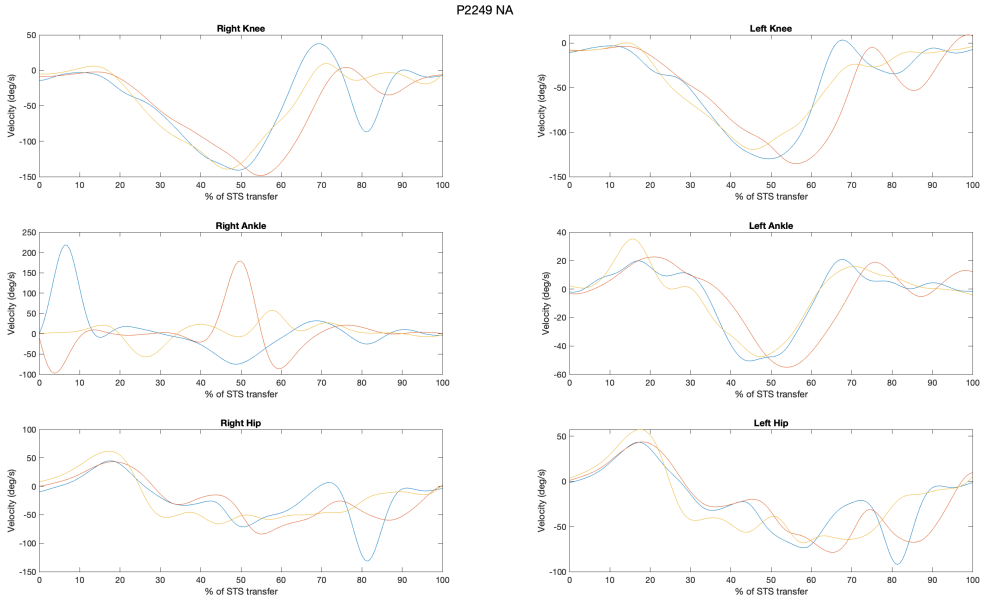

Figure 99: Joint velocities of the hip, knee and ankle joint in NA.

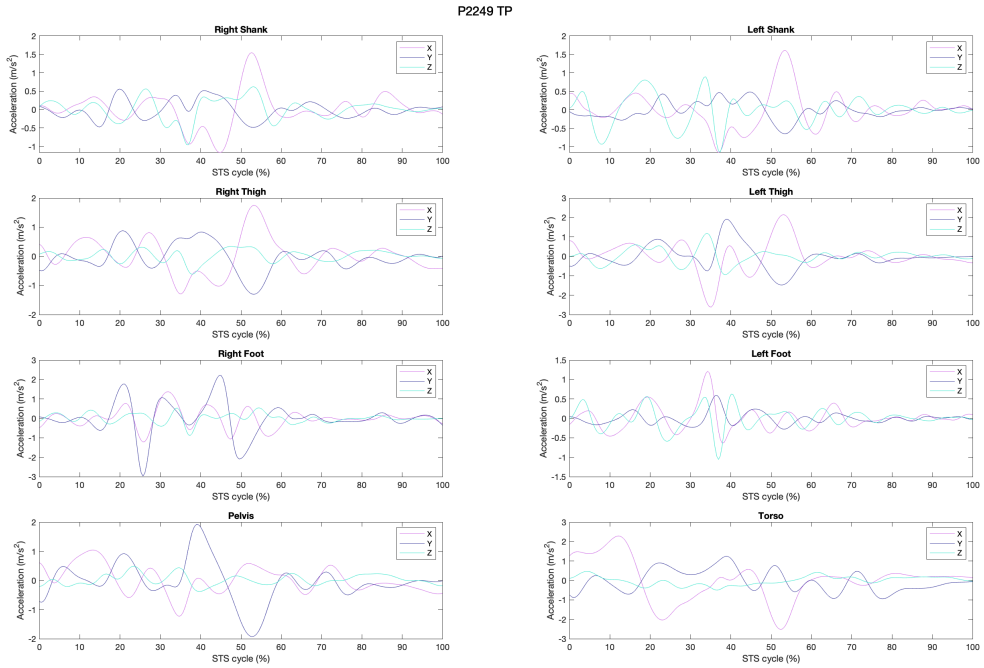

Figure 100: The segment accelerations in m/s^2 in TP.

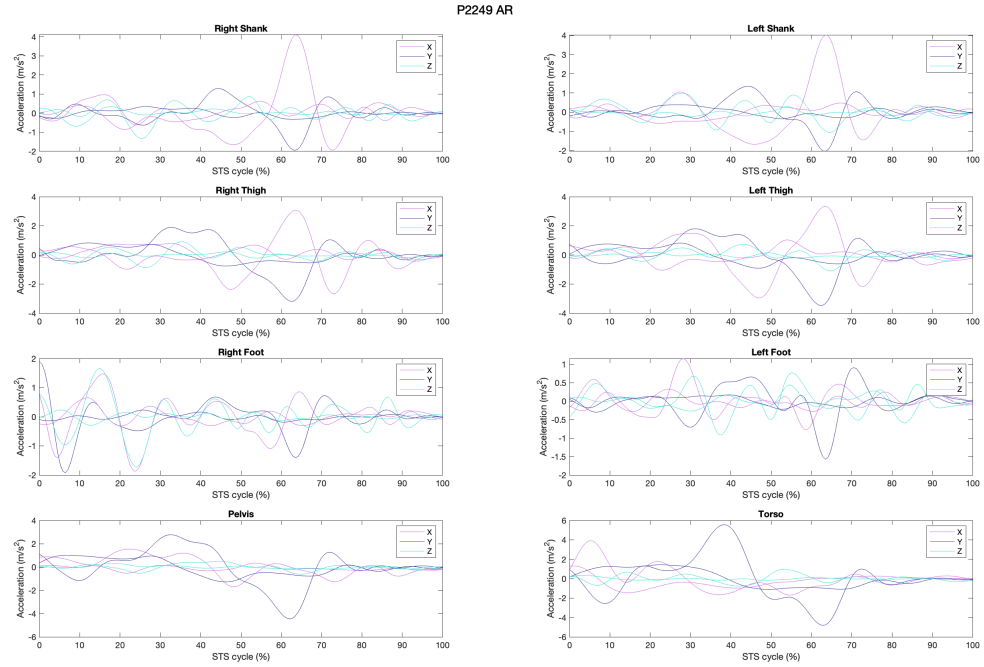

Figure 101: The segment accelerations in m/s^2 in AR.

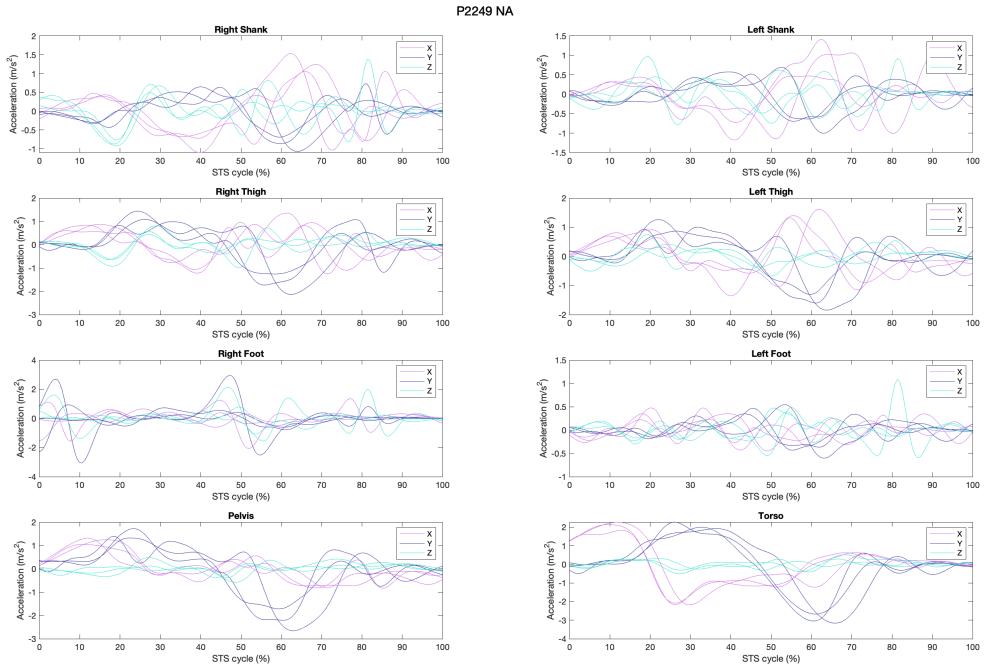

Figure 102: The segment accelerations in m/s^2 in NA.

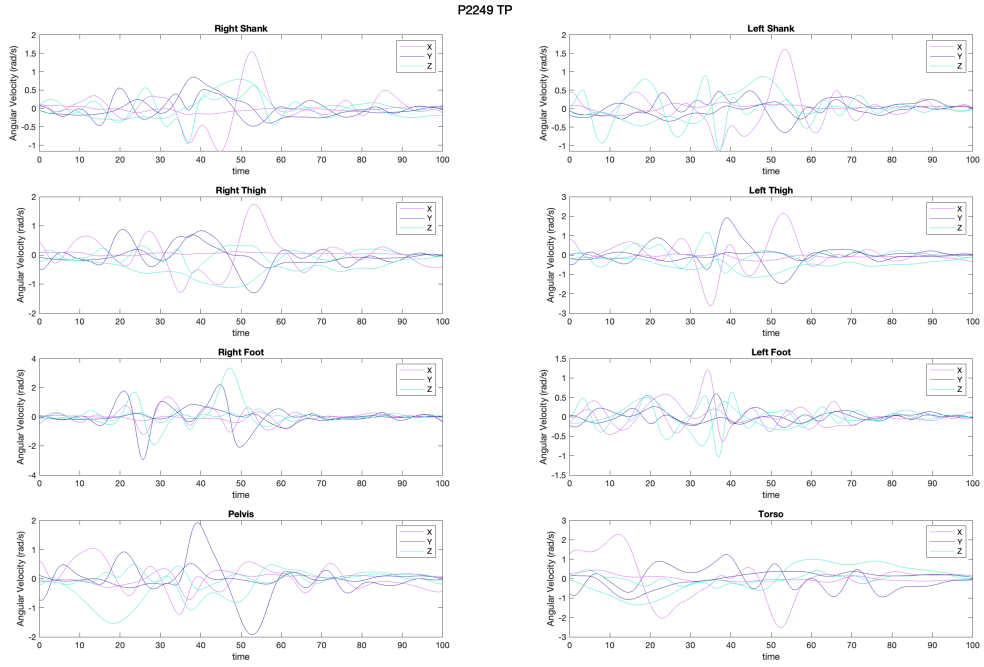

Figure 103: The segment angular velocity in radians per second in TP.

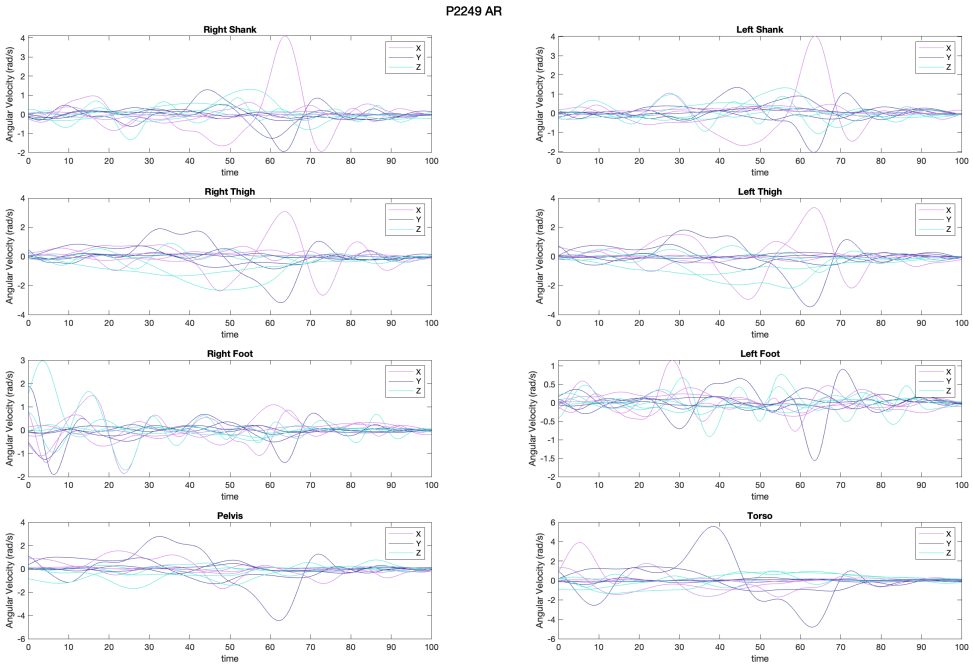

Figure 104: The segment angular velocity in radians per second in AR.

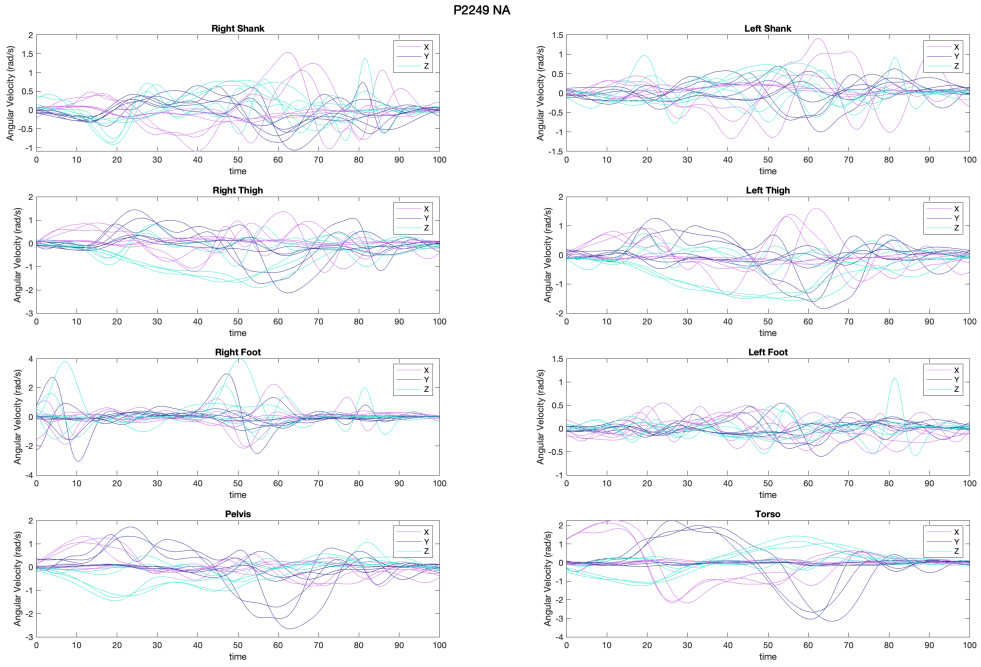

Figure 105: The segment angular velocity in radians per second in NA.

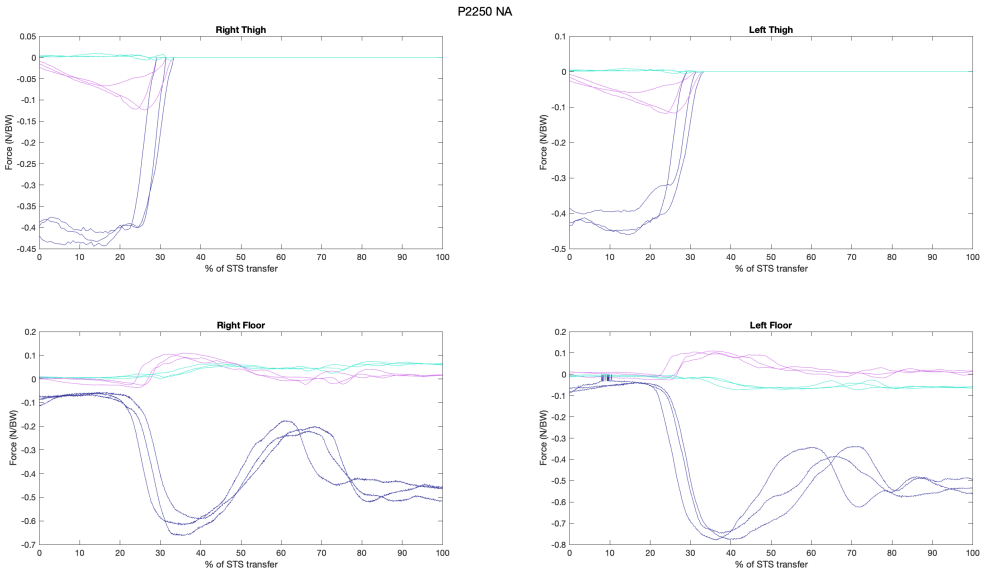

Figure 106: External Forces applied to the model in NA in N/BW.

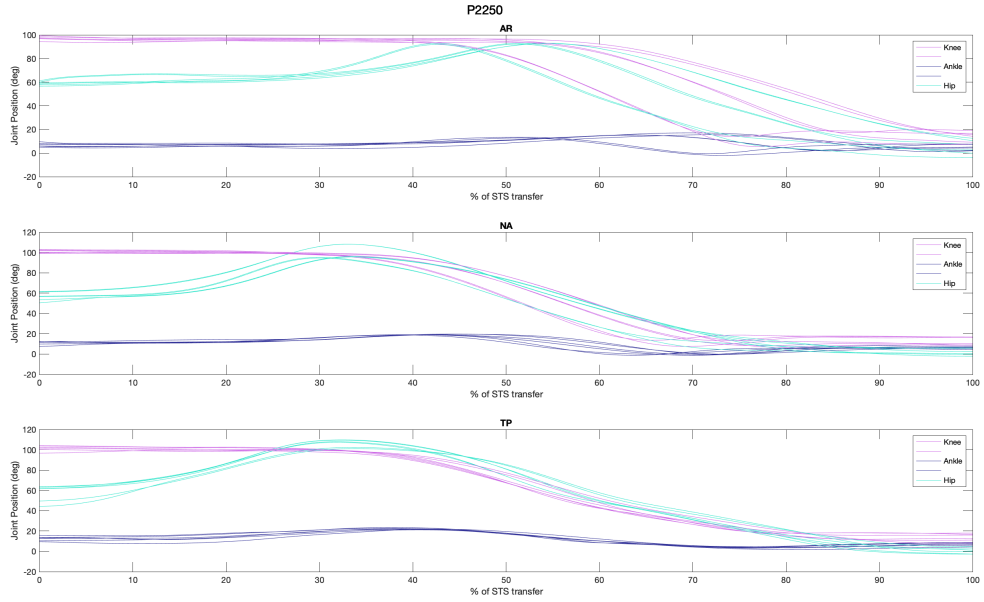

Figure 107: Joint Positions of the knee, hip, and ankle joint in the three different conditions

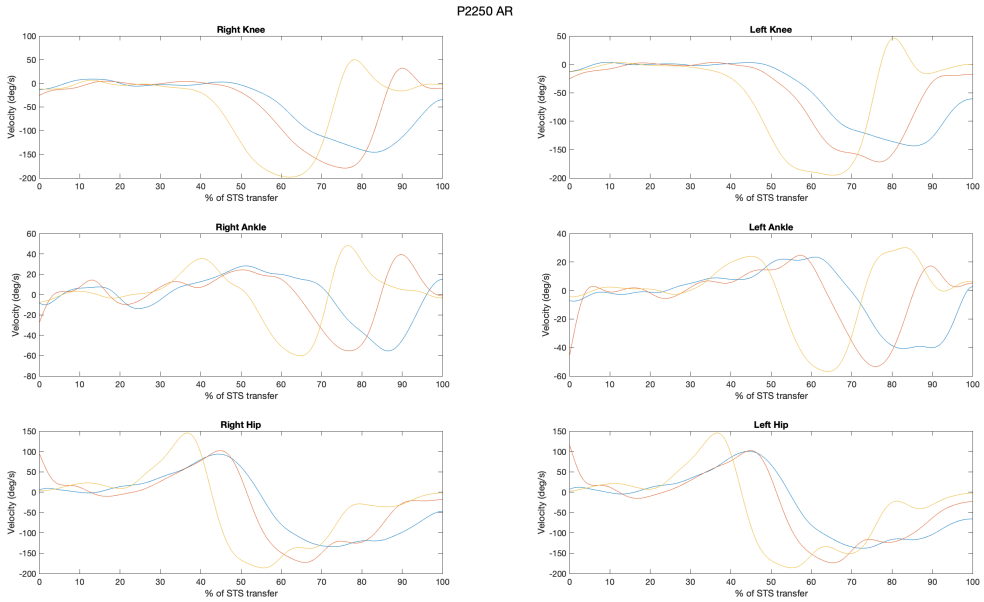

Figure 108: Joint velocities of the hip, knee and ankle joint in AR.

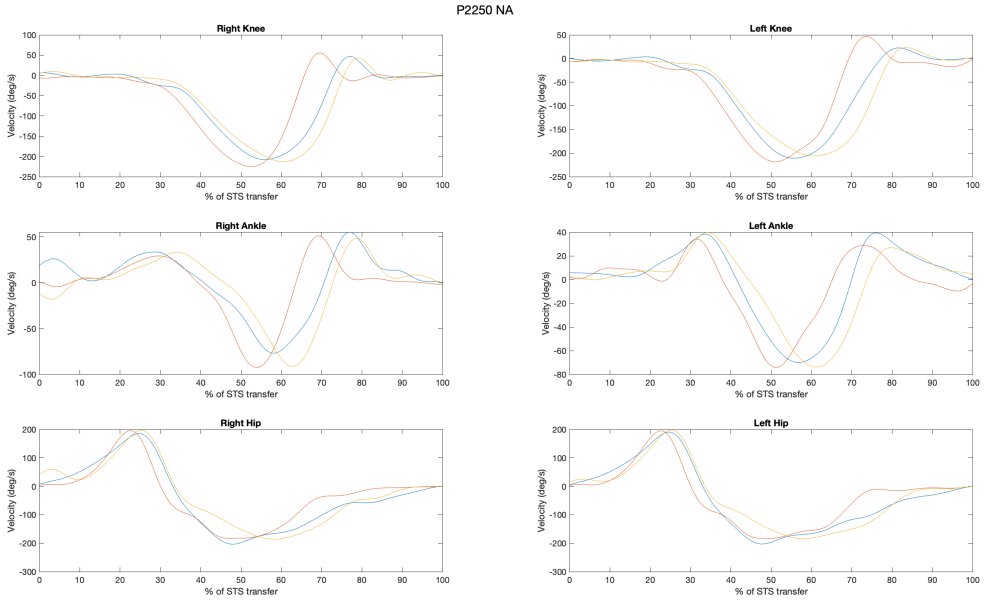

Figure 109: Joint velocities of the hip, knee and ankle joint in NA.

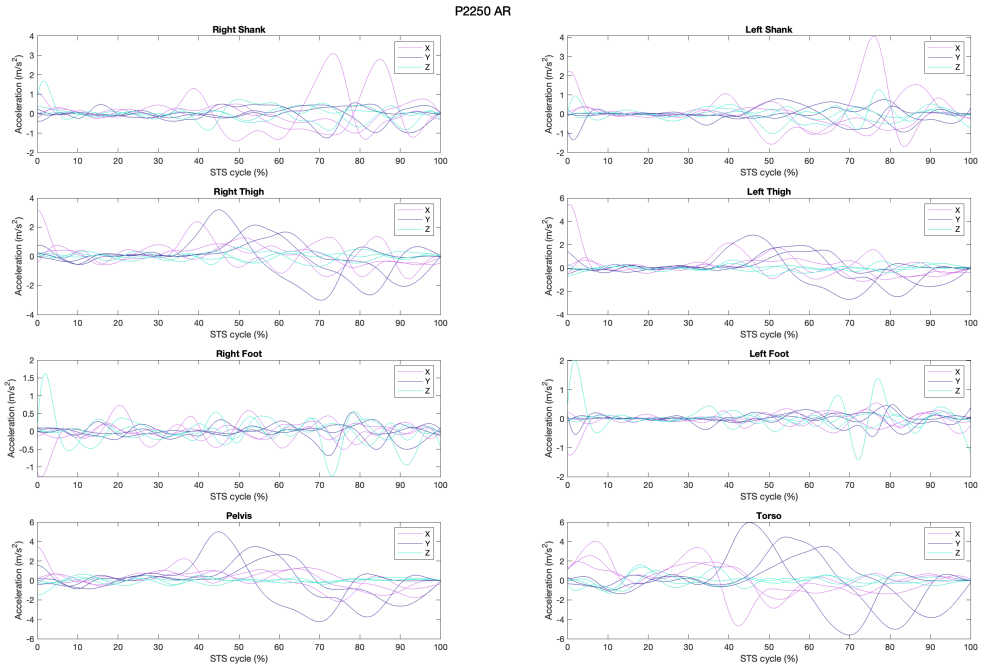

Figure 110: The segment accelerations in m/s^2 in AR.

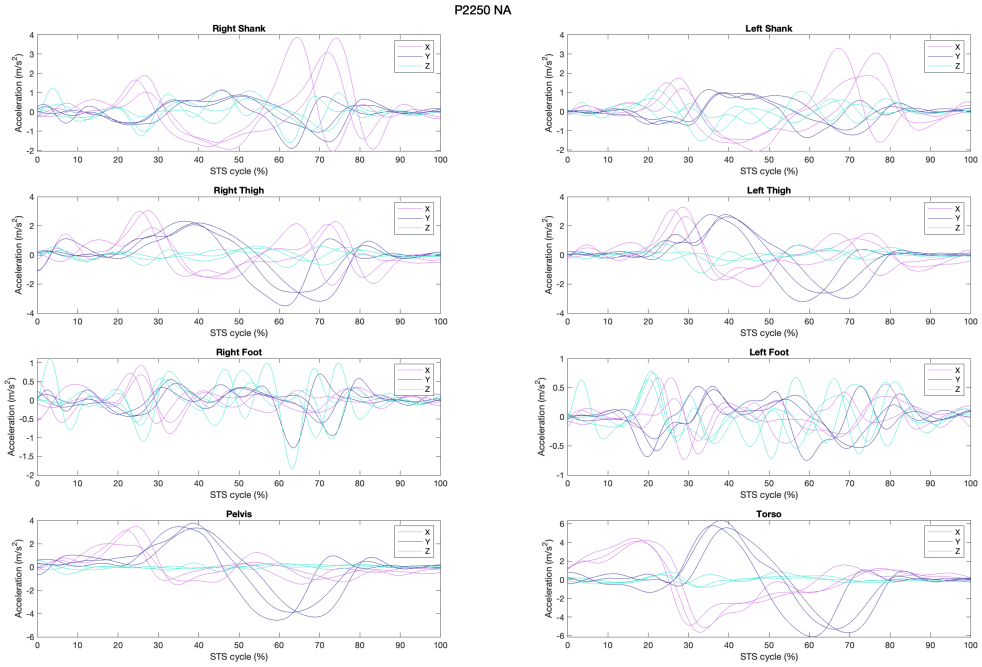

Figure 111: The segment accelerations in m/s^2 in NA.

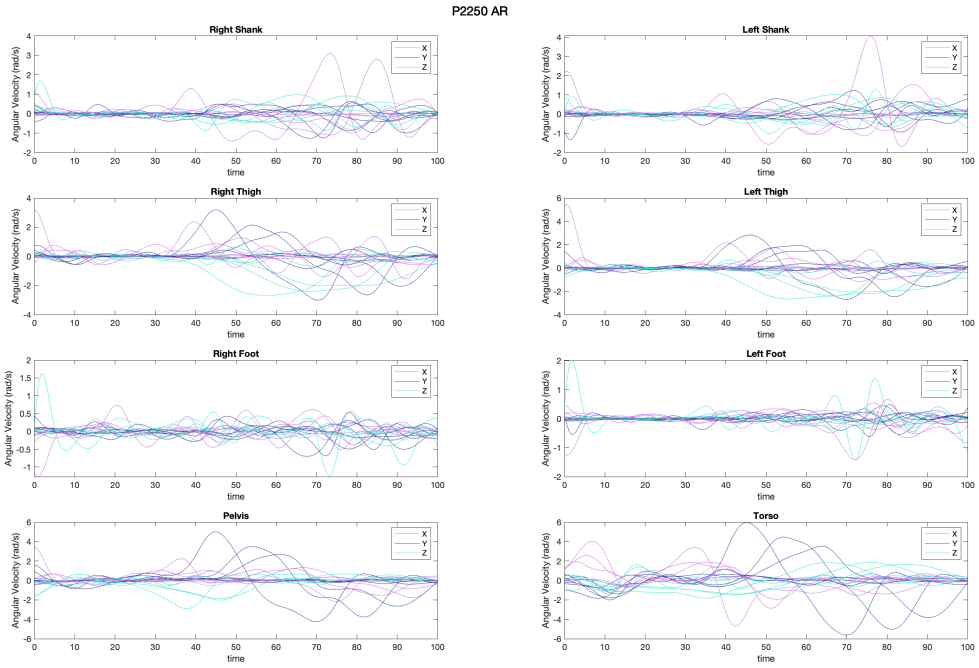

Figure 112: The segment angular velocity in radians per second in AR.

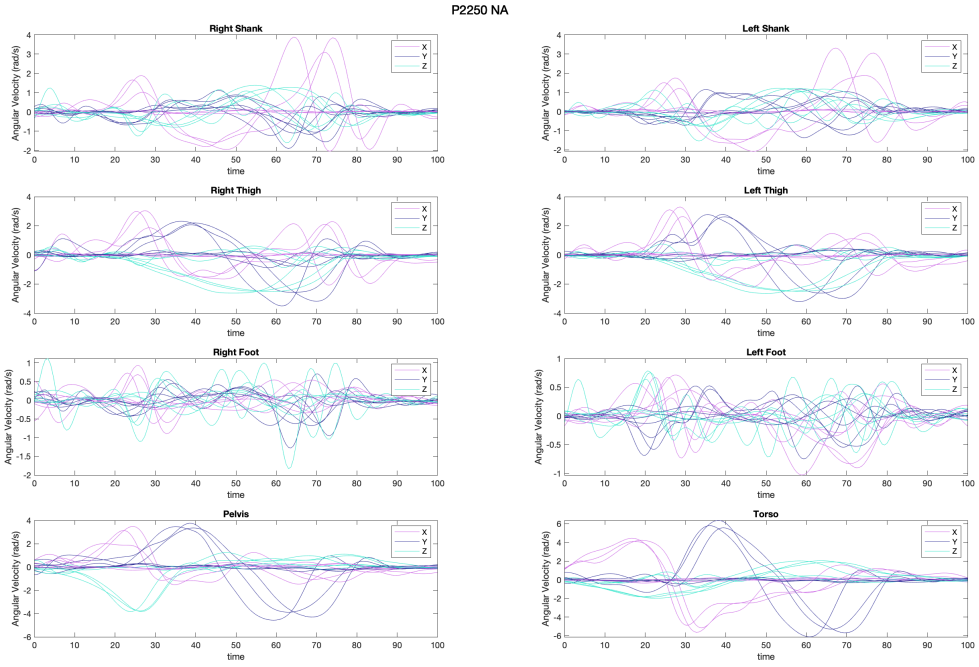

Figure 113: The segment angular velocity in radians per second in NA.